PB2001-103487

GRS Bridge Piers and Abutments

FHWA-RD-00-38

January 2001

US Department of Transportation
Federal Highway Administration

Research, Development, and Technology
Turner-Fairbank Highway Research Center
6300 Georgetown Pike
McLean, VA 221101-2296

REPRODUCED BY: NTIS
U.S. Department of Commerce
National Technical Information Service
Springfield, Virginia 22161

FOREWORD

This report describes three recent projects which evaluated the performance of Geosynthetic-Reinforced Soil (GRS) for bridge support applications. In all three projects the GRS mass was the primary structural element. The GRS abutments and piers were load tested and instrumented to evaluate performance. The concept of pre-loading GRS is explained. The report describes each of the projects in detail, presents the results, and offers recommendations on the applications of GRS in bridge abutment and pier construction. The report will be useful to researchers and practitioners in geotechnology, especially those interested in GRS applications.

T. Paul Teng, P. E.
Director, Office of Infrastructure
Research and Development

NOTICE

This document is disseminated under the sponsorship of the Department of Transportation in the interest of information exchange. The United States Government assumes no liability for its contents or use thereof. This report does not constitute a standard, specification, or regulation.

The United States Government does not endorse products or manufacturers. Trademarks or manufacturer's names appear herein only because they are considered essential to the object of this document.

Technical Report Documentation Page

1. Report No.	2. Government Accession No.	3. Recipient's Catalog No.
FHWA-RD-00-038		

4. Title and Subtitle	5. Report Date
GRS Bridge Piers and Abutments	January 2001
	6. Performing Organization Code
7. Author(s)	8. Performing Organization Report No.
Jonathan T. H. Wu, Kanop Ketchart, and Michael Adams	
9. Performing Organization Name and Address	10. Work Unit No. (TRAIS)
Reinforced Soil Research Center University of Colorado at Denver 1200 Larimer Street Denver, CO 80217-3364	Office of Infrastructure R&D Federal Highway Administration 6300 Georgetown Pike McLean, VA 22101-2296
	11. Contract or Grant No. N/A
12. Sponsoring Agency Name and Address Office of Infrastructure R&D Federal Highway Administration 6300 Georgetown Pike McLean, VA 22101-2296	13. Type of Report and Period Covered Staff Study Final Report June 1996 - July 1999
	14. Sponsoring Agency Code

15. Supplementary Notes

Technical Consultant: Jerry DiMaggio, HIBT-20

16. Abstract

This report presents the following three recent projects on load testing of geosynthetic-reinforced soil (GRS) bridge abutments and piers:

* a full-scale bridge pier load test conducted by the Turner-Fairbank Highway Research Center, Federal Highway Administration, in 1996 (referred to as the Turner-Fairbank pier),
* a full-scale, long-term load test of a bridge abutment and a bridge pier conducted by the Colorado Department of Transportation and the University of Colorado at Denver in 1996-1997 (referred to as the Havana Yard piers and abutment); and
* a production bridge abutment load test conducted by Yenter Companies in Black Hawk, Colorado, in 1997 (referred to as the Black Hawk Abutment).

All the bridge supporting structures were instrumented to measure their performance during the load test. The effect of pre-loading was also investigated in the Turner-Fairbank pier and the Black Hawk abutment. The report describes each of the projects in detail, presents the measured test results and discussion of the results, and offers recommendations on the applications of the GRS bridge abutments and piers.

17. Key Words	18. Distribution Statement
Geosynthetic-reinforced soil, abutments, piers, bridge support.	No restrictions. This document is available to the public through the National Technical Information Service, Springfield, Virginia 22161

19. Security Classif. (of this report)	20. Security Classif. (of this page)	21. No. of Pages	22. Price

Form DOT F 1700.7 (8-72) Reproduction of completed page authorized

This form was electronically produced by Elite Federal Forms, Inc.

SI* (MODERN METRIC) CONVERSION FACTORS

APPROXIMATE CONVERSIONS TO SI UNITS

Symbol	When You Know	Multiply By	To Find	Symbol
		LENGTH		
in	inches	25.4	millimeters	mm
ft	feet	0.305	meters	m
yd	yards	0.914	meters	m
mi	miles	1.61	kilometers	km
		AREA		
in^2	square inches	645.2	square millimeters	mm^2
ft^2	square feet	0.093	square meters	m^2
yd^2	square yards	0.836	square meters	m^2
ac	acres	0.405	hectares	ha
mi^2	square miles	2.59	square kilometers	km^2
		VOLUME		
fl oz	fluid ounces	29.57	milliliters	mL
gal	gallons	3.785	liters	L
ft^3	cubic feet	0.028	cubic meters	m^3
yd^3	cubic yards	0.765	cubic meters	m^3

NOTE: Volumes greater than 1000 l shall be shown in m^3.

		MASS		
oz	ounces	28.35	grams	g
lb	pounds	0.454	kilograms	kg
T	short tons (2000 lb)	0.907	megagrams (or "metric ton")	Mg (or "t")
		TEMPERATURE (exact)		
°F	Fahrenheit temperature	5(F-32)/9 or (F-32)/1.8	Celcius temperature	°C
		ILLUMINATION		
fc	foot-candles	10.76	lux	lx
fl	foot-Lamberts	3.426	candela/m^2	cd/m^2
		FORCE and PRESSURE or STRESS		
lbf	poundforce	4.45	newtons	N
lbf/in^2	poundforce per square inch	6.89	kilopascals	kPa

APPROXIMATE CONVERSIONS FROM SI UNITS

Symbol	When You Know	Multiply By	To Find	Symbol
		LENGTH		
mm	millimeters	0.039	inches	in
m	meters	3.28	feet	ft
m	meters	1.09	yards	yd
km	kilometers	0.621	miles	mi
		AREA		
mm^2	square millimeters	0.0016	square inches	in^2
m^2	square meters	10.764	square feet	ft^2
m^2	square meters	1.195	square yards	yd^2
ha	hectares	2.47	acres	ac
km^2	square kilometers	0.386	square miles	mi^2
		VOLUME		
mL	milliliters	0.034	fluid ounces	fl oz
L	liters	0.264	gallons	gal
m^3	cubic meters	35.71	cubic feet	ft^3
m^3	cubic meters	1.307	cubic yards	yd^3

		MASS		
g	grams	0.035	ounces	oz
kg	kilograms	2.202	pounds	lb
Mg (or "t")	megagrams (or "metric ton")	1.103	short tons (2000 lb)	T
		TEMPERATURE (exact)		
°C	Celcius temperature	1.8C + 32	Fahrenheit temperature	°F
		ILLUMINATION		
lx	lux	0.0929	foot-candles	fc
cd/m^2	candela/m^2	0.2919	foot-Lamberts	fl
		FORCE and PRESSURE or STRESS		
N	newtons	0.225	poundforce	lbf
kPa	kilopascals	0.145	poundforce per square inch	lbf/in^2

* SI is the symbol for the International System of Units. Appropriate rounding should be made to comply with Section 4 of ASTM E380.

(Revised September 1993)

TABLE OF CONTENTS

Chapter **Page**

1. INTRODUCTION.....1

2. THE TURNER-FAIRBANK PIER.....7

2.1 Overview.....7

2.2 Design Philsophy.....7

2.2.1 Reinforced Soil.....9

2.2.1 Prestrainning the Composite Mass.....9

2.2.3 Facing System.....9

2.2.4 Method of Construction.....10

2.3. Construction Phase.....11

2.3.1 Foundation.....11

2.3.2 Prestrainning Assembly.....13

a. Reaction Pad.....13

b. Vertical Rods.....13

2.3.3 Reinforced Soil.....15

a. Reinforced Material.....15

b. Fill.....15

2.3.4 Compaction Operation.....16

2.3.5 Instrumentation, Reaction and Load Test Procedures.....16

a. Loading System.....18

b. Displacements.....18

c. Strain Gauges.....18

2.4 Load Test Program.....19

2.4.1 Overview.....19

2.4.2 Load Test at Fill Height = 3.0m.....19

a. Vertical Settlement.....21

Chapter **Page**

2.4.3 Load Test at Full Height – July 3, 1996 24

a. Vertical Settlement 24

b. Lateral Deformation 24

c. Reinforcement Strain 27

2.4.4 Load Test at Full Height – July 23, 1996 36

a. Vertical Settlement 36

b. Lateral Deformation 36

c. Reinforcement Strain 42

2.4.5 General Observations from the Load Tests 42

a. Reinforcement Strain 42

b. Facing Blocks 46

(i) Bending Cracks 46

(ii) Tension Cracks 48

2.5 Findings, Observations and Recommendations 48

3. THE HAVANA YARD PIERS AND ABUTMENT 52

3.1 Overview 52

3.2 Construction Material 55

3.2.1 Backfill 55

3.2.2 Geotextile Reinforcement 55

3.3 Construction of GRS Piers and Abutment 58

3.4 Loading Scheme 58

3.4.1 The First-Stage Load Test 58

3.4.2 The Second-Stage Load Test 72

3.5 Instrumentation 72

3.5.1 Vertical Movement 72

3.5.2 Lateral Movement 72

3.5.3 Strains in Reinforcement 76

Chapter **Page**

3.6. Results and Discussion of the Results.....79
3.6.1 Short-Term Behavior.....79
3.6.1.1. Vertical and Lateral Displacements.....79
3.6.1.2. Strains in Reinforcement.....87
3.6.2 Long –Term Behavior under 1170kn Load.....90
3.6.2.1 Vertical and Lateral Creep Displacement.....90
3.6.2.2 Creep Strains in Reinforcement.....95
3.7. Summary and Conclusions.....99

4. THE BLACK HAWK ABUTMENT.....103

4.1. Overview.....103
4.2. Construction Materials.....107
4.2.1 Backfill.....107
4.2.2 Geotextile Reinforcement.....107
4.3 Instrumentation.....111
4.4 Preloading Configuration and Loading Sequence.....113
4.5 Test Results and Discussions..... 113
4.5.1 Loading Tests on Square Footings.....113
4.5.2 Loading Tests on the Strip Footings.....125
4.6 Summary and Conclusions.....131

5. CONCLUDING REMARKS.....134

REFERENCES.....136

LIST OF FIGURES

Figure		Page
2.1	Principal Elements in Internally Supported Geosynthetic-Reinforced Soil Bridge Pier	8
2.2	GRS Pier Foundation	12
2.2	Prestraining Elements	14
2.3	Density Results	17
2.5	Pad Pressure vs. Average Top Settlement	22
2.6	Lateral Displacement; 3-m # Prestrain	23
2.7	Load Settlement Curves	25
2.8	Lateral Displacement North Wall	26
2.9	Lateral Displacement North Wall Laser Measurements At 825 kPa (8.6 tst)	28
2.10	GRS Pier Constructed With External Confinement Straps	29
2.11	Strain Distribution, July 3, 1996 (Length Direction)	30
2.12	Strain Distribution, July 3, 1996 (Width Direction)	31
2.13	Pad Pressure vs. Average Strain (Width Direction)	33
2.14	Lateral Displacement; Calculated (SG) vs. Measured (LVDT)	35
2.15	July 23-26, 1996; GRS Pier Load Test History	37
2.16	Settlement vs. Time	38
2.17	Settlement Rate vs. Time (at Sustained Loads of 790 kPa/8.3 tsf, 670 kPa/7.0 tsf, and 890 kPa/9.3 tsf)	39
2.18	Lateral Displacement (0-780 kPa/8.2 tsf), 1st Half: July 23, 1996	40
2.19	Lateral Displacement (670kPa/7.0 tsf Load Hold and Unload Cycles), 2nd Half: July 23, 1996	41

Figure		Page

2.20 Lateral Displacement in the Length Direction (Potentiometer) 43
2.21 Fabric Strains.....44
2.22 Strain – Fabric Layer # 2.....45
2.23 Cracks in the Façade.....47
3.1 Side View of the Structures.....53
3.2 Top View of the Structures.....54
3.3 Gradation Curve.....56
3.4 First Stage Load Test.....73
3.5 Instrumentation for Vertical and Lateral Movements.....74
3.6 Locations of the Leveling Rods.....75
3.7 Locations of the Reinforcements with Strain Gauges and The Elastic Springs.....77
3.8 Strain Gauge Attachment 78
3.9 Strain Gauge Calibration in the Fill Direction of the Reinforcement.....80
3.10 Strain Gauge Calibration in the Warp Direction of the Reinforcement.....81
3.11 Vertical Displacement vs. Applied Load Relationships of the Abutment....82
3.12 Lateral Displacement vs. Applied Load Relationships of the Abutment.....83
3.13 Vertical Displacement vs. Applied Load Relationships of the Outer Pier....84
3.14 Lateral Displacement vs. Applied Load Relationships of the Outer Pier.....85
3.15 Vertical and Lateral Movements of the Outer Pier and The Abutment at 1170.....87
3.16 Reinforcement Strain Distributions in the Abutment.....89
3.17 Vertical Creep Displacement vs. Time Relationships of the Abutment.....91
3.18 Lateral Creep Displacement vs. Time Relationships of the Abutment.....92
3.19 Vertical Creep Displacement vs. Time Relationships of the Outer Pier.....93
3.20 Lateral Creep Displacement vs. Time Relationships of the Outer Pier.....94
3.21 Average Vertical Creep Rate at Tope of the Outer Pier and the Abutment...96
3.22 Reinforcement Creep Strain Distributions in the Abutment.....97

Figure **Page**

3.23 Reinforcement Creep Strain Distribution in the Outer Pier.....98

3.24 Calculated vs. Measured Lateral Creep Displacement of the Outer Pier....100

4.1 Configuration of the Black Hawk Abutment.....104

4.2 Cross Sections of (a) East Abutment and (b) West Abutment.....105

4.3 Thickness of the GRS Abutments: (a) West and (b) East Abutment.....106

4.4 Plan View of the Footings and Preloading Arrangement.....108

4.5 Gradation of Backfill.....109

4.6 Deviatoric Stress vs. Axial Strain Relationships and Volumetric Strain vs. Axial Strain Relationship.....110

4.7 Layout of Instrumentation 112

4.8 Setup for Preloading.....114

4.9 Loading Sequence Used for Each Footing.....115

4.10 a. Relationships Between Settlement at Four Corners of Footing # 1 and Applied Pressure.....116

b. Relationships Between Settlement at Four Corners of Footing # 2 and Applied Pressure.....117

c. Relationships Between Settlement at Four Corners of Footing # 3 and Applied Pressure.....118

4.11 Relationships Between Average Settlement and Applied Pressure.....121

4.12 a. Lateral Deformation Profiles of the Wall Under Footing 1.....122

b. Lateral Deformation Profiles of the Wall Under Footing 3.....123

4.13 Average Vertical Creep Displacement of the Square Footings.....126

4.14 Maximum Lateral Creep Displacements of the Square Footings 1 and 3.....127

4.15 Average Vertical Settlement vs. Applied Pressure Relationships of West Strip Footing.....128

4.16 Strains in Geosynthetic Reinforcement Beneath the West Strip Footing...129

4.17 Creep Strains Under Sustained Pressure of 80 kPa in the Preloading.....130

LIST OF PLATES

Plate		Page
1.1	Load Test of the Turner-Fairbank Pier	2
1.2	Long-Term Load Test of the Havana Yard Piers and Abutment	4
1.3	Preloading of the Black Hawk Abutment	5
1.4	The Black Hawk Abutment Supporting a Steel Arch Bridge	6
3.1	Excavation of the Construction Pit	59
3.2	Construction of the Reinforced Soil Foundation	60
3.3	Reinforced Soil Foundation With a Woven Geotextile Reinforcement	61
3.4	Laying the First Course Facing Block on a concrete pad (Note the lightweight compaction plant at he lower left-hand corner)	62
3.5	Compaction of the Center Pier	63
3.6	Placement of a layer of Geotextile Reinforcement	64
3.7	Alignment of Facing Blocks	65
3.8	Construction of the GRS Abutment With a Negative Batter	66
3.9	Cutting Concrete Blocks to Conform to the Designed Configuration	67
3.10	Placement of a Steel Bridge Girder	68
3.11	Three Steel Bridge Girders Welded Together	69
3.12	A Forklift Clamp Is Used to Lift a Jersey Barrier	70
3.13	Placement of Jersey Barriers	71

PROTECTED UNDER INTERNATIONAL COPYRIGHT
ALL RIGHTS RESERVED
NATIONAL TECHNICAL INFORMATION SERVICE
U.S. DEPARTMENT OF COMMERCE

Reproduced from best available copy.

LIST OF TABLES

Table **Page**

2.1 Highlights of the GRS Pier Load Test Program.....20

2.2 Summary of Creep Strains in Instrumented Reinforcement Layers.....34

3.1 Some Index Properties of the Reinforcement.....57

3.2 Maximum vertical and Lateral Movements of the Outer Pier and The Abutment at 1170 kN 88

Chapter 1
INTRODUCTION

Geosynthetic reinforced soil (GRS) technology has been widely used in the construction of retaining walls, embankments, slopes, and shallow foundations. Recently a number of studies have been conducted to investigate the applicability of GRS technology in the construction of bridge supporting structures, i.e., bridge piers and abutments. This report describes three of these studies:

- a full-scale GRS bridge pier load test conducted by Turner-Fairbank Highway Research Center, Federal Highway Administration in 1996 (referred to *as the Turner-Fairbank pier*);
- a full-scale long-term load test of a bridge abutment and a bridge pier conducted by the Colorado Department of Transportation and the University of Colorado at Denver in 1996-1997 (referred to *as the Havana Yard piers and abutment*);
- a production bridge abutment constructed by Yenter Companies in Black Hawk, Colorado in 1997 (referred to as *the Black Hawk abutment*).

The Turner-Fairbank pier is a 5.4-m high prototype GRS bridge pier constructed in McLean, Virginia in June and July of 1996. A series of load tests were conducted to examine load carrying capacity of the GRS bridge pier and to investigate the effects of various loading schemes, including preloading, on the pier performance (Adams, 1997). The pier was instrumented to monitor applied load, reinforcement strain, lateral movement of pier, and vertical settlement. Plate 1.1 shows the Turner-Fairbank pier subject to vertical loads.

The Havana Yard piers and abutment, comprising two piers and one abutment, were constructed in Denver, Colorado. One of the piers and the abutment, both 7.6 m in height, were load tested with concrete barriers stacked in

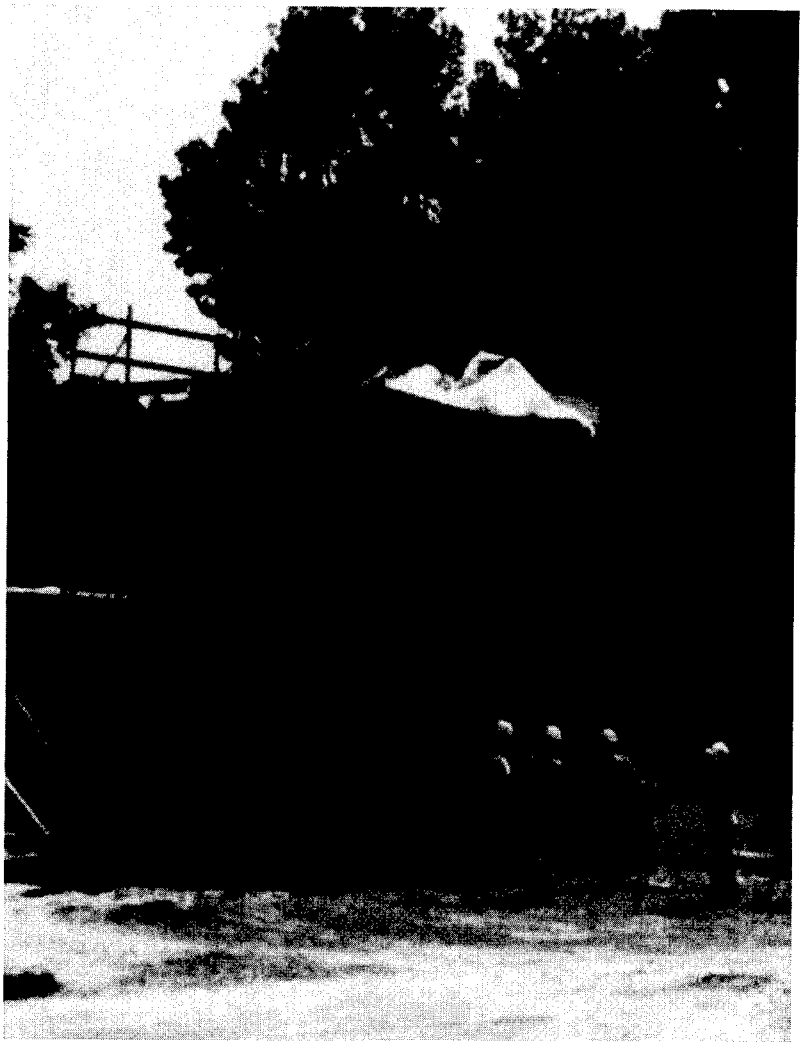

Plate 1.1 Load Test of the Turner-Fairbank Pier

seven layers. The use of dead weight facilitates long-term monitoring of the bridge supporting structures. The structures were instrumented to monitor their performance. The objectives of the study were twofold. The first objective was to investigate the performance of a GRS bridge support system when constructed in a less stringent condition than that in the Turner-Fairbank pier. The second objective was to investigate the long-term performance of the bridge supporting structure under a sustained design load. Plate 1.2 shows the completed Havana Yard piers and abutment supporting a bridge girder with concrete barrier dead weight.

The Black Hawk abutment was a production structure constructed in the city of Black Hawk, Colorado. The abutment was constructed to support a 36-m span steel arch bridge. Since the thickness of the reinforced soil abutment are quite different beneath the four footings directly supporting the weight of the bridge, the GRS abutment was preloaded to reduce post-construction settlement, especially the differential settlement between adjacent footings. The abutment was instrumented to monitor performance during preloading and subsequent reloading operation. Plate 1.3 shows the Black Hawk abutment. Plate 1.4 shows the steel arch bridge supported by the preloaded abutment.

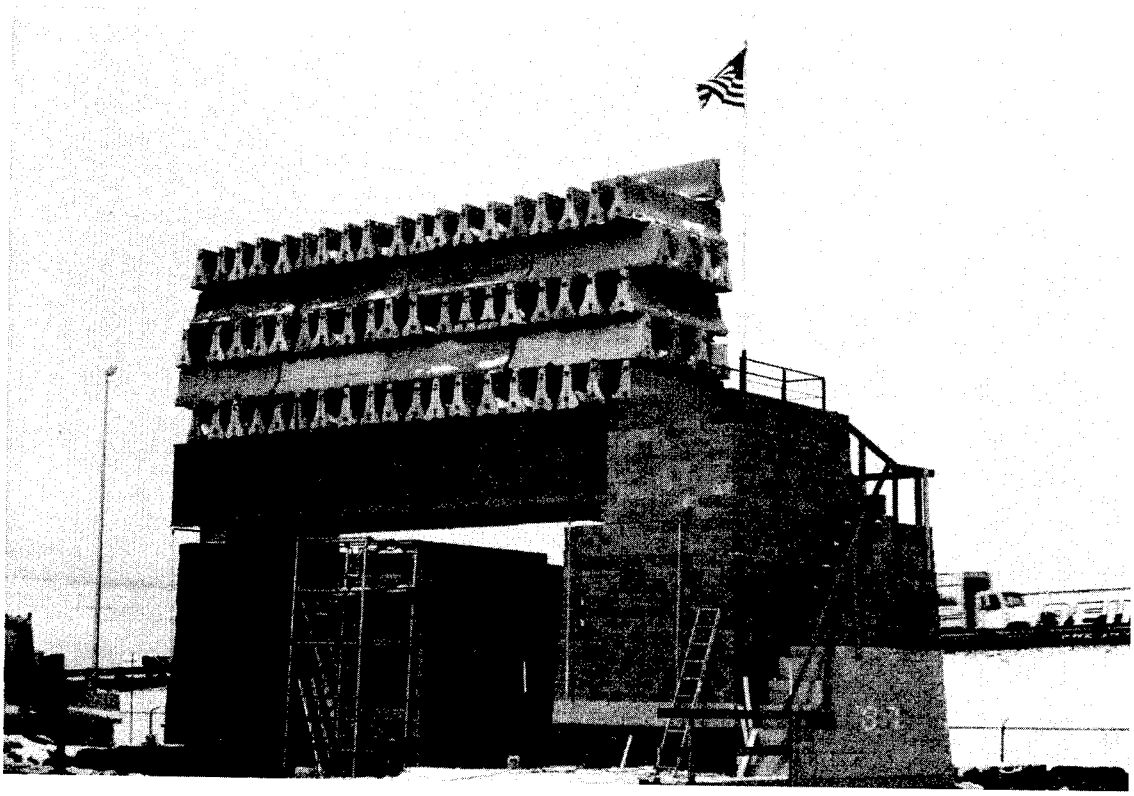

Plate 1.2 Long-Term Load Test of the Havana Yard Piers and Abutment

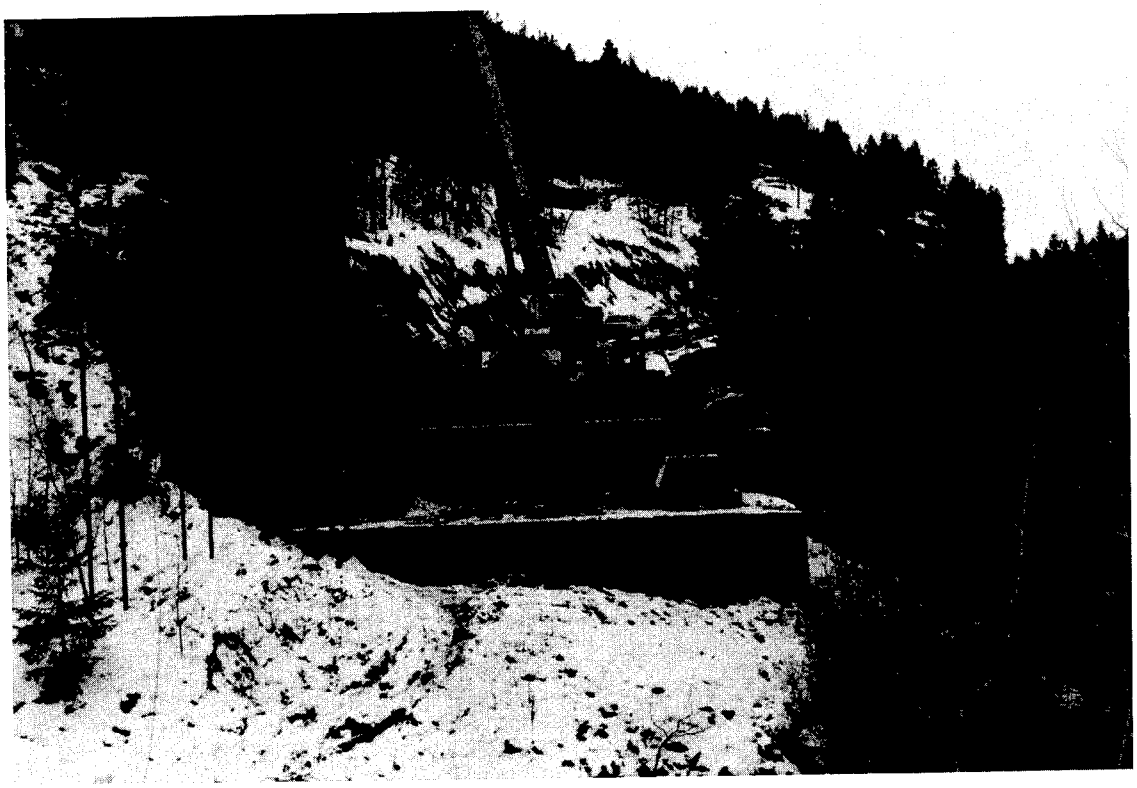

Plate 1.3 The Black Hawk Abutment

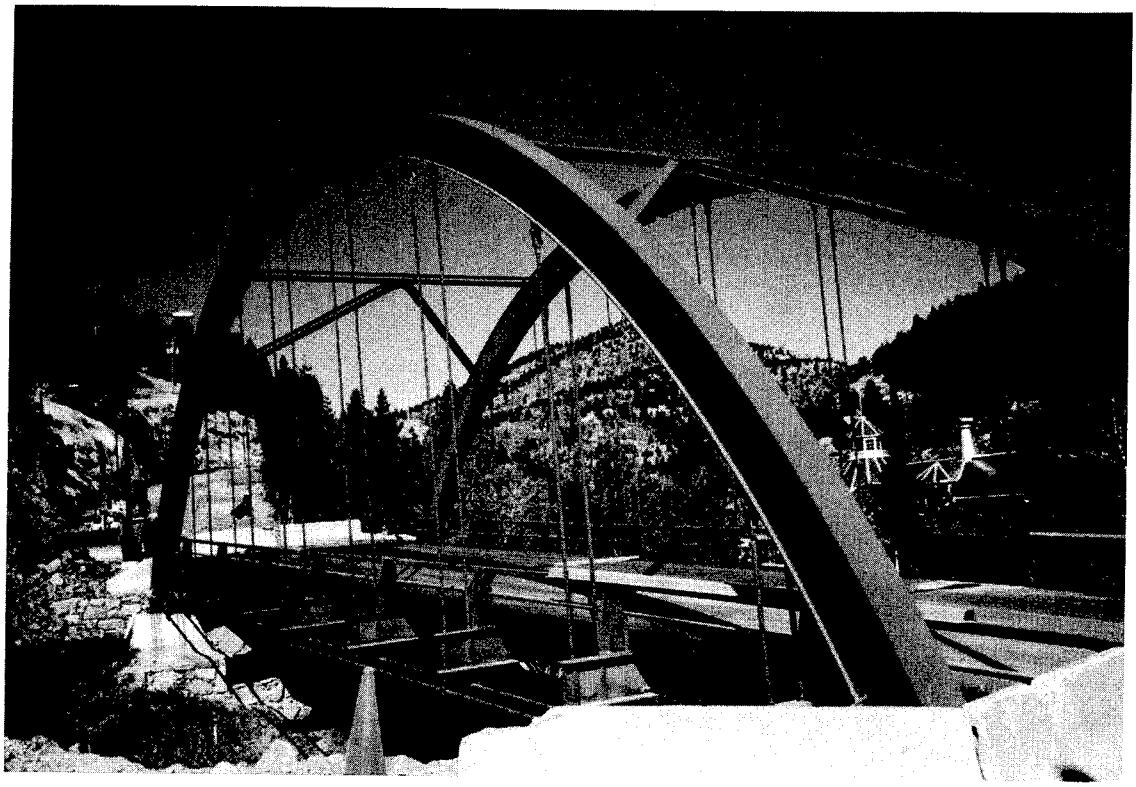

Plate 1.4 The Black Hawk Abutment Supporting a Steel Arch Bridge

Chapter 2
THE TURNER-FAIRBANK PIER

2.1 Overview

A prototype full-scale instrumented bridge pier was constructed and load tested at the Turner Fairbank Highway Research Center (TFHRC) in McLean, Virginia. The pier was 5.4m in height and was 3.6m by 4.8m at the base. The purposes of the study were to demonstrate the ability of constructing a GRS bridge pier with lightweight segmental blocks and to investigate the performance of the pier under various loading scenarios, including pre-straining/pre-loading. A generic method of constructing GRS structures was employed. This method utilizes closely spaced high-strength geosynthetic reinforcement and quality compacted road base. The pier was instrumented to monitor load, lateral deformation and vertical settlement. Several layers of the reinforcement were instrumented with strain gauges to measure deformation in the geosynthetic reinforcement.

2.2 Design Philosophy

The focus of this study was to advance the state of practice of reinforced soil technology by demonstrating what is known about the technology based on experimental testing and practice, as well as what is possible. An additional objective was to demonstrate the ease and speed of construction when faced with limited resources. The prototype pier took two weeks to construct, but a typical production pier would have taken half the time. Additional time was needed in this case to prepare the instrumentation and conduct the pre-straining experiment at approximately mid-height.

Some of the key elements of the GRS pier design are the reinforcement spacing, the act of pre-straining (pre-loading) the soil, the facing system, and the method of construction. Figure 2.1 shows the principal elements of the GRS pier.

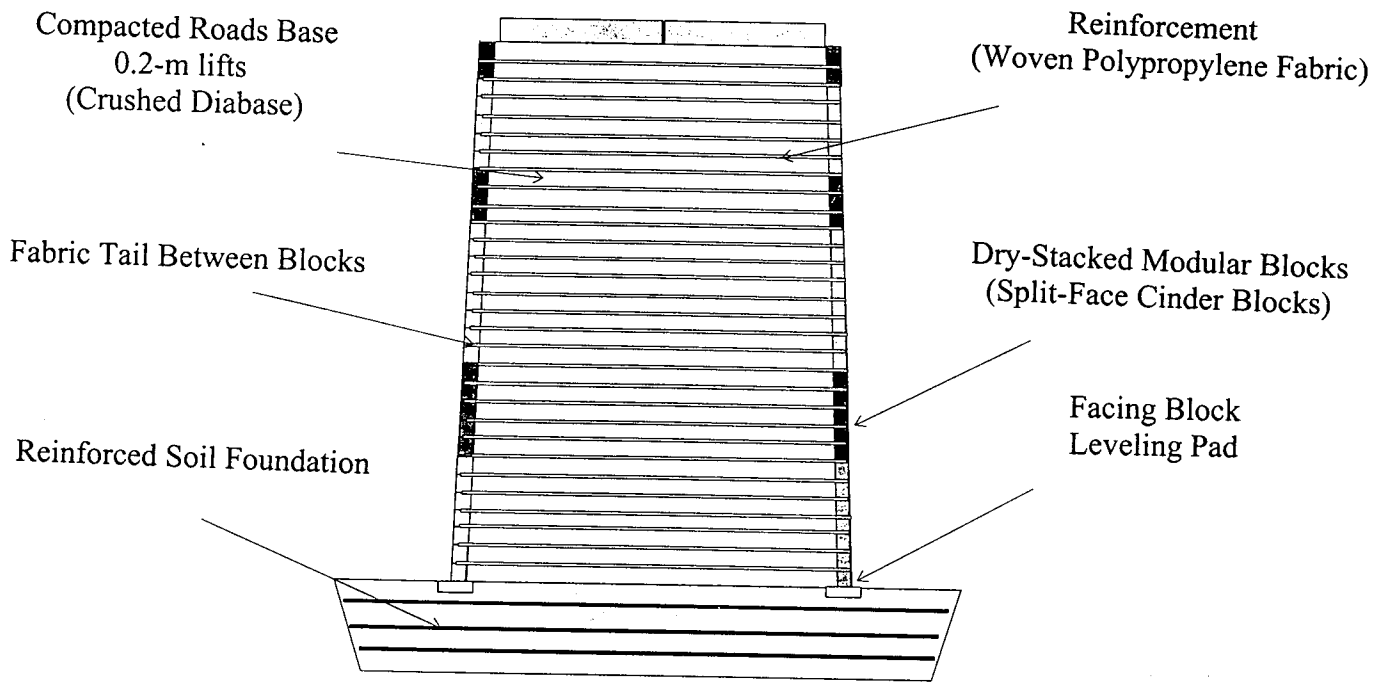

Figure 2.1 Principal Elements in Internally Supported Geosynthetic-Reinforced Soil Bridge Pier

2.2.1 Reinforced Soil (RS)

In the case of this GRS pier, the default reinforcement spacing was selected at 0.2m, which is the height of the facing blocks. This spacing was selected because it is a warranty of good compaction of each lift. Superior performance depends largely upon good compaction. With a smaller spacing, the contractor is bound to compact the backfill in thin lifts.

For this bridge support application, the additional cost of placing the reinforcement between each layer of fill did not add significantly to the cost of construction. This closer spacing, combined with high strength reinforcement and quality compacted road base, forms a stronger composite mass more suitable for bridge support.

2.2.2 Pre-straining the Composite Mass

A technique of pre-straining the reinforced soil (RS) was incorporated into the design of the pier to determine what effect, if any, it would have on construction and performance.

Construction of the pier was in two parts to evaluate the technique of incremental pre-straining, and to resolve any problems associated with the pre-straining assembly before the pier reached its full height.

Pre-straining the reinforced soil mass offers many advantages, including (1) compression of the reinforced mass; (2) mobilization of the reinforcement; (3) proof test the structure; and 4) reduction in post-construction settlement of the reinforced soil mass. In addition, pre-straining may be necessary in some pier applications where it is impractical to use large, heavy compaction equipment.

It is known that pre-loading a soil mass beyond the expected service load will typically increase its stiffness and decrease its compressibility. This is because the confining pressure tends to be "locked-in" the soil mass after the load is removed. The significance of this effect depends, among others, on the degree of restrain to the lateral deformation of the soil mass. The higher the restrain, the more pronounced is the effect. Because the frictional resistance at the soil-

reinforcement interface tends to restrain internally the lateral deformation of a reinforced soil mass, the effect of pre-loading can be quite significant in reinforced soil structures.

2.2.3 Facing System

One of the current issues of debate is the connection strength between the segmental wall block and the reinforced soil mass. Much of this debate concerns the equations to resolve the forces on the blocks. The facing system for this experiment was designed to demonstrate the connection strength requirement between a lightweight segmental block wall and the RS mass for this type of loading scenario.

The connection strength of the blocks to the reinforced soil depends on the frictional bond between the blocks, the fabric reinforcement, and the compacted soil. To demonstrate how well the fabric tail connection works, a 0.2m-thick block was used instead of a 0.3m-thick block, which is typically used in practice and has more frictional bond strength than a 0.2m block. Fill was compacted into the core of the blocks.

In this system, the blocks accept as much a load as they can, then they move outward to relieve the lateral pressure. The facing system was designed to move and retain its shape. The walls were battered 20:1 to offset any lateral deformations which were expected to occur at intense pressures.

A standard cinder block (0.2mx0.2mx0.4m) with a split-face was used for this prototype pier. The blocks were dry-stacked and attached to the reinforced soil mass with a fabric tail from the layers of reinforcement. In this style, the primary function of the facing block was to act as a form for each lift of fill, and provide an attractive facade. The facing is not considered to contribute structural confinement; it's contribution to soil retainment is minor compared to the effect of closely spaced reinforced soil.

Additionally, many believe that a stiff facing system is necessary to increase global rigidity and limit long-term creep deformation of the reinforced

soil mass. This experiment was designed without a rigid face, to determine if one is required.

2.2.4 Method of Construction

A notable advantage of modular block GRS construction is that it does not require specialized equipment, labor or material. All of the equipment and material required to construct the pier were commonly found and relatively available. Necessary equipment included a backhoe, small crane, hopper bucket, vibratory plate tamper and garden tools to spread the road base.

Construction of the pier is simple, but a learned skill. Training is required for proper construction practice. As a part of the demonstration, the intent was to keep the construction crew simple. The number of people required to construct a pier depends upon the size and desired speed of construction. In this experiment, labor was limited to a four to five man team led by a foreman with considerable experience in segmental block wall construction. The other team members, a crane operator, backhoe operator, and two general laborers, had no previous experience.

2.3 Construction Phase

2.3.1 Foundation

The pier was supported on a Reinforced Soil Foundation (RSF). Design of the RSF was based on previous experiments at Turner-Fairbank Highway Research Station. The size of the RSF was determined by the width of the superstructure and the allowable loads of the soils beneath the RSF. Generally, the dimensions of the RSF with respect to the footing are (L+B) x 2B (see Figure 2.2). In the case of the RSF for this project, the depth of the RSF was 0.4 B or 1.2m. The area of RSF was 7.3m x 8.5m.

After the excavation of soil, the base of the pit was compacted. A fabric separator was lined along the walls of the pit. The pit was refilled with compacted road base and bi-axial geogrid reinforcement. The fill was compacted in 0.15m lifts, with three layers of geogrid reinforcement spaced 0.3m apart. The

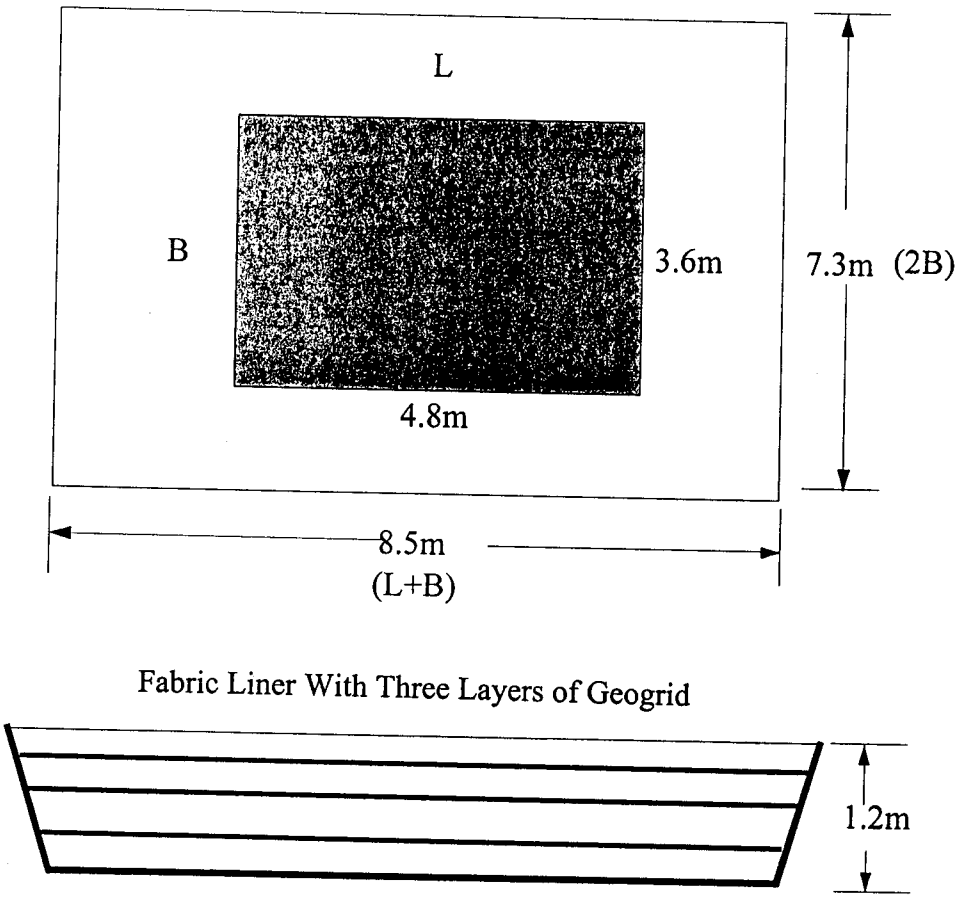

Figure 2.2 GRS Pier Foundation

pier was centered on the RSF to ensure uniform settlement (see Figure 2.2). The RSF was instrumented with inclinometers to evaluate its long-term performance under the load of the pier.

Additional research will further optimize the design of the RSF for pier foundations. Since the intention of this project was to evaluate the performance of the pier and not the shallow foundation, the performance of the RSF was not analyzed in detail.

2.3.2 Pre-straining Assembly

The GRS pier was pre-strained using hydraulic jacks and a specially designed reaction system. The jacks were used to squeeze the reinforced soil mass between the concrete pads on the bottom and top of the pier. The jacks and concrete pads were bolted together with vertical steel rods as shown in Figure 2.3. For experimental purposes, the reaction pads were very thick because the applied loads were very high. For routine pre-straining on a typical construction project, the reaction system would be reduced by half or more.

a. *Reaction Pads*

After completion of the RSF, six concrete reaction bottom pads were poured on the center of the RSF. The dimensions of the base pads were 1.3m x 1.4m x 0.3m thick. Four sections of dywidag rods were anchored into each pad. Each pad was separated with wood and designed to work independently with a top pad.

The top pads were poured on the base pads. The top pads were numbered and matched to the base pads. Four 150mm-diameter holes were cast into each of the six top pads; the holes in the top pad mated to the location of the dywidag rods anchored to the bottom pads. Top pads were removed. A plastic sheet was used to separate the top pads from the bottom pads.

b. *Vertical Rods*

Since the intent of the experiment was to demonstrate the load bearing capabilities of a GRS pier, a considerable number of vertical rods

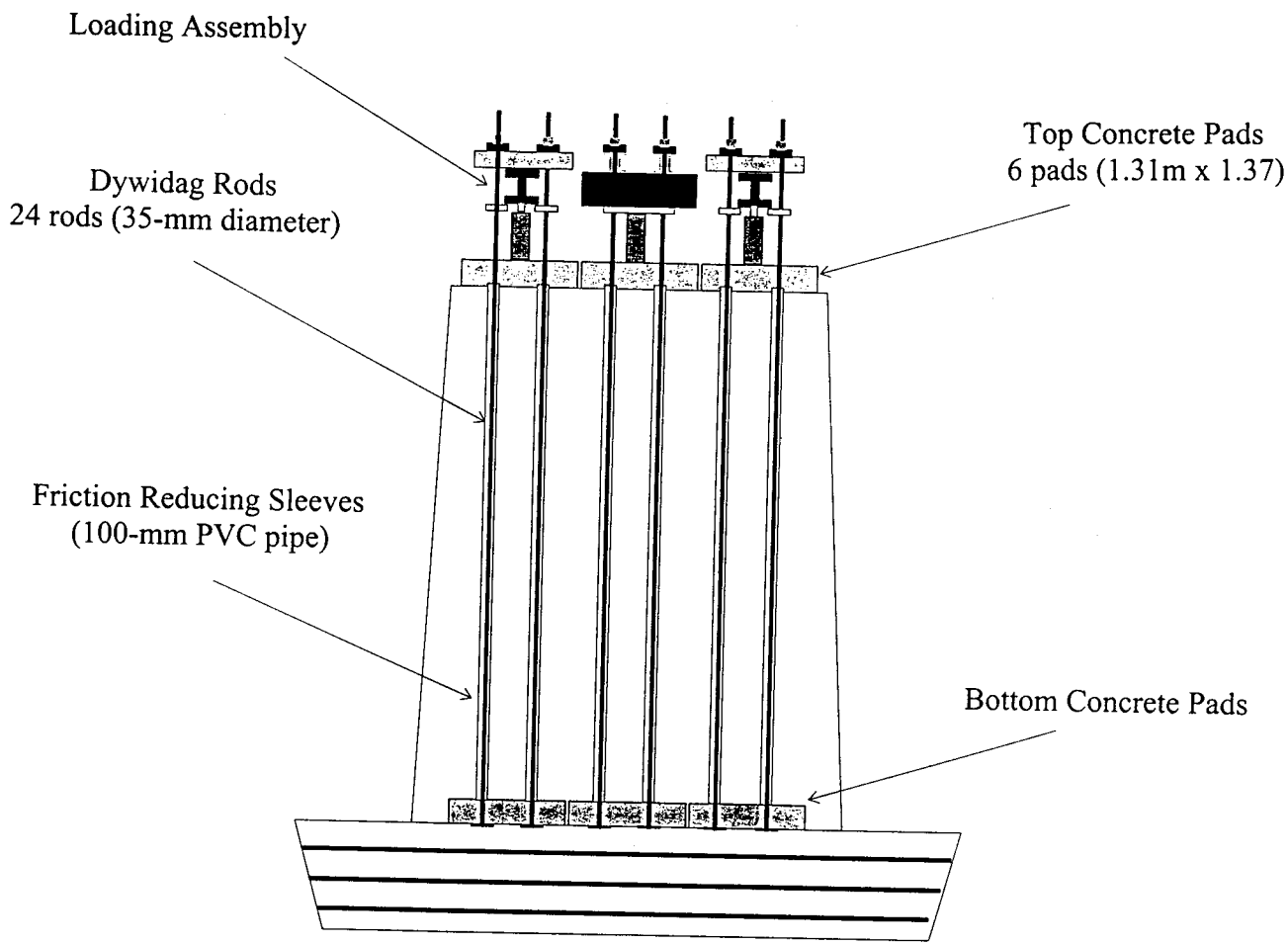

Figure 2.3 Prestraining Elements

were included in the design because of the capacity of the reaction system. A total of 24 rods were used to provide the reaction. The rods were high strength grade 150 steel, 36mm in diameter. In production, a pre-stressing assembly would have 6-12 rods.

The steel rods were isolated from the reinforced soil mass by PVC pipes to negate the rod's contribution to increased reinforcement in the vertical direction. Both the rods and the PVC friction sleeves (100mm diameter) were coupled together in 1.5m lengths.

The addition of the friction sleeves is believed to have lessened pier strength; without the friction sleeves, the addition of rods probably would have increased pier strength because they would have resisted deformation of the soil.

The technique of constructing reinforced soil with many vertical reinforcing rods was investigated to determine feasibility of construction. It is suggested that the combination of the reinforced soil's ability to absorb ground shocks and the vertical rods resistance to lateral load may produce a system capable of protecting a bridge during an earthquake.

2.3.3 Reinforced Soil

a. Reinforcement Material

The reinforcement material used was a high strength woven polypropylene geosynthetic (Amoco 2044), which ruptures at 18% strain.. Because the fabric was stronger in the length direction, the width and length directions were alternated on each layer.

To easily fit the fabric over the pre-straining rods, a template was placed over each layer. The fabric was then cut to match the location of the rods, fitted over the rods, and stretched into place.

b. Fill

The backfill was a crushed Diabase rock from a local source near Washington, D.C. The material was classified as a well graded gravel (A-1a or GW-GM) according to AASHTO M-15 and ASTM D2487. The

maximum density is 24 kN/m^3 (154 lb/ft^3). The optimum moisture content is (5.0%). The backfill moisture was monitored to ensure efficient compaction.

Nuclear density testing was performed on each lift (see Figure 2.4). The average compaction of all the lifts was 95%.

2.3.4 Compaction Operation

Construction of the pier began with a 90mm thick concrete leveling pad for the facing system. The leveling pad ensured a proper start with horizontal rows of blocks. A fabric tail was used to connect the facing blocks to the RS mass. A hopper bucket and light crane were used to lift and help spread the fill. Care was taken to get good compaction of fill directly behind the facing blocks in order to keep the facing block from slipping out of alignment during compaction.

The fill behind the facing blocks had to be tamped in 0.1m lifts to set the blocks in place. During these thin 0.1m lifts, the laborers walked around the perimeter with one foot on the facing blocks to keep them in place, while the other foot compacted the fill. This process continued until the fill behind the blocks was compacted near the level of the blocks. The laborers walked the area again, to further compact the fill.

After the fill behind the blocks was compacted by foot, laborers raked and compacted the material with a vibratory plate tamper. Each lift was compacted evenly. During the last quarter of construction, it was necessary to compact areas near the facing blocks with a hand tamper because the vibratory plate tamper was too wide to compact the fill between the facing blocks and pre-straining rods. Construction adhesive was used to glue the last row of facing blocks in place.

2.3.5 Instrumentation, Reaction and Load Test Procedures

The pier was instrumented to monitor its performance during the load test for vertical and lateral displacement of the reinforced soil. Strain gauges were mounted on some layers of the reinforcement to measure strain and creep in the reinforcement.

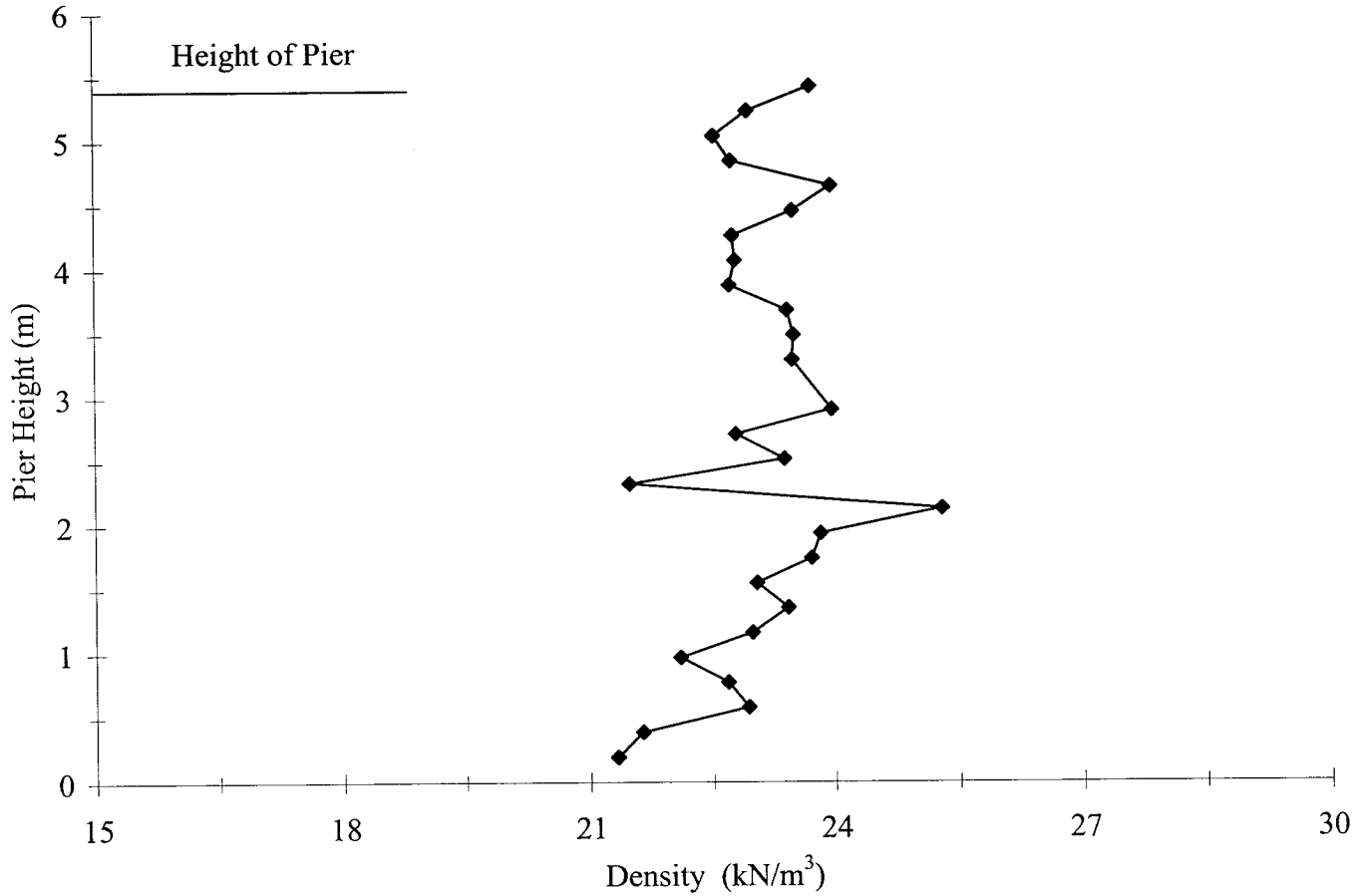

Figure 2.4 Density Results

a. *Loading System*

Load was measured with load cells and calculated from the hydraulic jack pressure. The load cells were mounted on jacks from three of the pads. Load was maintained with an electrical hydraulic pump and strain indicator box connected to a load cell.

The experiment was designed to apply the load evenly over the entire area of the pier. An hydraulic system for the jacks consisted of a high capacity electric hydraulic pump and manifolds to feed the jacks simultaneously and equally. A pressure transducer was connected to the hydraulic line to monitor jack pressure. Hydraulic jack pressure was also used to calculate load on the pads. Results were compared to the load values measured from the load cells.

As explained earlier, the pier was loaded by squeezing the reinforced soil between concrete pads on the top and bottom of the pier. Jacks were placed on the top of each pad. Each pad had 2670kN (600kips) of jack capacity. Three of the pads had a single 2670kN (600kips) jack. The other three pads had two 1335kN (300kip) jacks teamed together to equal the capacity of the 2670 kN (600kip) jack.

b. *Displacements*

Displacements were measured with a variety of devices: Linear Potentiometers, Linear variable displacement transducers (LVDTs), and mechanical/digital dial gauges. The displacement devices were referenced off scaffolding constructed around the pier.

Vertical settlements were measured from top pads. Lateral displacement was measured along the height of the pier walls. A laser displacement measuring device was also used to map movement on two faces of the pier during the first full height load test on July 3, 1996.

c. *Strain Gauges*

In the second half of the pier construction, the upper 2.4 m of pier, four sheets of strain gauge instrumented fabric were layered into the reinforced soil. A total of 21 gauges were placed on each layer. The

strain gauges were placed at 0.3m intervals along the centerline in the width and length directions. The rolled direction on the instrumented sheets was matched for each layer to insure comparative strain readings. Holes were drilled through the facing blocks for the wires.

The strain gauges were a high elongation foil type. To mount the gauges, they were first glued onto a heat-bonded nonwoven fabric swatch. The swatch was then oriented and glued onto the fabric. The area on the fabric was then covered with a silicon wax mixture to seal water from the gauge. Separate strain gauges were mounted on fabric samples and calibrated in the laboratory. The calibration factors were used to compute strain in the fabric.

All data, with the exception of the dial gauges, were recorded using an automated data acquisition system.

2.4 Load Test Program

2.4.1 Overview

The pier was load tested three times: first, on June 24, 1996 when the pier height was 3.0m; second, on July 3, 1996, when pier construction was completed; and third, on July 23, 1996. Details of the load test program and results are summarized in the remainder of this report. A more detailed analysis of the results will follow in an official FHWA document.

It should be noted again that the intent of the experiment was to evaluate the performance of a GRS pier and not the RSF. All the references to settlement refer to deformation in the pier, and not the foundation soil. Table 2.1 provides an overview of the highlights of the three load tests.

2.4.2 Load Test at Fill Height = 3.0m

Construction of the pier was stopped at 3.0 m to pre-strain. There were several reasons for the 3.0m pre-strain, one of which was to explore the concept of incremental pre-straining. Some of the technical review committee members for this study believed that loading the GRS incrementally or at different stages

June 24, 1996	3 m Prestrain, 600 kPa (6.3 tsf)
July 3, 1996	415 kPa (4.3 tsf) Initial Load 900 kPa (9.4 tsf) Prestrain 415 kPa (4.3 tsf) Reload
July 23, 1996	670 kPa (7.0 tsf) for 18 hr

Table 2.1 Highlights of the GRS Pier Load Test Program

during the construction would more effectively compress the fill material.

Another reason for incremental pre-straining was to correct any problems associated with the loading system before the pier reached full height. One of the most important aspects of the study was to evaluate strain in the reinforcement. At considerable time and expense, several layers of reinforcement were instrumented with strain gauges during the second half of construction. The expected life of strain gauges is very short, perhaps only a few days. A significant time delay in the first full-height load test could have compromised the quality of the strain data.

A final reason was to correct any gross lateral offset that may have occurred during a single full-height pre-strain. The plan was to load the pier far beyond any previous experiments. It was expected the pier would bulge more in the middle under intense load but the amount was unknown. For this reason, the pier was pre-strained at half the height to determine the magnitude of lateral deformation and correct any significant offset in the walls by realigning the blocks during the top half of construction.

a. *Vertical Settlement*

LVDT's were used to monitor lateral and vertical deformations. Displacements were monitored on four of the six pads. Vertical deformations were collected on four points along the wall.

Results of the load test are illustrated below in Figures 2.5 and 2.6. These graphs show the vertical settlements and lateral deformations during the load test.

The 3.0m pier was loaded to about 600kPa (6.3tsf). For the 3.0m pre-strain, the average settlement at 200kPa (2.1tsf) was about 15mm and about 27mm at 415kPa (4.3tsf).

b. *Lateral Deformation*

At 200kPa (2.1tsf), lateral displacement was about 6mm (see Figure 2.6); at 400kPa (4.2tsf), it was about 12mm; and at 600kPa (6.3tsf), it was about 20mm. Some cracks in the facing block developed after about 270kPa (2.8tsf) vertical load. More detailed comments about the

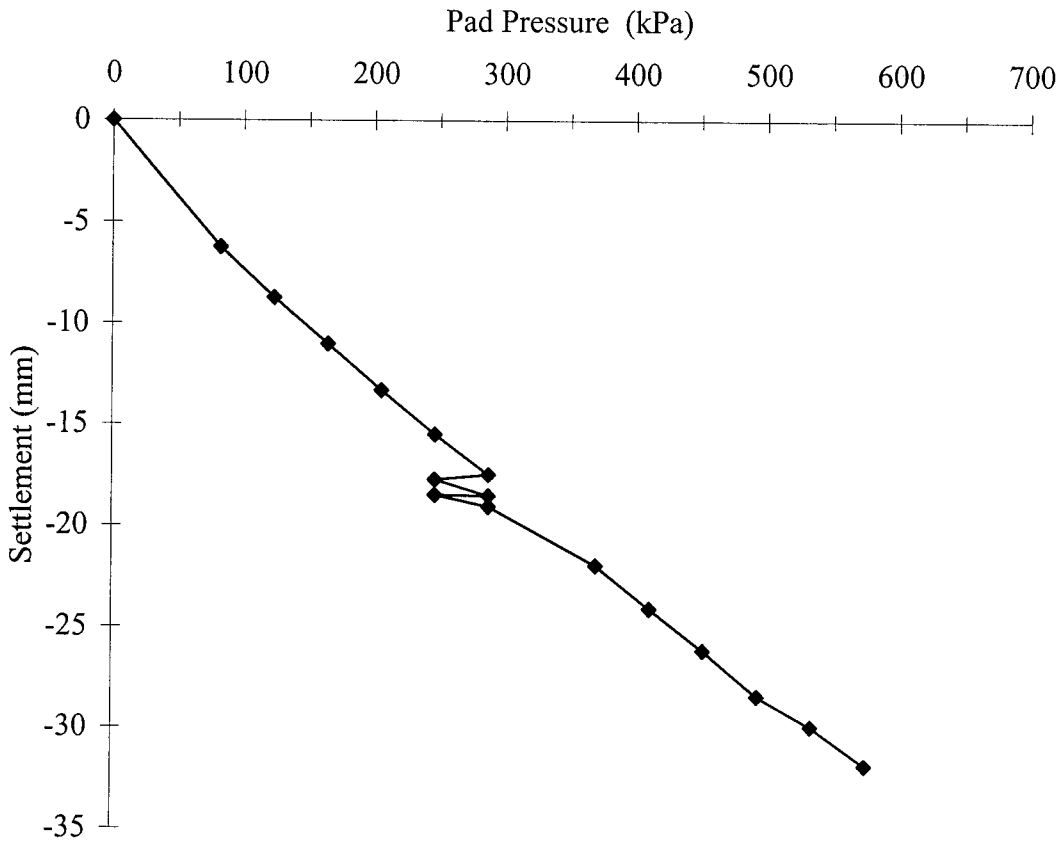

Figure 2.5 Pad Pressure vs. Average Top Settlement

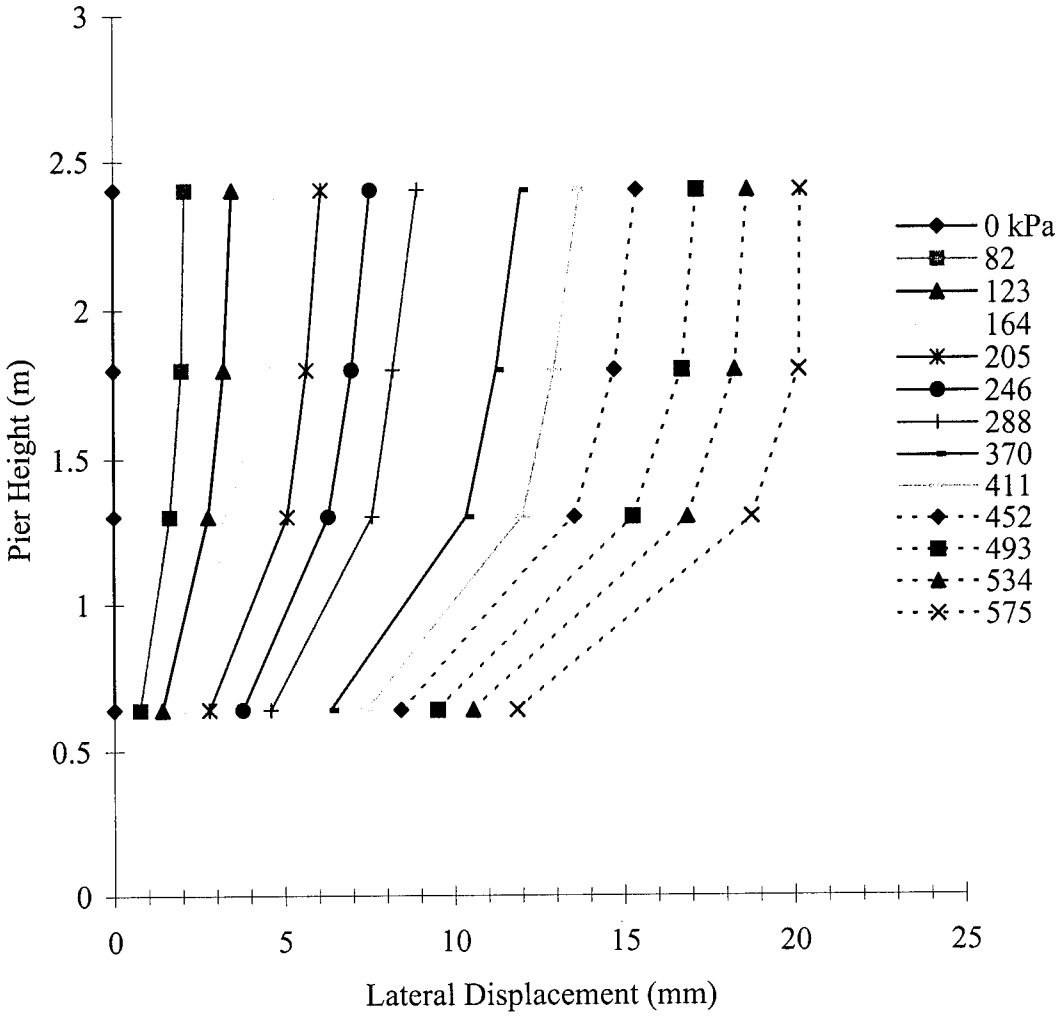

Figure 2.6 Lateral Displacement; 3-m Prestrain

cracked blocks are addressed later.

2.4.3 Load Test at Full Height -- July 3, 1996

The intent of this test was to initially load the pier to twice the allowable load recommended for reinforced soil bridge abutments, 200kPa (2.1tsf) and to further evaluate the concept of pre-straining.

To evaluate the concept of pre-straining, the experiment was conducted in three parts: 1) the pier was incrementally loaded to 415kPa (4.3tsf), then held for 100 minutes; 2) load was then ramped up to 900kPa (9.4tsf), and held for 150 minutes and released; and 3) the pier was then reloaded to 415kPa (4.3tsf), and held for 100 minutes. Parts 1 and 3 were compared to evaluate the benefits of pre-straining the reinforced soil mass.

a. Vertical Settlement

Figure 2.7 shows the load settlement curves for the full height load tests (July 3 and 26). It can be seen that the RS response is slightly stiffer after each load cycle.

At the initial pressure of 415kPa (4.3tsf), the pier settled about 25mm then consolidated 70 mm at 900kPa (9.4tsf). The stress-strain response is very linear until about 700kPa (7.3tsf). Settlement begins to accelerate after 800kPa (8.4tsf), because the whole pier is contributing to settlement. Up to 600kPa (6.3tsf), most of the settlement came from the top 2.5m of pier because the bottom 3.0m had been pre-loaded during the first pre-straining at 600kPa (6.3tsf).

During the 415kPa (4.3tsf) reload cycle, settlement was 12mm. The settlement at 200kPa (2.1tsf) for the initial and reload cycles was 15mm and 8mm, respectively. This indicates that the settlement within this reinforced soil mass was reduced by a factor of 2 because of pre-straining.

b. Lateral Deformation

During the first cycle, lateral deformation measurements from seven LVDT's are shown in Figure 2.8. At 200kPa (2.1tsf) the pier deformed laterally less than 3mm. At 415kPa (4.3tsf), the pier deformed

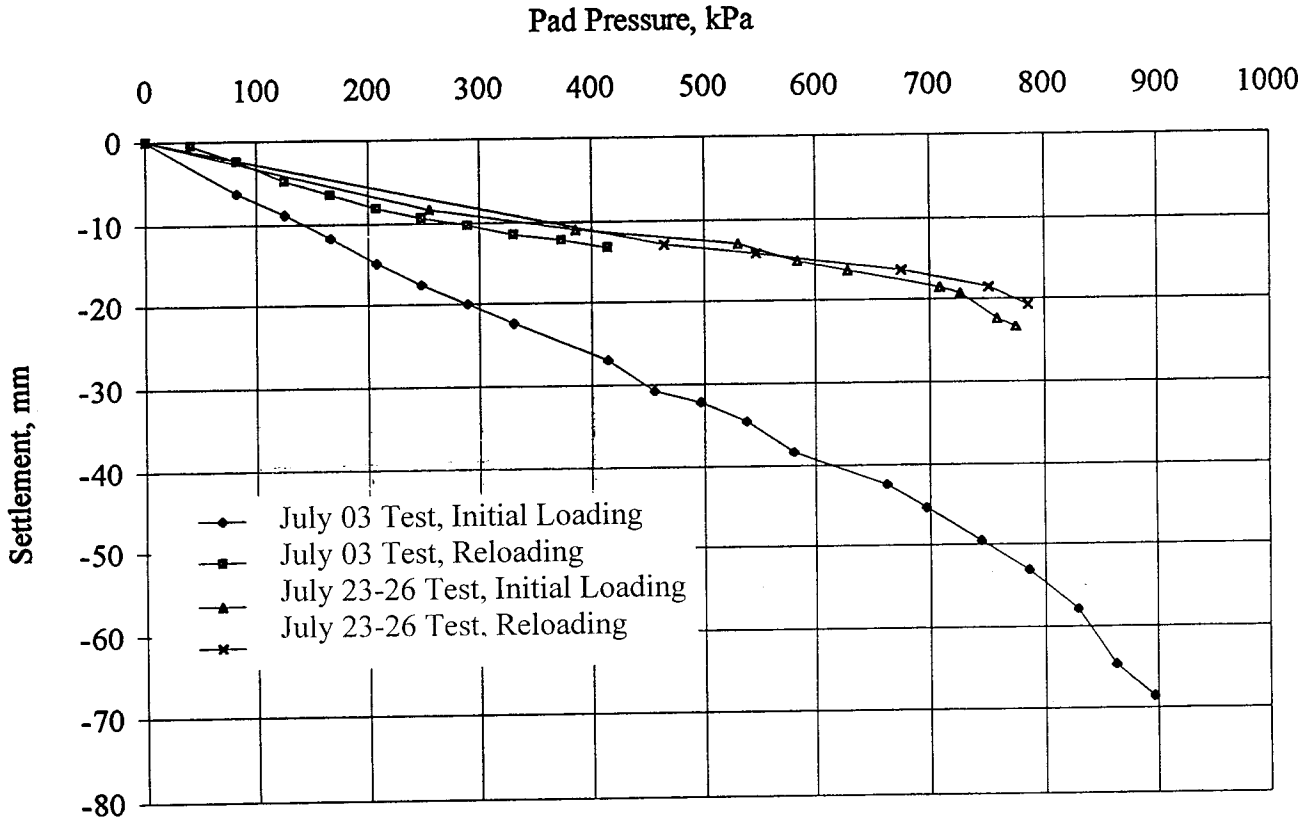

Figure 2.7 Load Settlement Curves

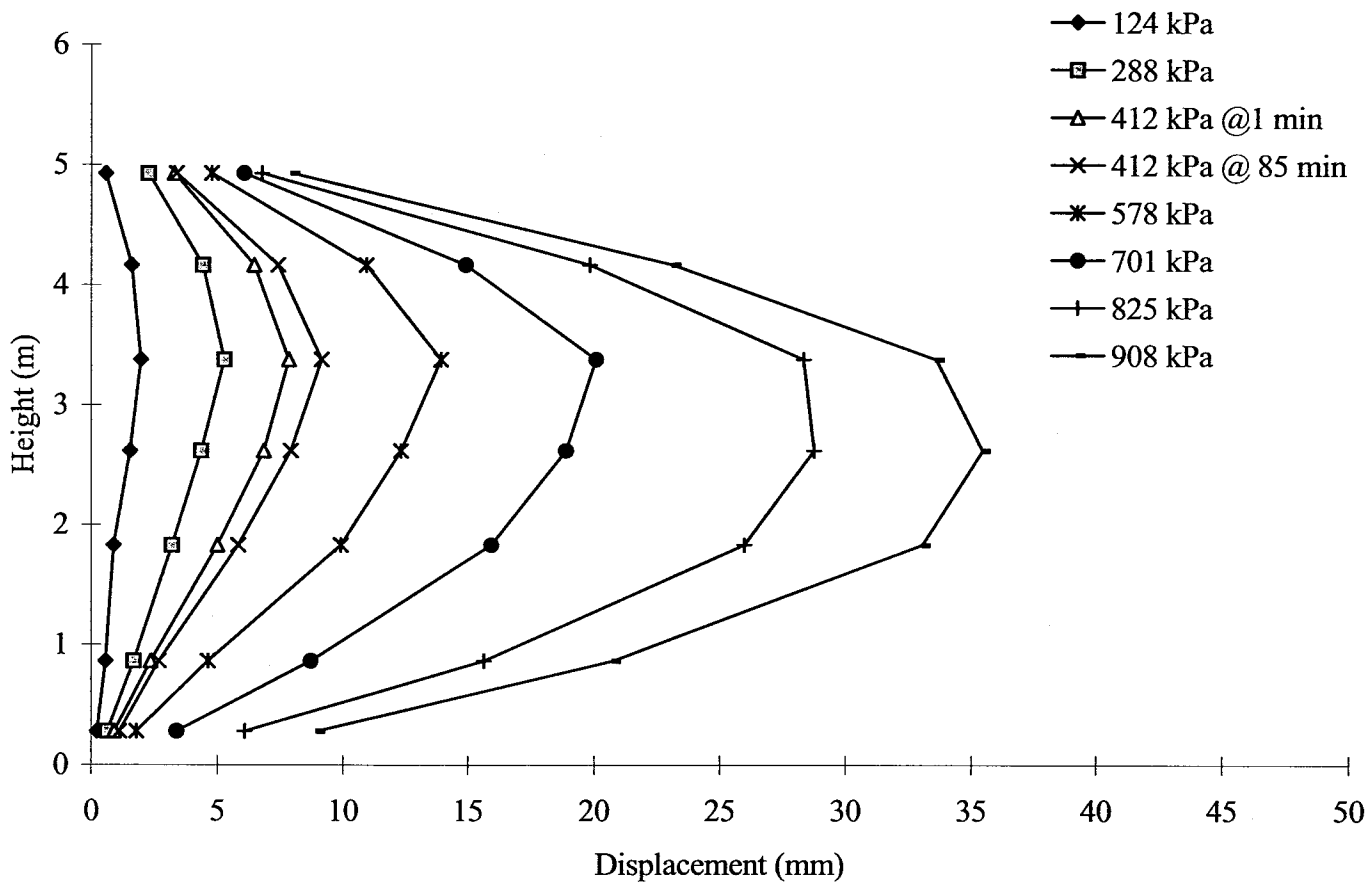

Figure 2.8 Lateral Displacement North Wall

9mm laterally in the middle, which is about 0.5% of the width of the pier at mid-height. In other words, deformation was unrecognizable except for a few cracked facing blocks.

Because the pier was pre-strained at 3.0 meters, the lateral deformation in the middle of the pier was not symmetrical. The bottom half of the pier deformed slowly until the load exceeded the 3.0m pre-strain load of 600kPa (6.3tsf), where deformation was more symmetrical about the middle.

A laser displacement measurement device was also used to record lateral deformation during the initial July 3 load cycle. Figure 2.9 shows a detailed contour map of a face (long wall) for the 825kPa (8.6tsf) load increment. A bulge is clearly developed in the center area of the face. To limit creep deformation and to inhibit the development of the bulge (lateral deformation) in the center area, it is proposed to include in the design a supplemental external confinement system as shown in Figure 2.10.

Placement of the confinement straps can be achieved by laying horizontal rods across the reinforced soil mass during construction. After construction is completed, the external straps can be easily bolted to the rods. The use of external confinement straps would probably require two stage construction to integrate the straps into the facing system.

c. *Reinforcement Strain*

The measured strain along each fabric layer was uniform which means the load was applied evenly over the entire area of the pier.

The bar charts, Figures 2.11 and 2.12, show the magnitude of strain in the length and width directions. Of the four layers of instrumented fabric that were placed in the top half of the pier, layer 1 was on the bottom and layer 4 was on the top. At 900kPa (9.4tsf), the maximum strain is recorded on the bottom layers of fabric, near the middle of the pier. In the width direction, the maximum strain is 2.3% in layers 1 and 2. In the length direction, the maximum strain is recorded in

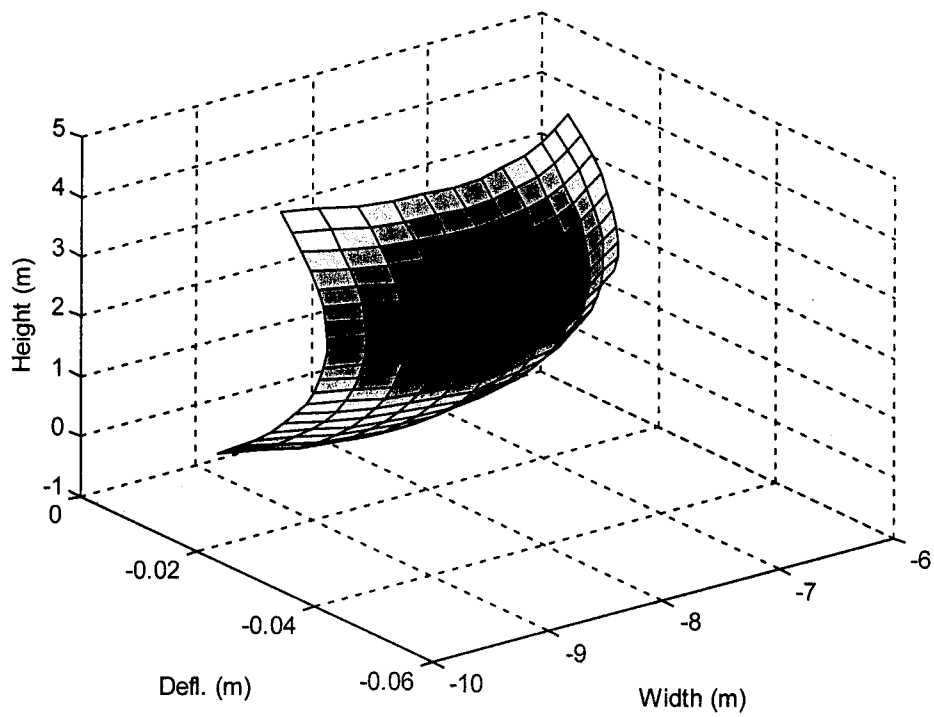

Figure 2.9 Lateral Displacement North Wall; Laser Measurements at 825 kPa (8.6 tsf)

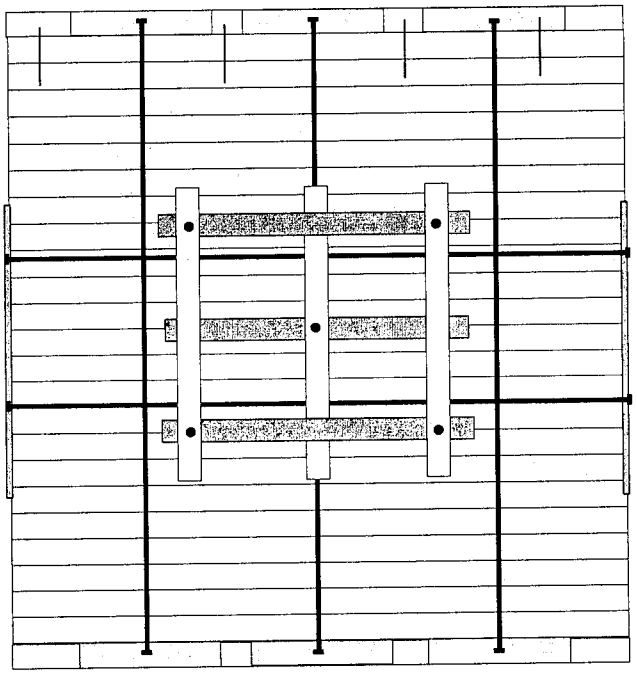

Figure 2.10 GRS Pier Constructed With External Confinement Straps

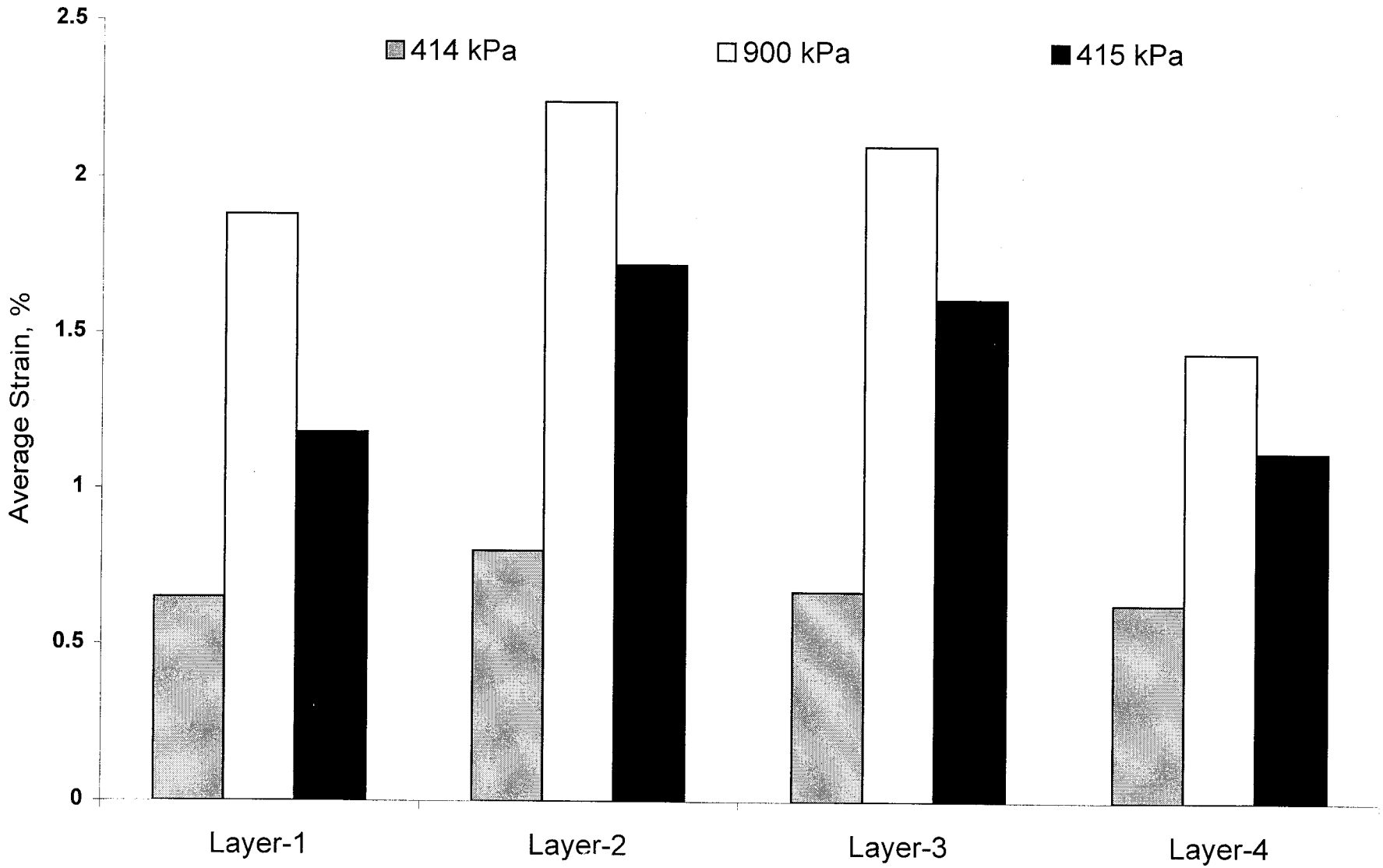

Figure 2.11 Strain Distribution, July 3, 1996 (Length Direction)

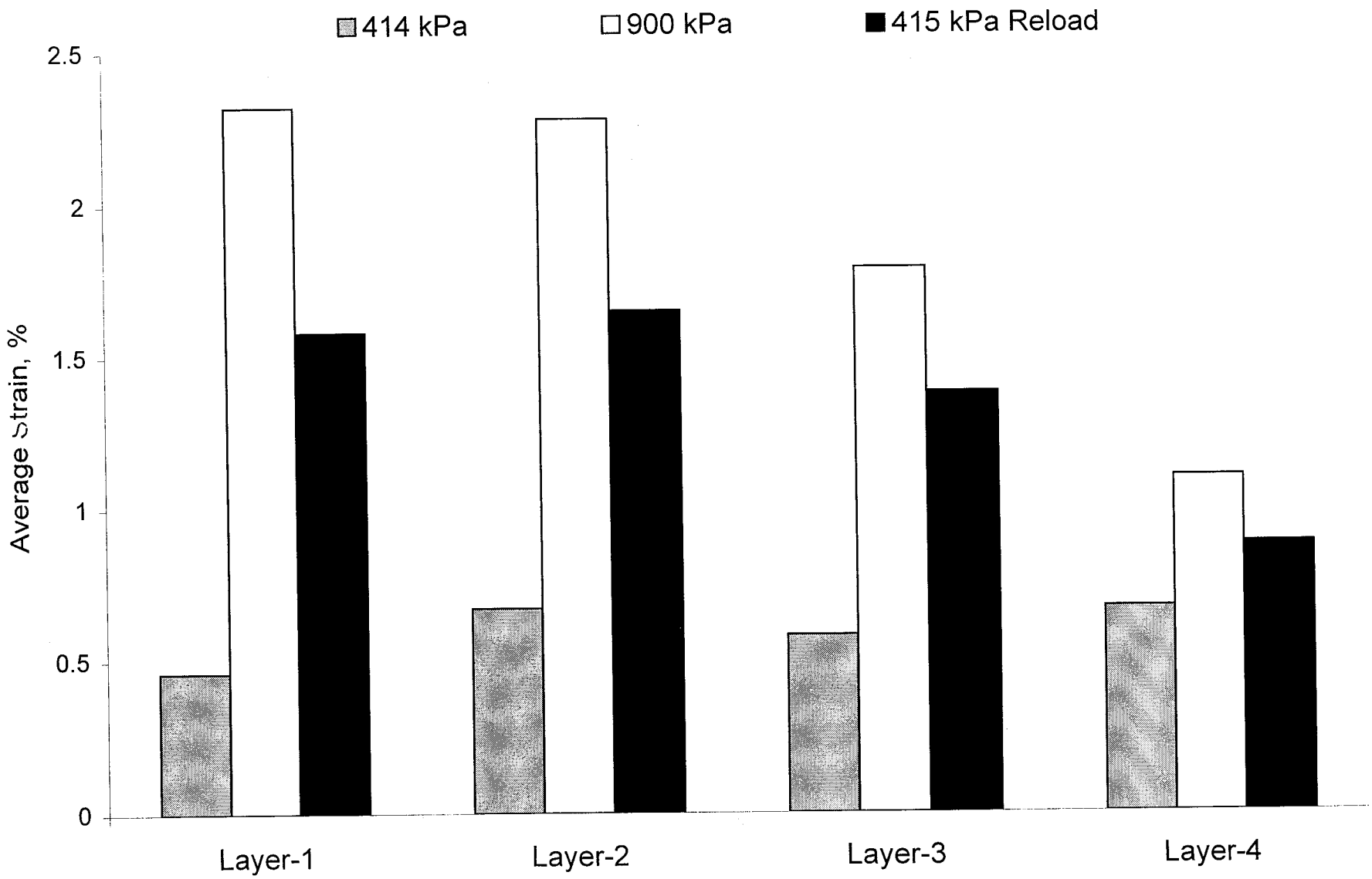

Figure 2.12 Strain Distribution, July 3, 1996 (Width Direction)

fabric layers 2 and 3. During the first load cycle, the strain at 400kPa (4.2tsf) was about 0.5%.

The difference in the strain between the initial 415kPa (4.3tsf) load and 415kPa (4.3tsf) reload gives an indication of the degree of confinement stress locked into the RS mass. During the reload cycle, the creep strain results show that the stress locked in the RS mass relaxed a little.

The 415kPa (4.3tsf) load and reload had different stress paths. In both cases, the soil and reinforcement will continue to transform until equilibrium is established. The duration of the 100- minute load cycle was insufficient to determine the final strain in the fabric.

The fabric reinforcement strain for the instrumented layers in the width direction is shown in Figure 2.13. The strain at 200kPa (2.1tsf) is only 0.25% and about 0.5% at 415kPa (4.3tsf).

Table 2.2 shows the creep rate for the July 3, 1996 load test. During the initial 415kPa (4.3tsf) load and reload 100-minute cycle, a strain increase of 0.02% to 0.04% and decrease of -0.01% to 0.02% was observed. During the initial load cycle, the fabric and soil moved out together; the fabric reinforcement strain increased and soil continued to displace laterally. During the 415kPa (4.3tsf) reload cycle, the fabric and soil moved in opposite directions. The fabric retracted and the soil displaced laterally outward. Figure 2.14 compares the lateral displacement calculated from the strain gauge to the measured displacement calculated from the LVDT's. The data agree well in the lower layers of fabric, but does not agree well in the upper layers.

An explanation for the discrepancy between the strain gauges and the LVDT's in Figure 2.14 is that the LVDT's measure lateral deformation but not vertical deformation. The soil and the fabric respond together. The principal direction of soil movement near the top and bottom of the pier is vertical compression. The upper and lower layers of fabric move with the fill and are strained downward into a bowl shape. The

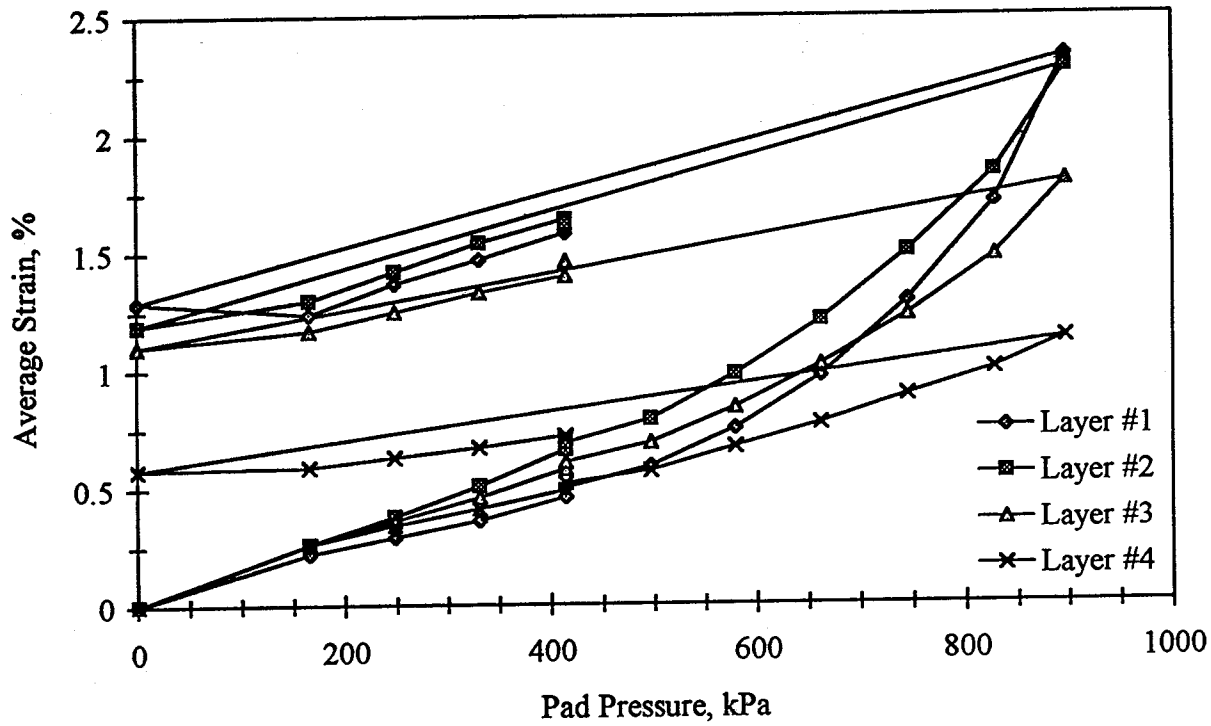

Figure 2.13 Pad Pressure vs. Average Strain (Width Direction)

Test Date	Pad Pressure kPa (tsf)	Elapsed Time (min)	Creep Strain (%)
July 03, 1996	415 (4.3)	100	0.02 - 0.04
	415(4.3) Reloading	100	decreased 0.01 - 0.02
July 23-26, 1996	785 (8.2)	140	0.02 - 0.2
	670 (7.0)	1050	decreased 0.05 - 0.17
	890 (9.3)	152	0.05 - 0.12

Table 2.2 Summary of Creep Strains in Instrumented Reinforcement Layers

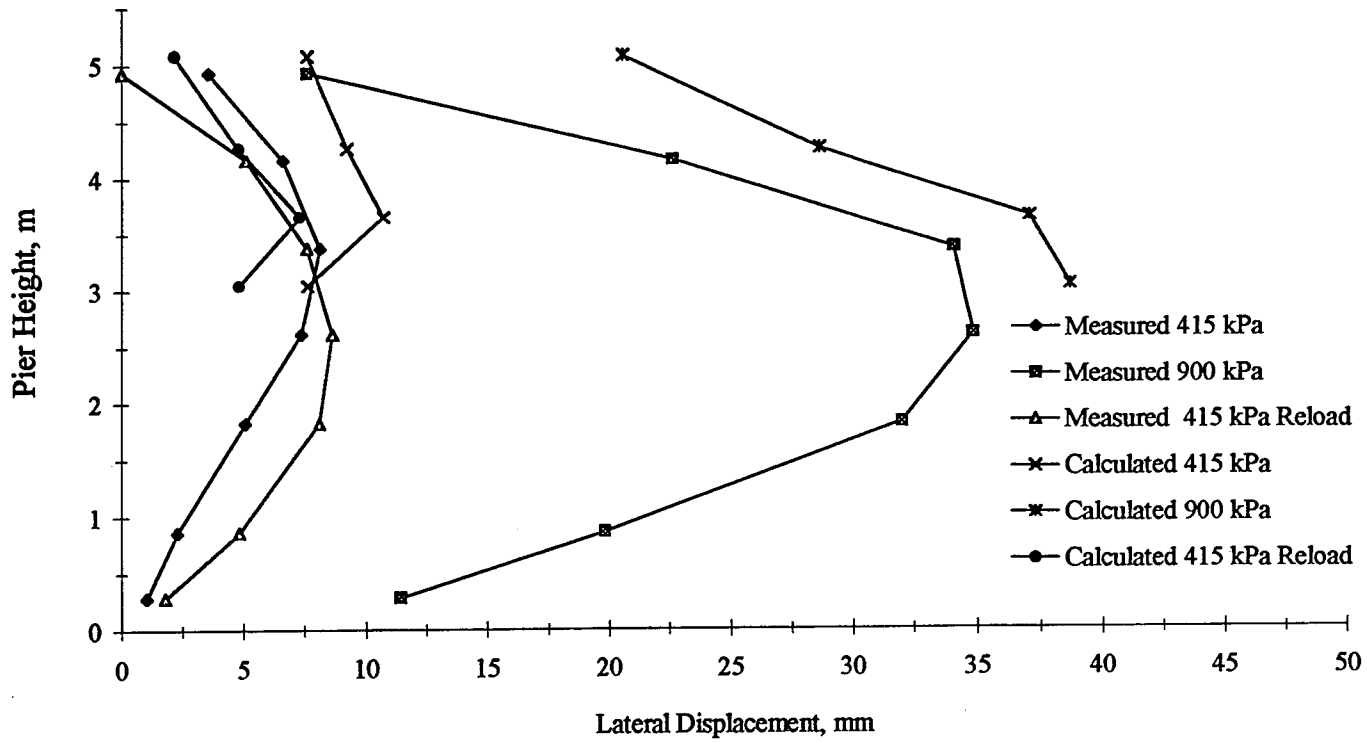

Figure 2.14 Lateral Displacement; Calculated (SG) vs. Measured (LVDT)

fabric reinforcement strain is not laterally outward, as is the case in the middle of the pier, where the displacement agree well because both the fabric and soil are moving in the same direction that the LVDT's are measuring.

2.4.4 Load Test at Full Height -- July 23, 1996

The intent of the July 23 load test was to evaluate creep at a higher load than the July 3 experiment. Figure 2.15 shows the load history for the July 23 experiment. Initially, load was stepped up, then stepped down a little for numerous cycles until it was gradually increased in this manner to 785kPa (8.2tsf) and held for 140 minutes; then load was decreased to 670kPa (7.0tsf) for 1,050 minutes (18 hours) and then increased to 890kPa (9.3tsf) for 152 minutes.

a. *Vertical Settlement*

Figure 2.7 shows the load-settlement curves for the July 23 load test. The pier's response to load was similar to the July 3 reload test. As expected, each reload cycle showed a slightly stiffer response to load. When load was held constant for 1050 min at 670kPa(7.0tsf) (see Figure 2.15), settlement was insignificant until the end of the 670kPa (7.0tsf) increment (see Figures 2.16 and 2.17).

b. *Lateral Deformation*

Figures 2.18 and 2.19 show lateral displacement from three manual gauges along one of the long walls. Figure 2.18 shows lateral displacement up to and during the 780kPa (8.2tsf) pre-strain, before the 670kPa (7.0tsf) load hold. Very little deformation occurred until the 780kPa (8.2tsf) pre-strain load hold. During the 780kPa (8.2tsf) load cycle, their was considerable creep within the RS mass and disfigurement to the facing blocks. Many of the blocks split and separated apart.

Figure 2.19 shows the results of the second part of the July 23 load test, because of the 780kPa (8.2tsf) pre-strain very little insignificant lateral deformation occurred during the 670kPa (7.0tsf) 17.5 hour load cycle. Creep was reinitiated when the load was increased to 870kPa

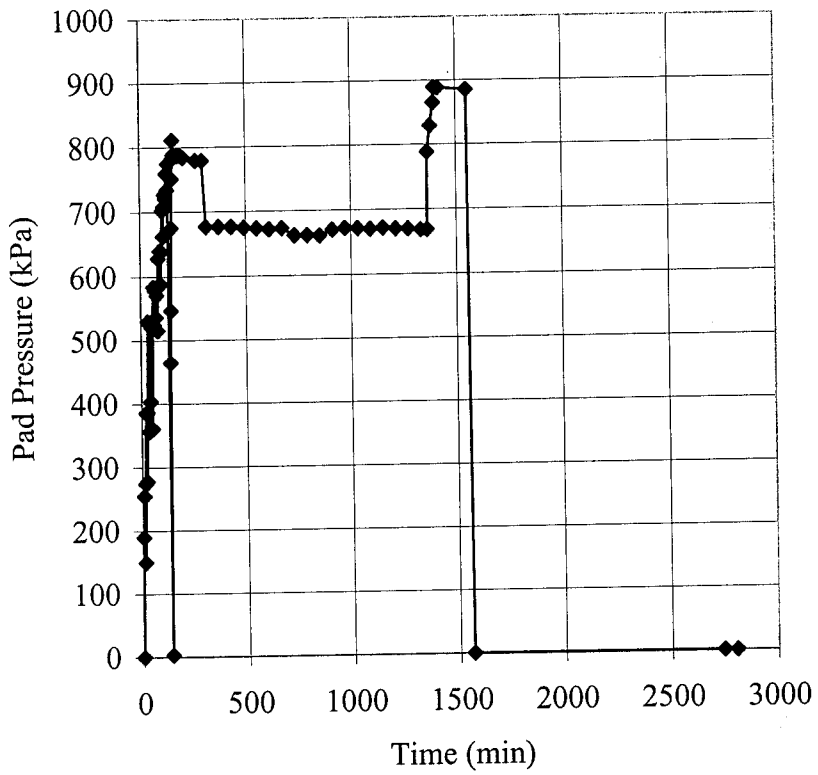

Figure 2.15 July 23-26, 1996; GRS Pier Load Test History

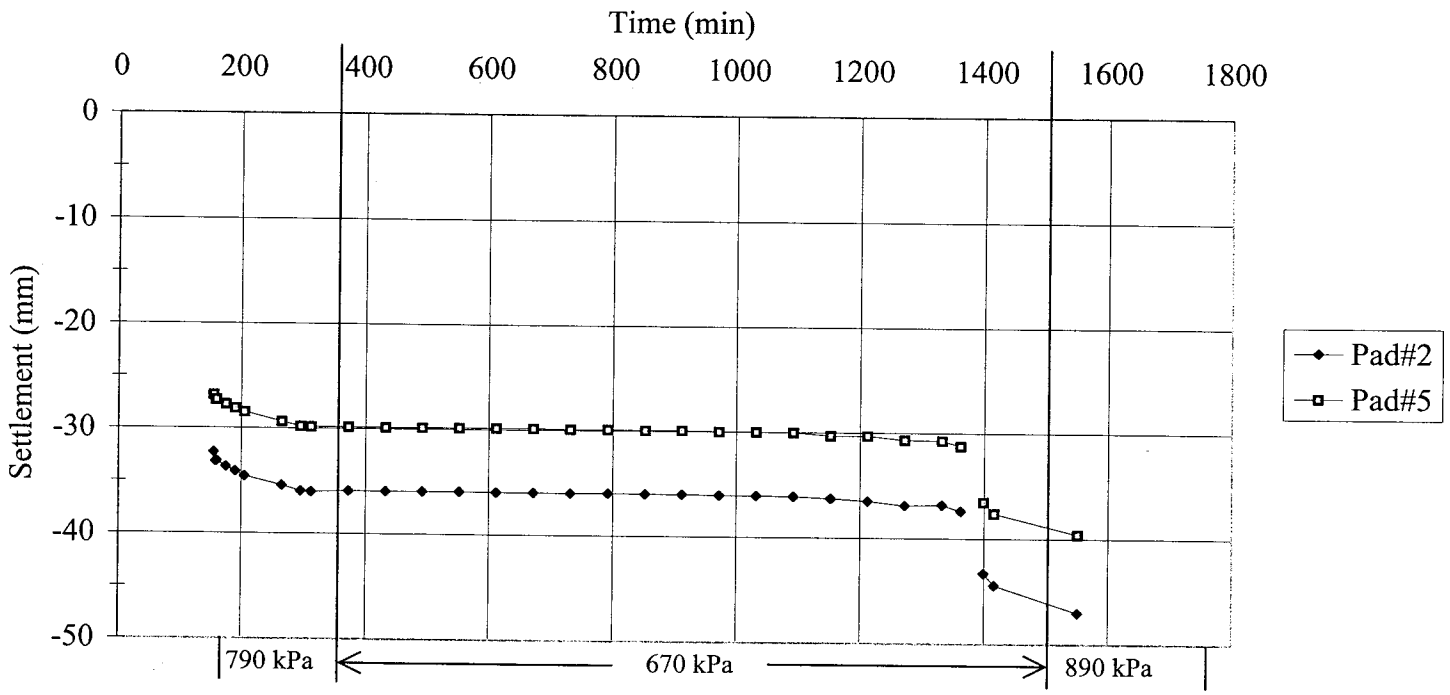

Figure 2.16 Settlement vs. Time

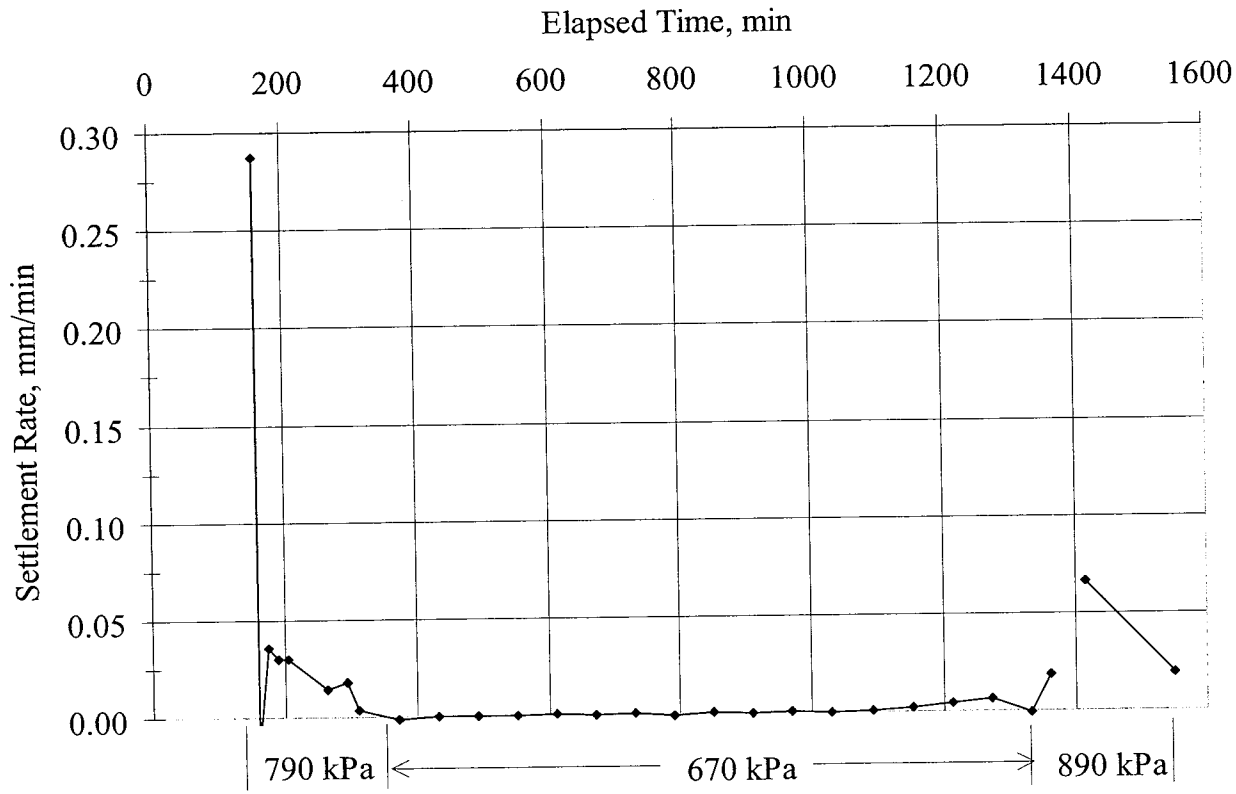

Figure 2.17 Settlement Rate vs. Time (Sustained Loads of 790 kPa/8.3 tsf, 670 kPa/7.0 tsf, and 890 kPa/ 9.3 tsf)

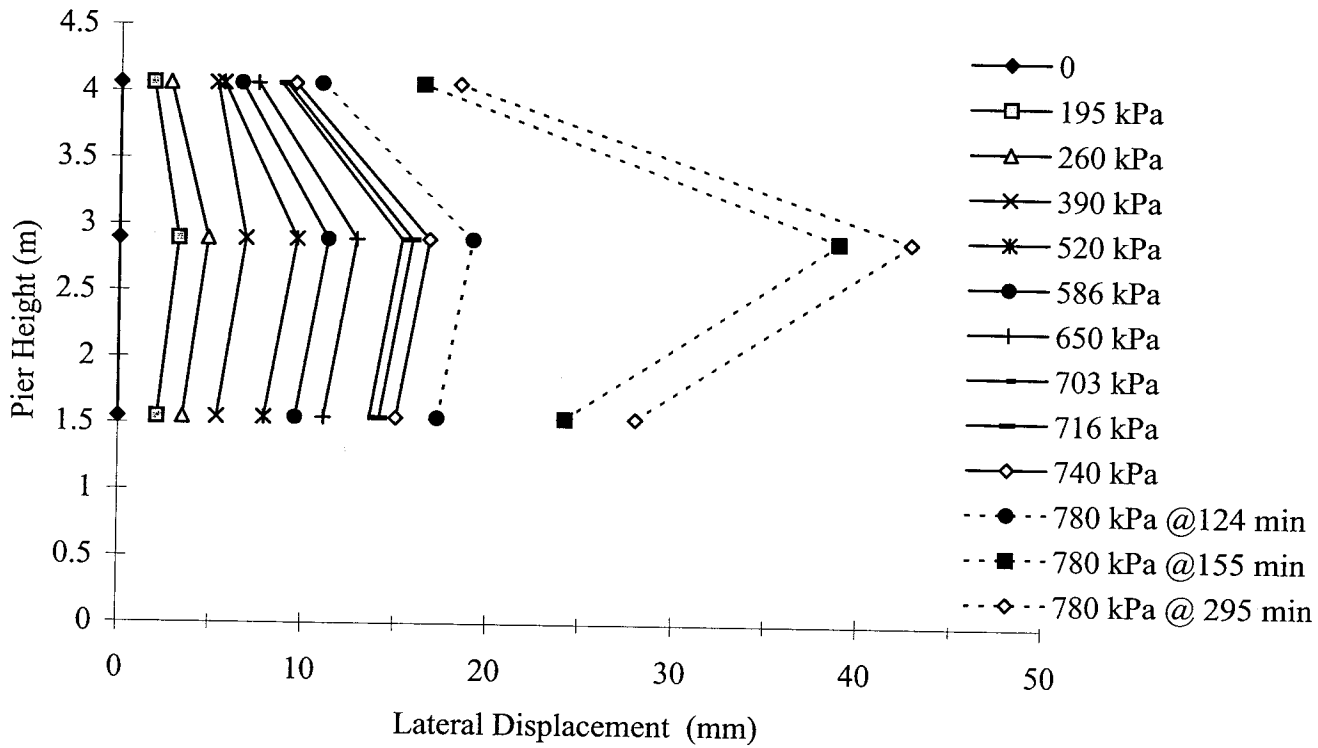

Figure 2.18 Lateral Displacement (0-780 kPa/8.2 tsf), 1st Half: July 23, 1996

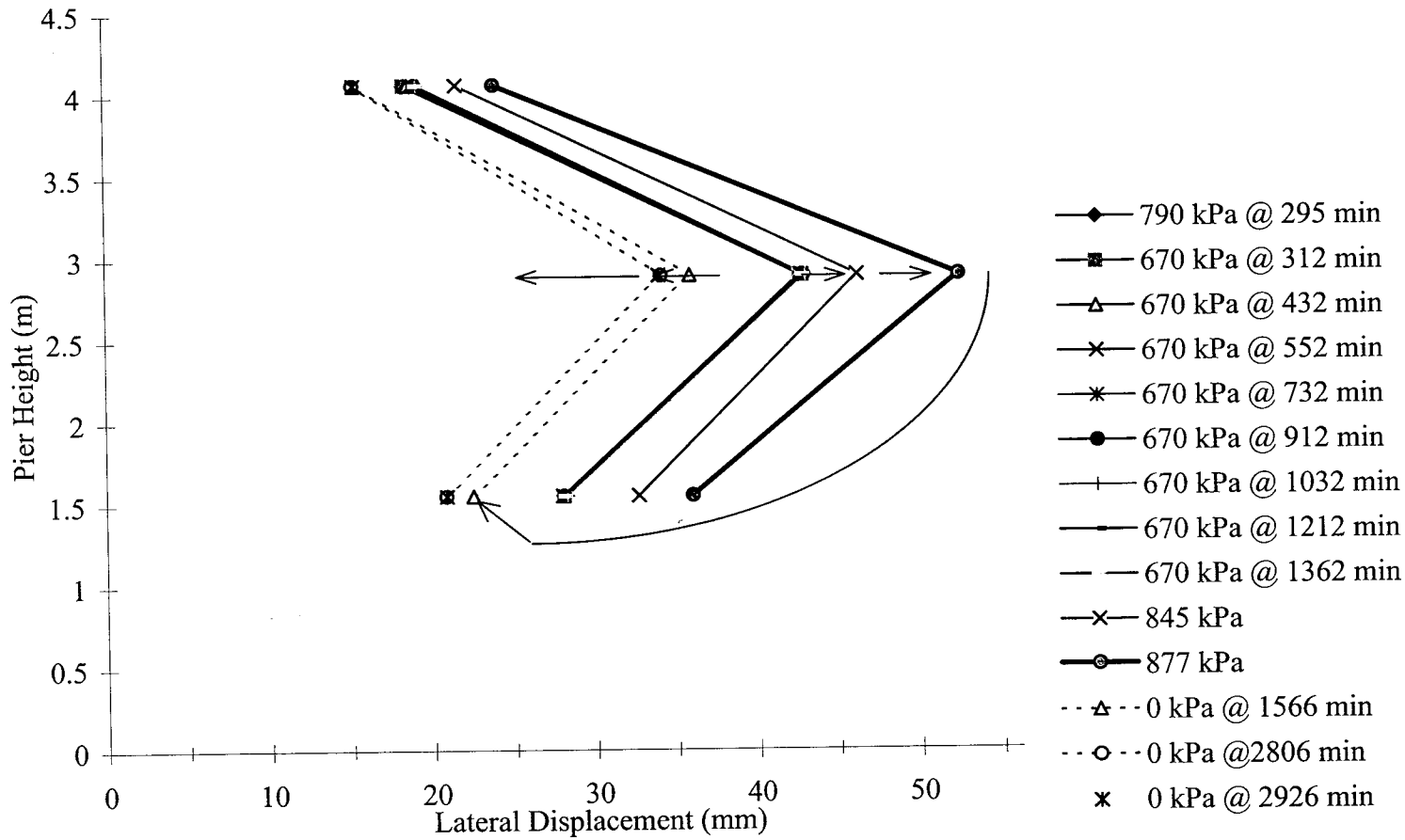

Figure 2.19 Lateral Displacement (670 kPa/7.0 tsf Load Hold and Unload Cycles), 2nd Half: July 23, 1996

(9.1tsf). Figure 2.19 also shows considerable elastic rebound, about 50 %, after the load was released, the walls continued to retract several millimeters, for about one day after the load test was terminated.

Pre-straining did not reduce the lateral deformation. Lateral deformation during the July 23 test was about 50mm more than what was recorded during the July 3 load test, 35 mm. More deformation occurred during the July 23 test because the RS was permitted to creep longer (the July 23 test had a longer time duration). Lateral deformation and creep limit the allowable load of this RS system.

Figure 2.20 shows lateral deformation vs. pad pressure curves for two potentiometers at 2.7m and 4.1m from the base of the pier. A slight increase in lateral creep is recorded during the 670kPa (7.0tsf) load hold.

c. Reinforcement Strain

Results for fabric reinforcement strain in the July 23 test show less strain than the July 3 test, but had a similar trend (see Figures 2.21 and 2.22). Fabric reinforcement strain was greatest in lower layers (middle of pier). Insufficient number of gauges in Layer #1 were active to obtain a reliable average value and therefore Layer #1 was eliminated from Figure 2.21.

For the July 23 test, it is difficult to determine the total strain in the fabric because strain was already locked into the fabric from the July 3 test. Strain reduction between these two tests is not known. Nevertheless, there was a maximum 1.8% strain increase recorded during the July 23 test.

2.4.5 General Observations from the Load Tests

a. Reinforcement Strain

The experiments were set up so that the total strain recorded on a particular direction would not exceed 4%, even though this particular fabric ruptures at 18% strain, because creep accelerates at around 5%. Total strain recorded in the fabric was assumed to be equal the sum of the

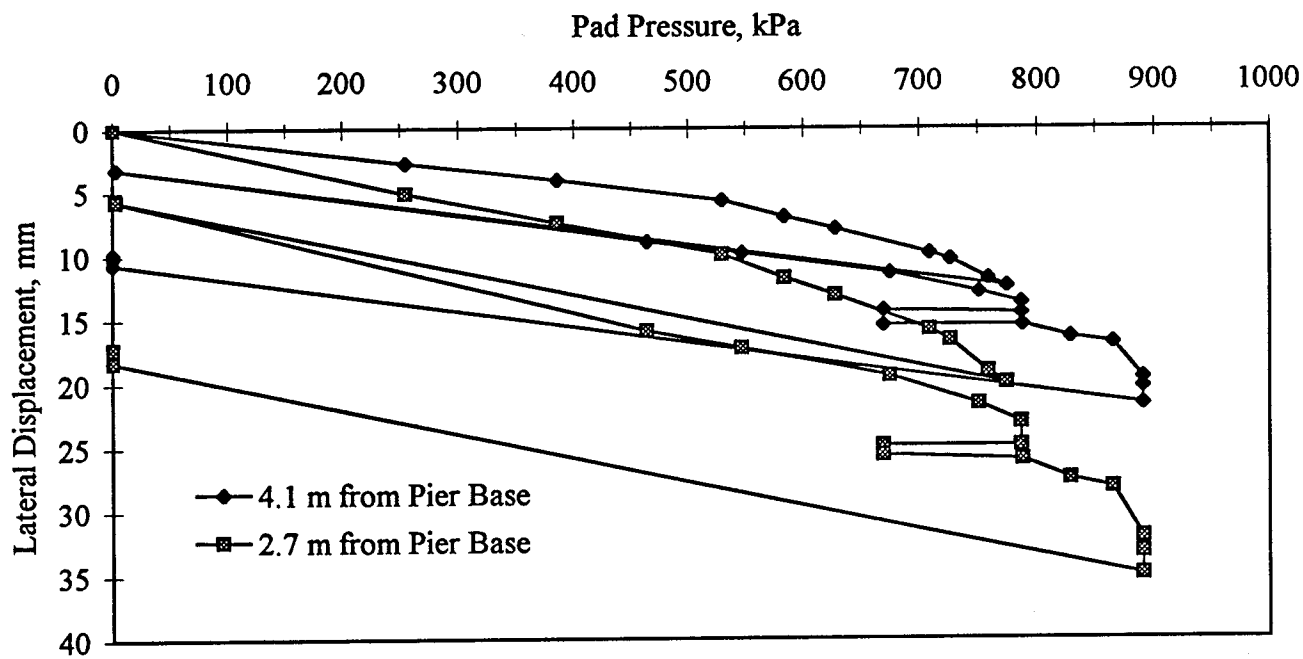

Figure 2.20 Lateral Displacement in the Length Direction (Potentiometer)

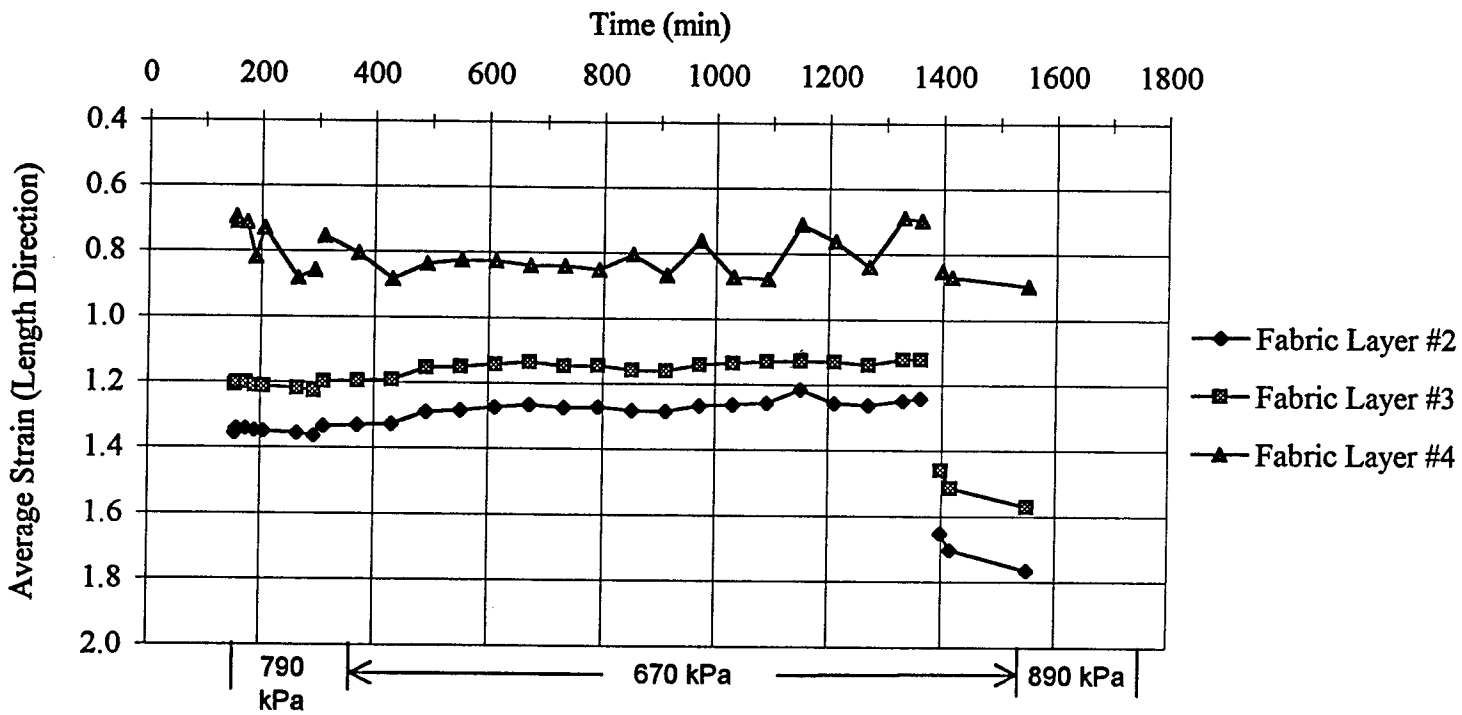

Figure 2.21 Fabric Strains

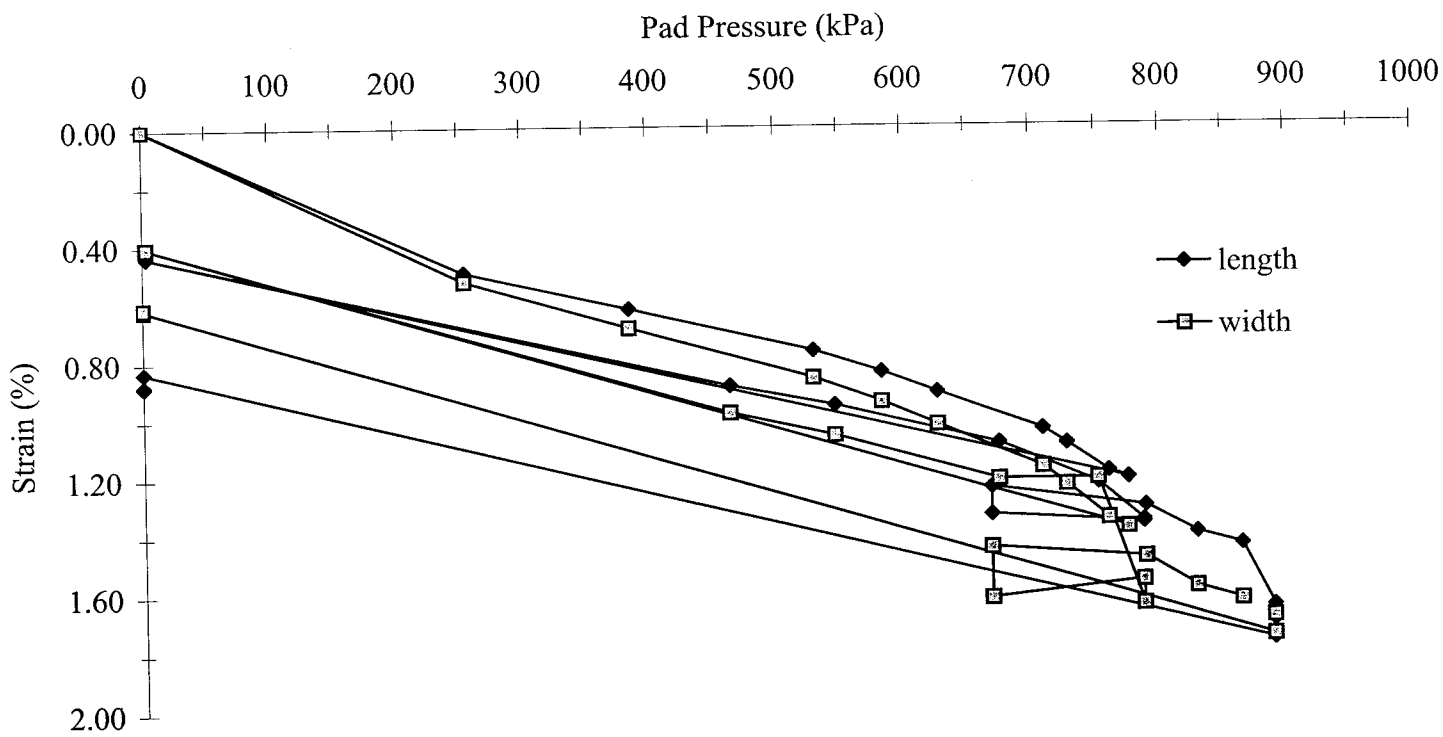

Figure 2.22 Strain - Fabric Layer #2

July 3 and July 23 tests. At 4% fabric reinforcement strain, which was the set limit for deformation, the pier would still maintain a uniform shape. Lateral deformation correlates well with the strain in the middle, where maximum lateral displacement occurs.

At the 1100-minute mark, 670kPa (7.0tsf) load hold on July 23, an unexpected event occurred in the RS mass causing a release in fabric reinforcement strain and an increase in settlement rate. Also, during this load hold, a reduction in strain (between 0.05 to 0.17% in both the width and length directions) was recorded in the instrumented layers (see Figure 2.21). It is believed that the wavy pattern of strain reduction in Layer 4 is somehow related to creep reduction in the fabric and lateral deformation of the soil. Clearly, during the 670kPa (7.0tsf) load hold, there was a reduction in fabric reinforcement strain (see Figures 2.21 and 2.22) while an increase in lateral displacement was recorded (see Figure 2.20).

The creep reduction process is very slow and steady, and is believed to occur as follows. Under high pressures >415kPa (4.3tsf), some zones within the RS mass de-bond or slip from the fabric. Fabric reinforcement strain is reduced. The load is again transferred to the fabric, strain is increased a little, then slips a little again.

A summary of the creep strains for both full height load tests can be obtained from Table 2.2.

b. *Facing Blocks*

The facing system performed as anticipated. The connection of the blocks to the RS was excellent. A superficial problem of cracks in the facing system became notable at pressures greater than 275kPa (2.9tsf). Two types of cracks developed in the blocks, bending and tension cracks (see Figure 2.23):

(i) Bending Cracks

The intent of the experiment was to demonstrate the connection strength of a 0.2m thick block, therefore, cinder blocks were used instead of the standard, 0.3m segmental wall block. The bending cracks were

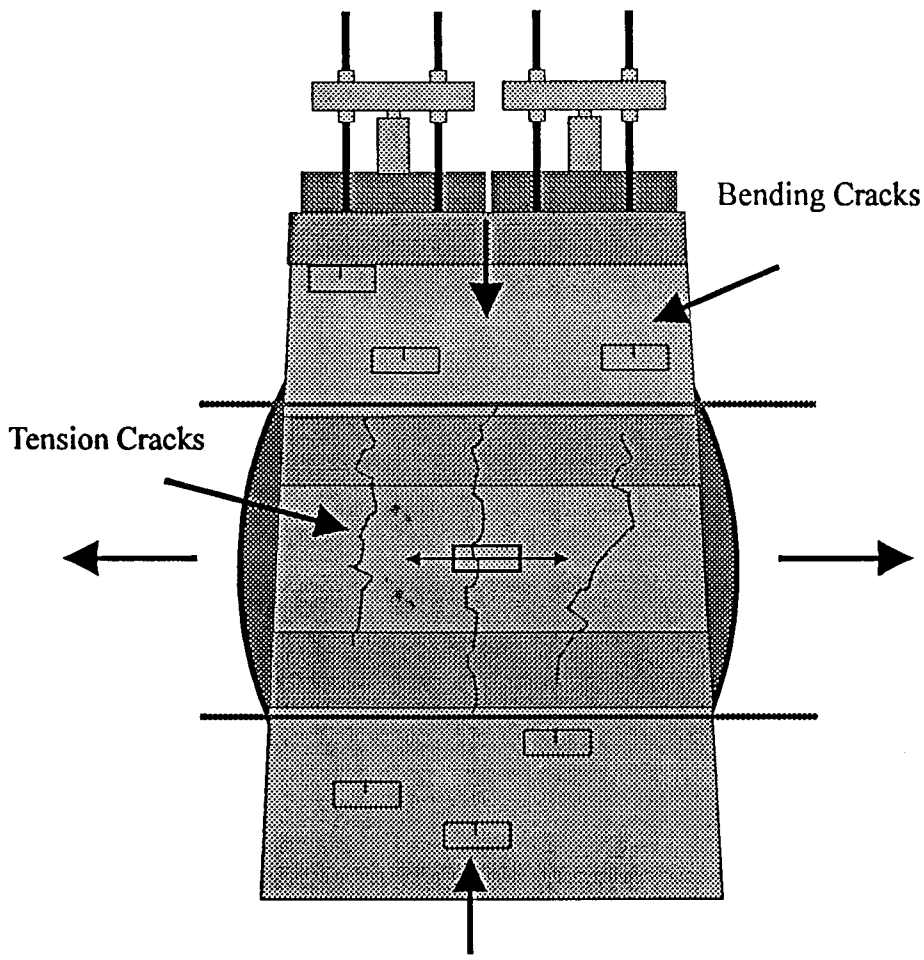

Figure 2.23 Cracks in the Facade

caused by variations in the height of the cinder blocks used, and occurred predominantly along the top and bottom thirds of the pier. Vertical loads were transferred to the blocks by drag forces from the fabric and the soil.

The frequency of bending cracks would have been reduced if a segmental wall block had been used, because the height tolerance specifications are tighter. The height tolerance on the corners of a cinder block must be within 3.0mm of each corner, whereas the height tolerance for a segmental wall block can be 1.6mm. Also, a segmental block wall is designed to be dry stacked, while the cinder block used here was designed to be stacked with mortar between the blocks. A few blocks on the bottom two rows were crushed outward. This is probably due to poor compaction on the bottom two lifts of fill (see Figure 2.4).

(ii) Tension Cracks

The tension cracks formed in the middle area of the pier, and propagated to the top and bottom areas. The expansion of the wall caused the block to split and move apart. As shown from the lateral deformation measurements, the center third of the pier expanded the greatest. Often when a block cracked, the crack would follow the joints between blocks and cause other blocks to crack. The connection strength between the blocks and RS mass was stronger than the tensile strength of the block.

Since the facing block is not considered to be a structural element in this style of GRS construction, the problem of cracked blocks is regarded as minor. Many propose the placement of mortar as a solution to limiting cracks in the blocks. Others advocate a rigid face system for some RS structures. Future experiments will address this topic.

2.5 Findings, Observations and Recommendations

Reinforced soil has been used to support bridge abutments on major highways, and has been shown to be economical. Given the limited funds available to construct and replace old bridges, it is reasonable and justifiable to explore alternative methods of bridge support. The style of GRS construction

used in this experiment performed well and should be considered for use on experimental field projects.

The following are some observations, findings, and general remarks concerning GRS bridge supporting structures:

- FHWA's manual, "Mechanically Stabilized Earth Walls and Reinforced Soil Slopes Design and Construction Guidelines," (October 1996) discusses RS for bridge support applications. The manual recommends that bridge loads on RS not exceed 200kPa (2.1tsf). At 200kPa (2.1tsf), the performance of the pier was very good, strain in the fabric was 0.25%, lateral deformation was 3mm, and no cracks occurred in the facing blocks. For the full height load tests, the vertical settlement was about 15mm on the initial load cycles and about 5mm during the reload cycles.
- Small vertical reinforcement spacing, say 0.2m to 0.3m, generally lead to better compaction of the backfill, which is the key to good performance. Closely spaced reinforcement and quality compacted fill should be considered as a standard method for RS bridge support applications. The additional cost of closely spaced reinforcement is minimal for bridge support applications because the area is much smaller than most RS applications.
- The pre-straining reduced vertical settlement of the pier by approximately 50% and limited the vertical creep deformation. Pre-straining is especially beneficial in reducing differential settlement between bridge supports.
- Pre-straining did not reduce lateral deformation, except near the top of the pier where the lateral movement was partially restrained.
- The pier was loaded uniformly over the entire surface area of the pier, including near the edge. The pier remained stable with very high edge loads. Although it is not recommended that the edge of a reinforced soil mass be used to support girders and economize on the length of the bridge, the study clearly demonstrated that load can be supported very close to the facing without failure.

- Integrating the approach embankment with the abutment and bridge may eliminate the settlement demarcation between the approach and abutment, and provide a smooth transition between the embankment and the bridge deck.
- Modification to the facing design employed in this study is required if the surcharge load or pre-straining is greater than 300kPa. There are many possibilities to improve the performance of the facing system; for example, a two- stage construction approach could be used. Initially, a very low cost block could be used. After pre-straining or the placement of bridge loads, attractive panels could be hung on the face over the low-cost block.
- The face was not fabric wrapped for this demonstration. For permanent applications, it is recommended that the face be wrapped in situations where there is a possibility that facing elements could be severely damaged or removed. A wrapped face will eliminate the possibility of erosion of fill material.
- Moderate traffic loads are not considered to be a problem. Some secondary settlement is expected because of traffic vibrations. Wrapping the face of the fill material at the top adds another layer of reinforcement near the face to inhibit lateral displacement.
- The durability of geosynthetics is not considered to be a problem. Results of a comprehensive FHWA study indicate that geosynthetics do not suffer any serious degradation when properly used. Construction damage of the geosynthetic is not considered to be a factor in a pier application because fill material can only be spread by manual labor.
- This technology is well suited for remote locations, where specialized equipment or concrete is unavailable. The materials used to construct the pier are commonly available. In emergency situations, a GRS pier can be constructed and put into service in only a few days.
- Although the GRS pier may be the optimal choice in many bridge assignments, it is not suited for all bridge building assignments. It should

not be used in scour environments, or when it would not prove economical, or where the assignment is too large, or not within allowable loads.

- The pier design is considered to have seismic protection potential, which requires further research and development.
- At 200kPa (2.1tsf), creep is not considered to be a problem in a closely spaced RS system with a well- compacted granular backfill.

Chapter 3
THE HAVANA YARD PIERS AND ABUTMENT

3.1 Overview

The Havana Yard piers and abutment consisted of two piers and one abutment. These structures were situated in a 3.53-m deep pit as depicted in Figure 3.1. The outer pier and the abutment were 7.6 m tall. The center pier was 7.3 m tall, 0.3 m shorter than the outer pier and the abutment. The pier was made shorter for the purpose of a second-stage load test to be conducted at a later time.

The center pier and the abutment were of a rectangular shape and the outer pier was of an oval shape, as shown in Figure 3.2. The bases of the outer pier, the center pier, and the abutment were 2.4 m by 5.2 m (major and minor axes), 2.7 m by 5.4 m, and 4.6 m by 7.2 m, respectively. The tops of the outer pier, the center pier, and the abutment were, respectively, 1.8 m by 4.6 m (major and minor axes), 2.1 m by 4.8 m, and 3.6 m by 5.2 m. The edge to edge distance between the outer pier and the center pier and between the center pier and the abutment was 2.7 m.

At the bottom of the pit was a geosynthetic-reinforced soil foundation. The reinforced soil foundation comprised three layers of geotextile reinforcement with a constant vertical spacing of 0.3 m. The geotextile reinforcement was the same type as those used in the piers and the abutment.

The piers and the abutment were constructed on a 0.15-m thick concrete pad placed over the reinforced soil foundation (see Figure 3.1). The vertical spacing of the geotextile reinforcement in all three structures was 0.2 m. The reinforcement covered the entire top surface area of backfill and facing blocks at each construction lift. The top four layers of the reinforcement in the abutment employed a wrapped-around procedure behind the facing block. A center geotextile "tail", 1.2 m in length, was placed between each of these four layers to connect the backfill to the facing blocks. Modular blocks, 0.2 m in height, were used as the facing element for all three structures. Compaction of the backfill was conducted at each course of the facing blocks. The facing element was made to

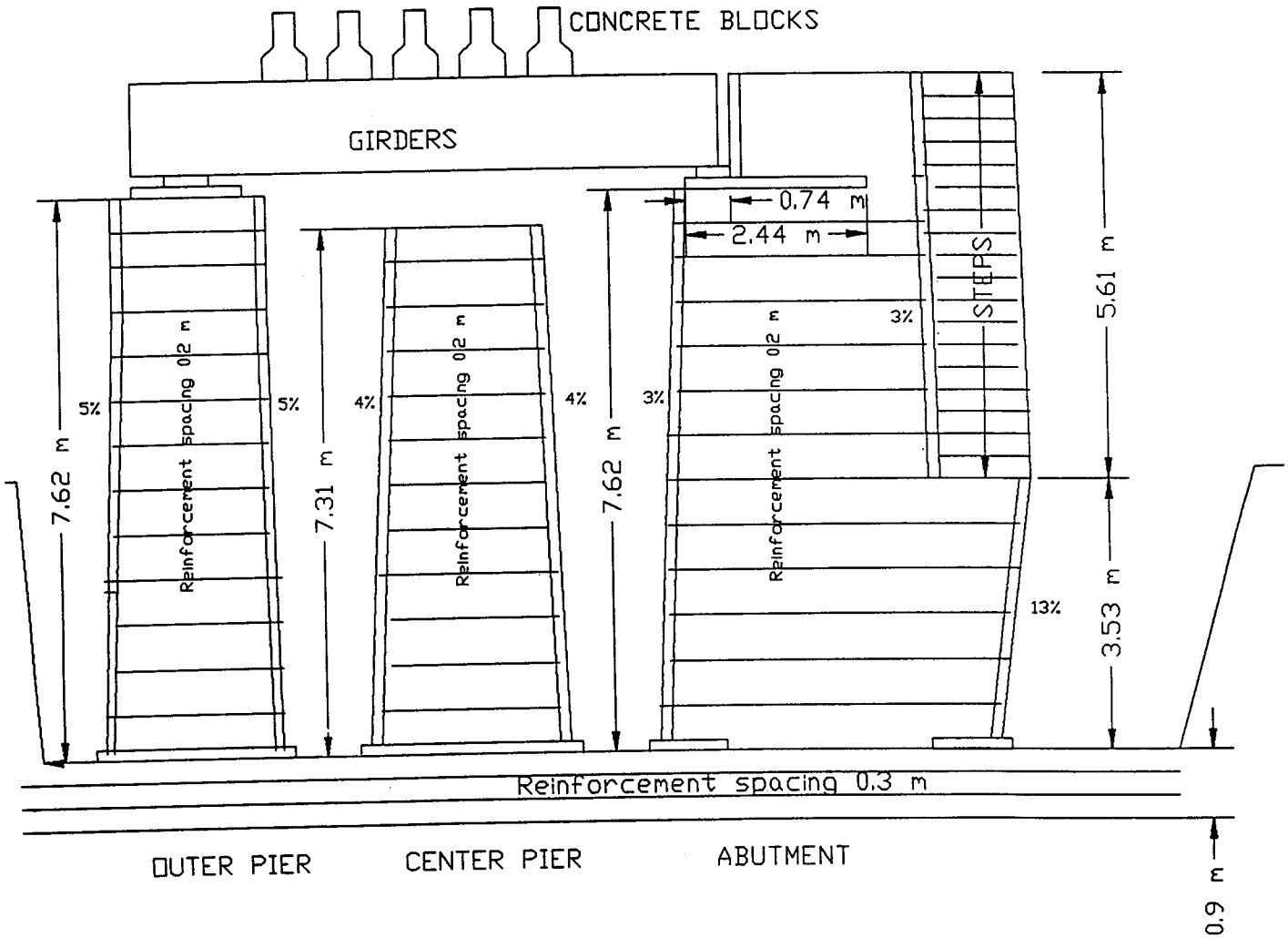

Figure 3.1 Side View of the Structures

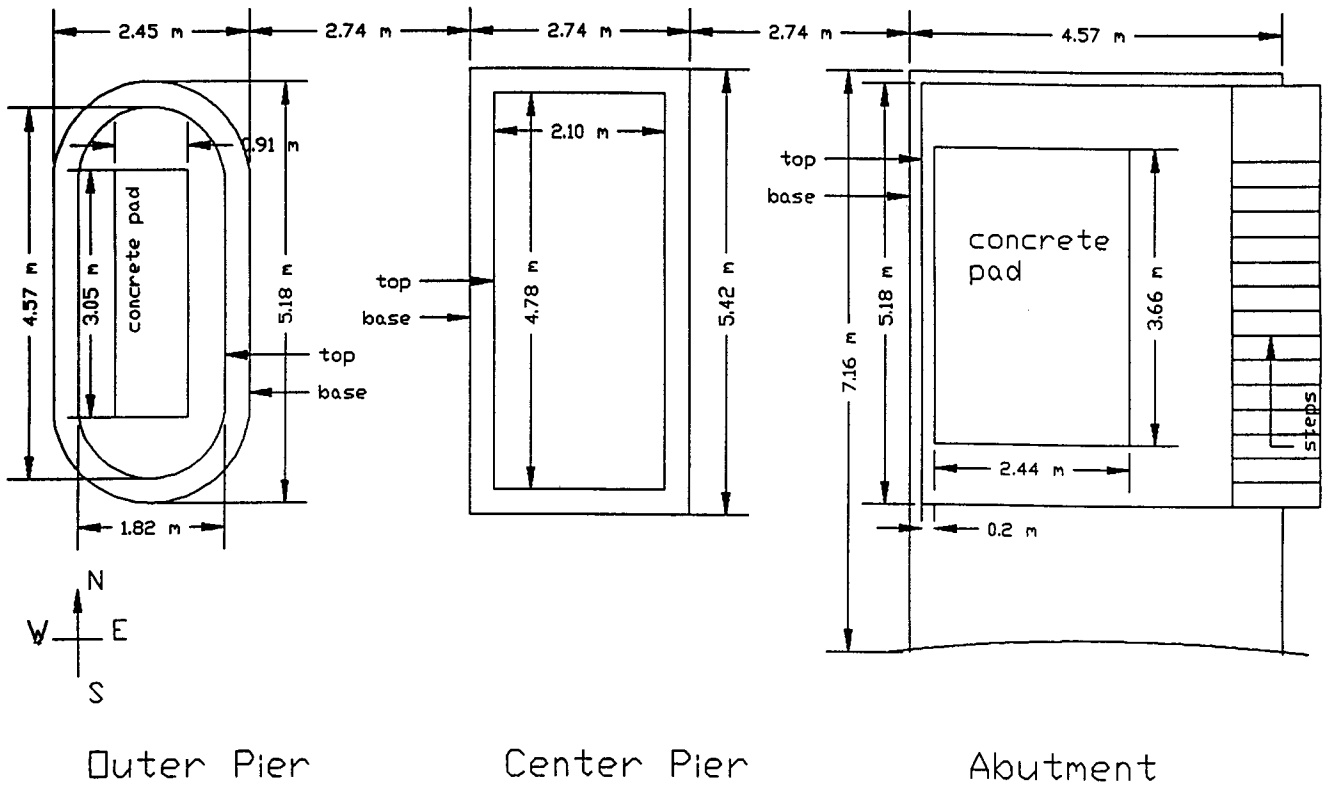

Figure 3.2 Top View of the Structures

incline from the base to the top of approximately 5% in outer pier, 4% in the center pier and 3% in the abutment. On the east face of the abutment, the facing assumed a 13% negative batter up to a height of 3.5 m. From 3.5 m to the top of the abutment were walking steps as shown in Figure 3.1. The negative batter was made to examine the feasibility and stability of such a facing configuration.

On top of the piers and the abutment were 0.3 m-thick concrete pads to support steel bridge girders. The concrete pads were 0.9 m wide and 3.1 m long for the piers and 2.4 m wide and 3.7 m long for the abutment, as shown in Figure 3.2. It is to be noted that the clearance of the concrete pad was only about 0.02 m behind the back face of the abutment facing blocks (see Figure 3.1).

3.2 Construction Material

The backfill and the geotextile reinforcement employed in the construction are described as follows.

3.2.1 Backfill

The backfill was a "road base" material classified as A-1-A(0) according to AASHTO. It has 13% of fine particles (passing sieve #200). The gradation curve is shown in Figure 3.3. The maximum dry density, per AASHTO T180 method D, is 21.2 kN/m^3. The optimum moisture is 6.7 %.

3.2.2 Geotextile Reinforcement

The reinforcement was a woven prolyproplylene geotextile. The geotextile reinforcement was the same as that used in the Turner-Fairbank pier. The wide width tensile strength in both fill and warp directions of the geotextile is kN/m. The tensile strengths at 5% strain of the fill and the warp directions are 38 kN/m and 21 kN/m, respectively. Some index properties of the geotextile reinforcement are shown in Table 3.1.

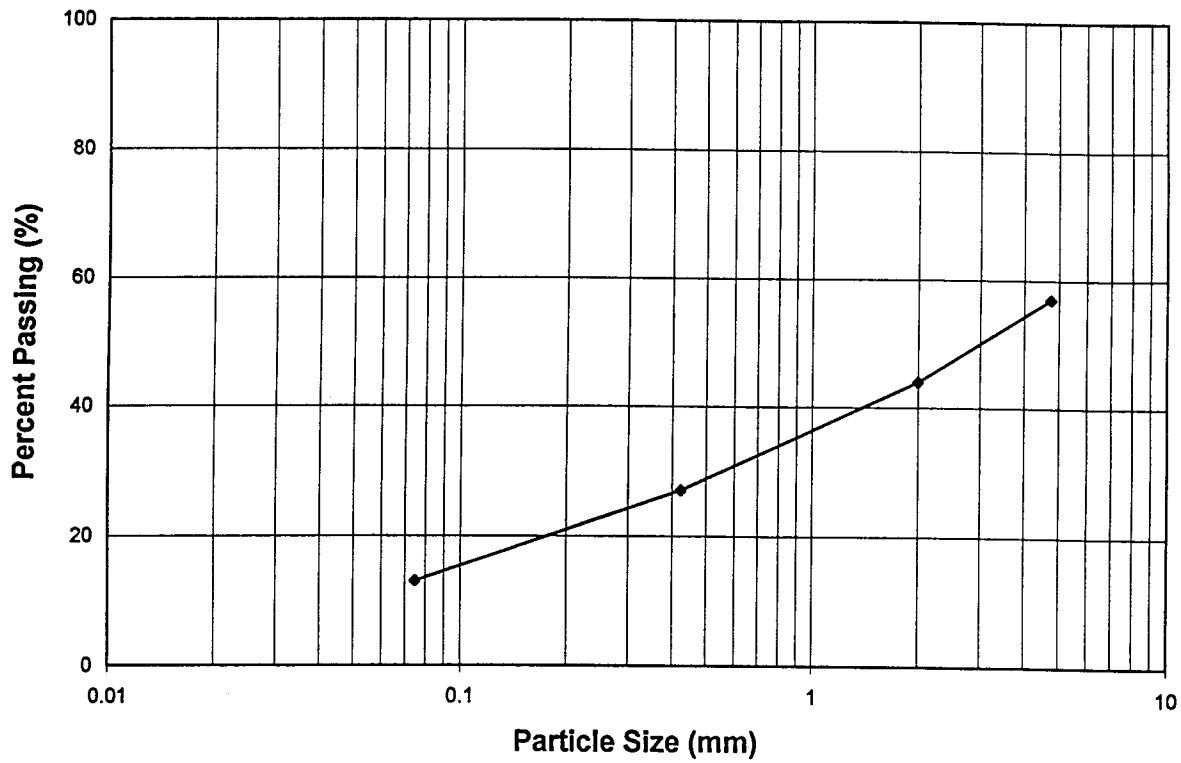

Figure 3.3 Gradation Curve

Polymer Type	Structure	Wide-Width Tensile Strength ASTM D 4595 (kN/m)				Grab Tensile Strength ASTM D4632-86 (kN) (% @ Break)	
		Strength @ 5% Strain		Ultimate Strength (% @ Break)			
		Fill Direction	Warp Direction	Fill Direction	Warp Direction	Fill Direction	Warp Direction
Polypropylene	Woven	38	21	70 (18%)	70 (18%)	2.6 (20%)	2.2 (20%)

Table 3.1 Some Index Properties of the Reinforcement

3.3 Construction of GRS Piers and Abutment

The construction procedure of the GRS piers and abutment is described in the following steps:

1. Excavate a 3.5-m deep test pit;
2. Prepare the geosynthetic-reinforced soil foundation;
3. Pour and level a 0.15-m thick concrete pad on top of the geosynthetic-reinforced soil foundation;
4. Lay a course of facing blocks conforming to the designed shape of the structure;
5. Backfill and compact in 0.2 m lifts;
6. Place a layer of geotextile reinforcement covering the entire top surface area of the compacted fill and the facing blocks;
7. Repeat steps 4, 5 and 6 until completion.

Selected photos taken during construction of the abutment and piers are shown in Plates 3.1 to 3.13.

Field density tests were performed on the center pier and the abutment during construction. The average dry density of the center pier was 19.2 kN/m^3 (91% of the modified Procter relative compaction) with the average moisture of 2.5%. For the abutment, the average dry density was 19.0 kN/m^3 (90% of the modified Procter relative compaction) and the average moisture was 1.6%. The density of the outer pier was believed to be lower than these measured values as a lighter compaction plant was employed.

3.4 Loading Scheme

There are two stages in the load test. The first stage was conducted on the outer pier and the abutment. The second stage was to be conducted on the center pier, but the plan was subsequently abandoned.

3.4.1 The First-Stage Load Test

Three steel bridge girders were placed over the top concrete pads of the outer pier and the abutment. Each girder was supported by steel bearing plates

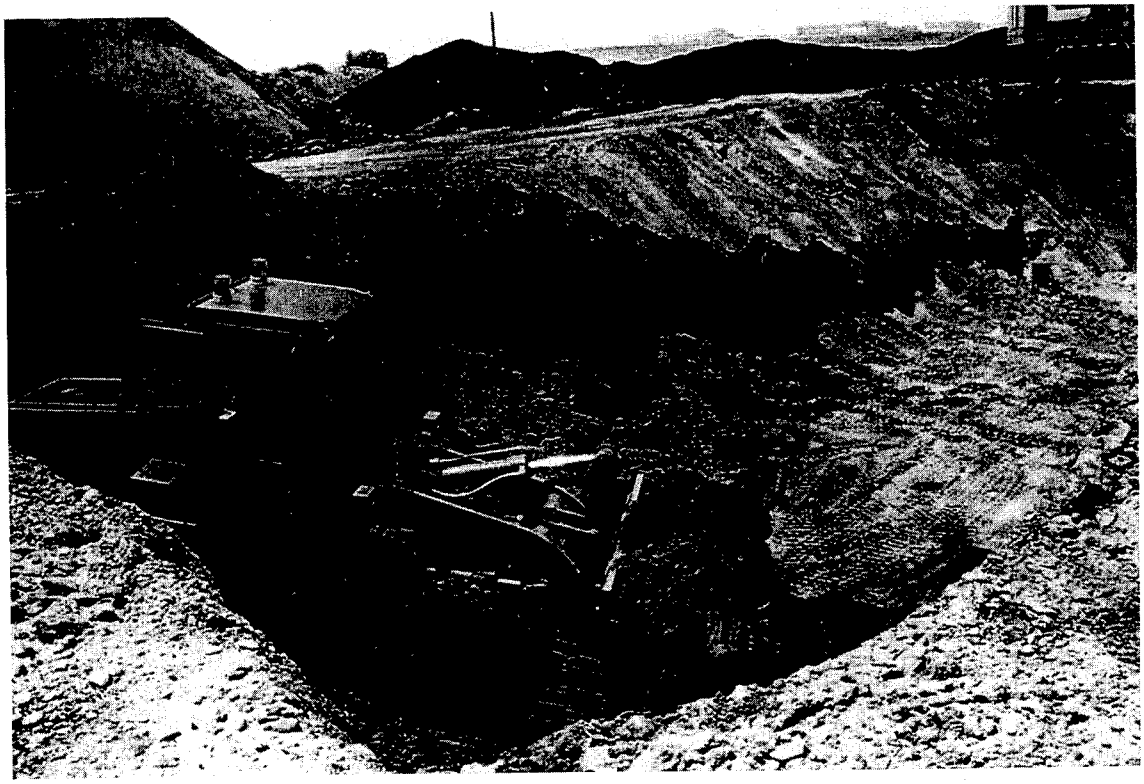

Plate 3.1 Excavation of the Construction Pit

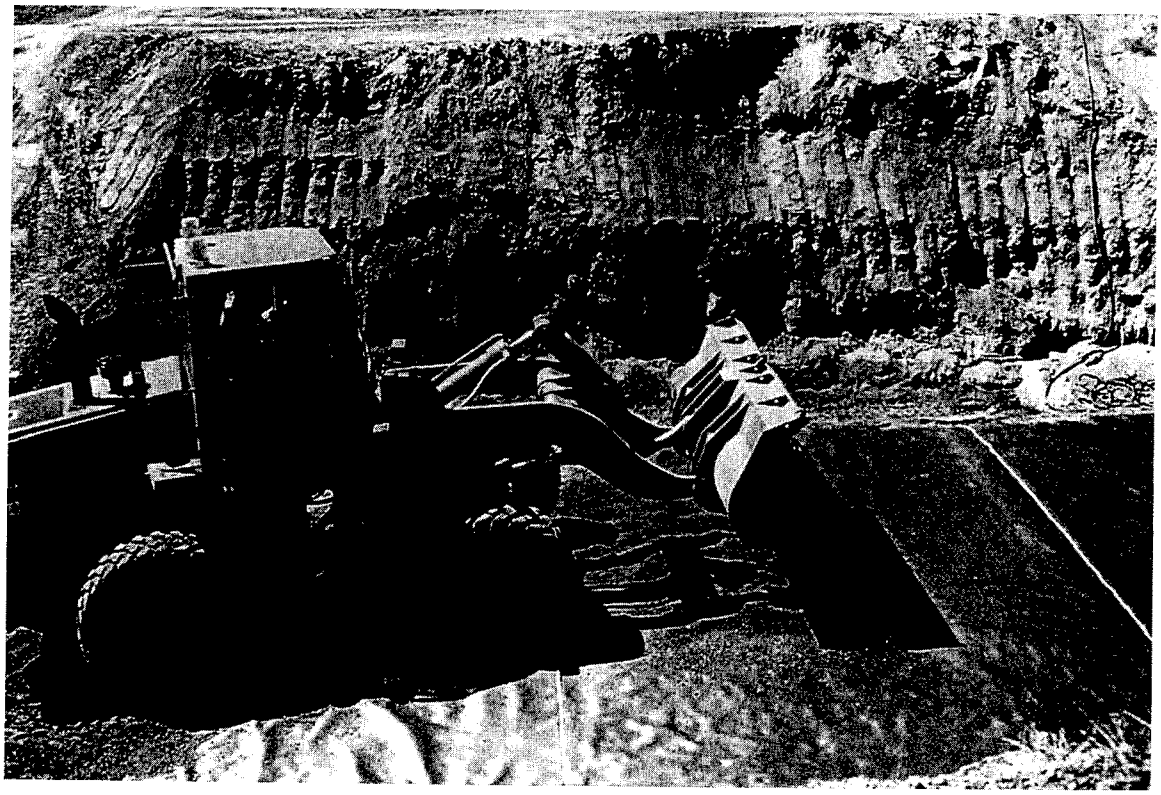

Plate 3.2 Construction of the Reinforced Soil Foundation

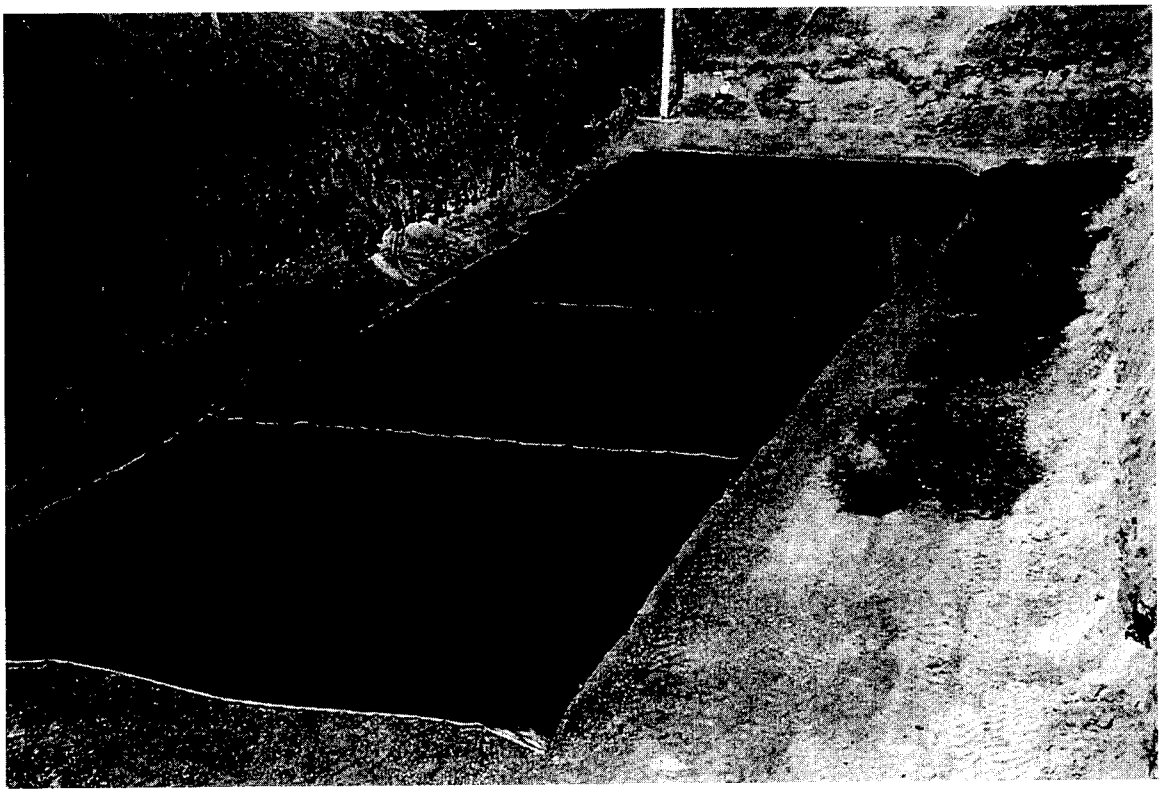

Plate 3.3 Reinforced Soil Foundation with a Woven Geotextile Reinforcement

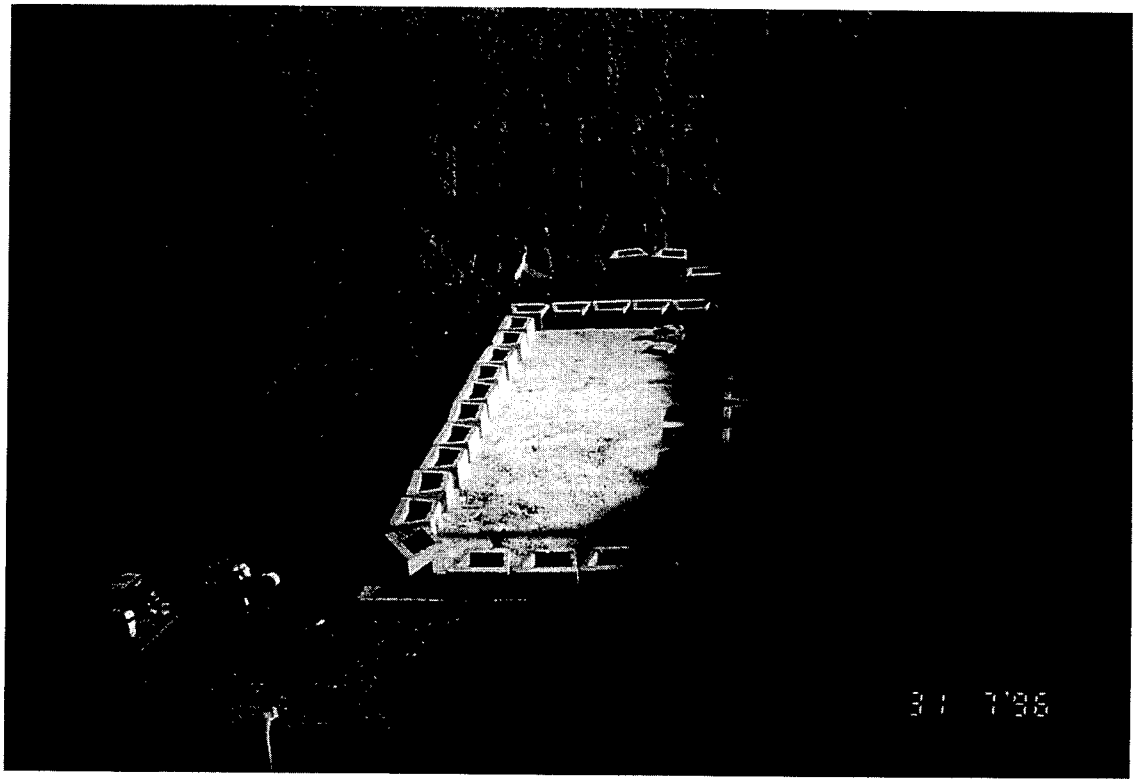

Plate 3.4 Laying the First Course Facing Block on a Concrete Pad
(Note the light-weight plate compactor at the lower left-hand corner)

Plate 3.5 Compaction of the Center Pier

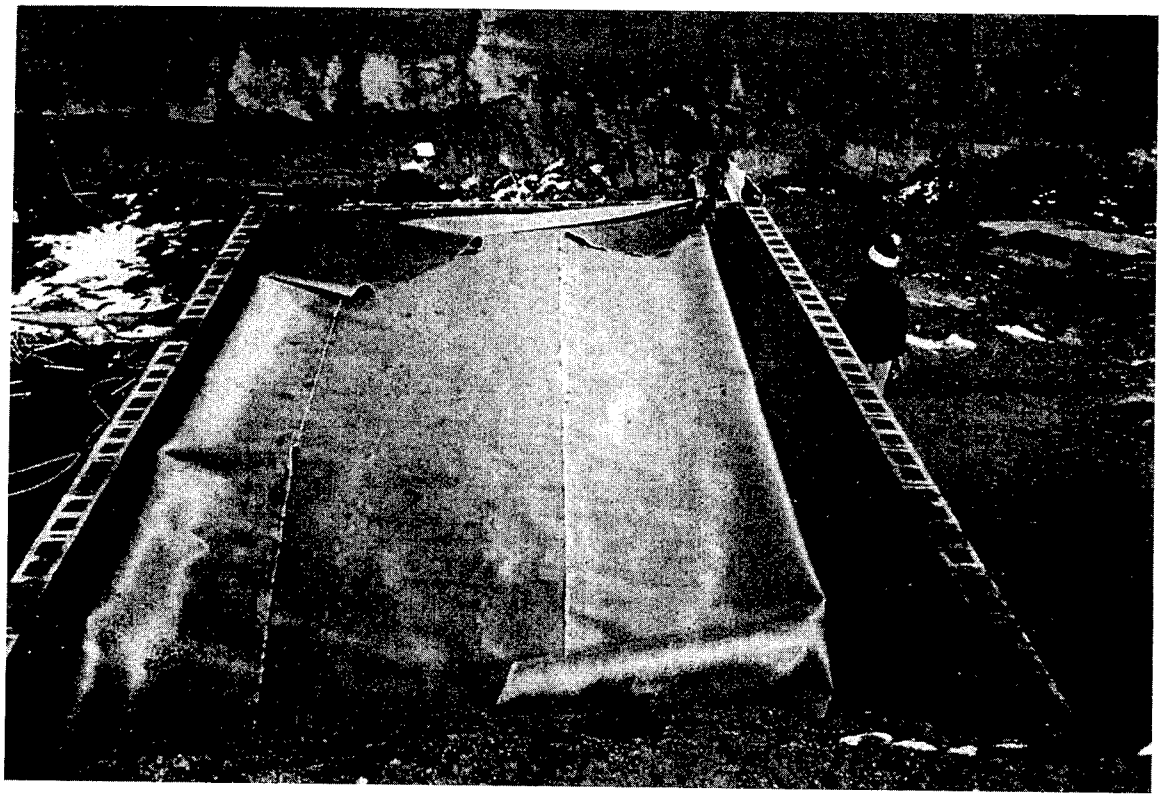

Plate 3.6 Placement of a Layer of Geotextile Reinforcement

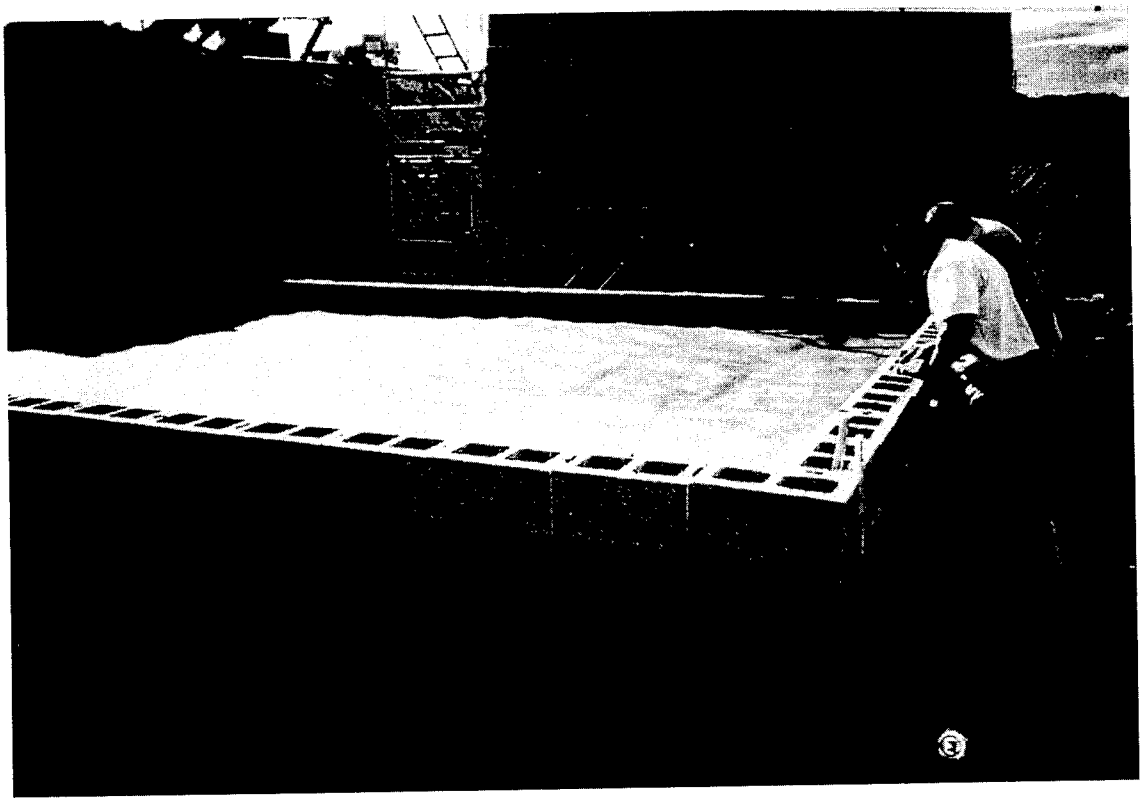

Plate 3.7 Alignment of Facing Blocks

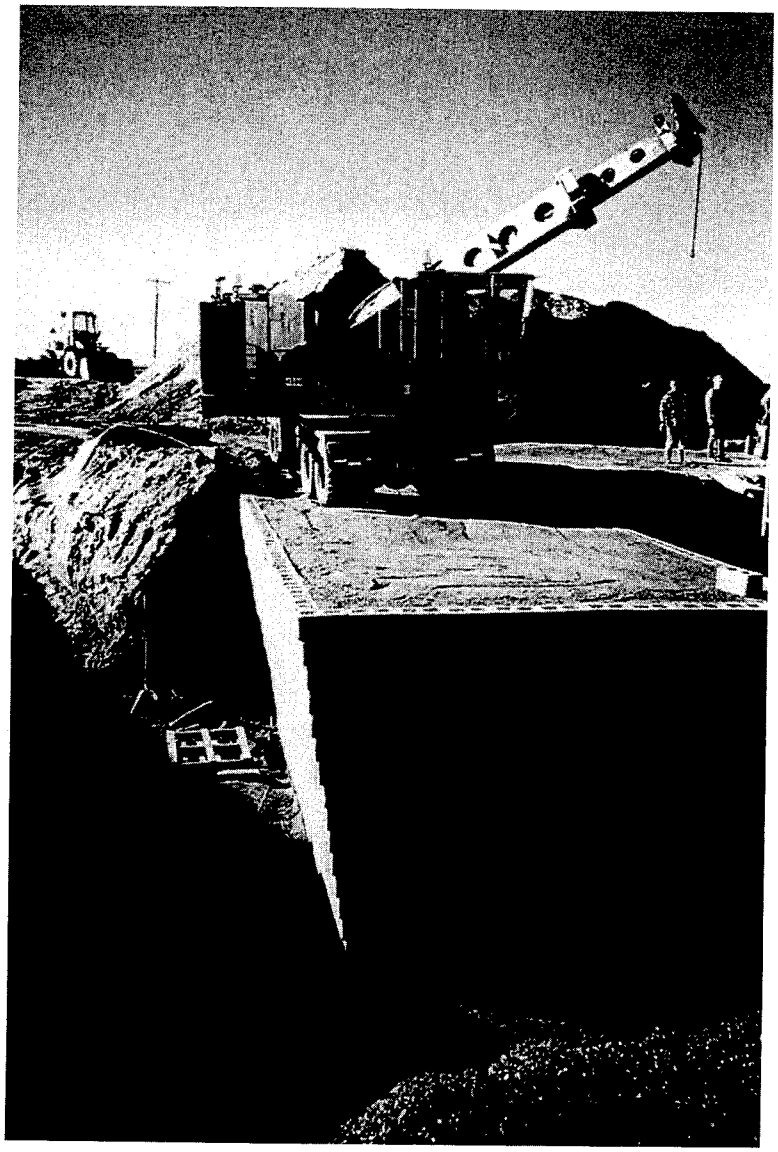

Plate 3.8 Construction of the GRS Abutment With a Negative Batter

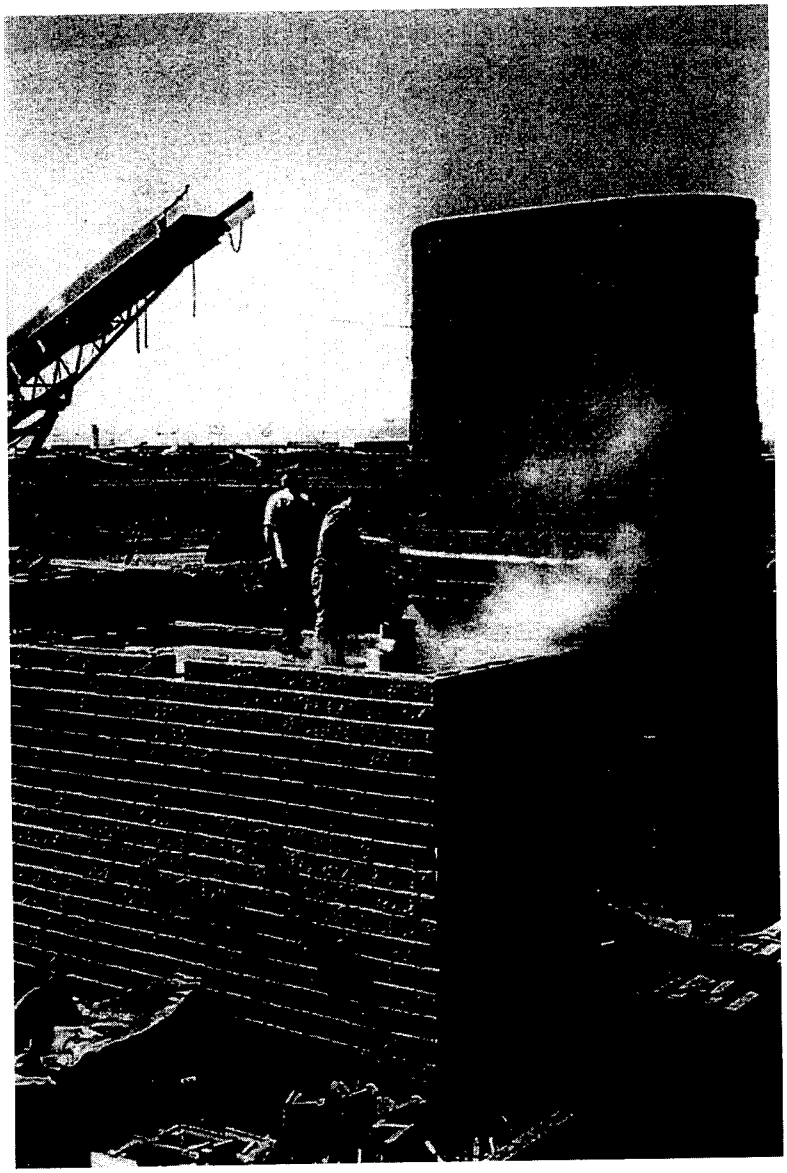

Plate 3.9 Cutting Concrete Blocks to Conform to the Designed Configuration

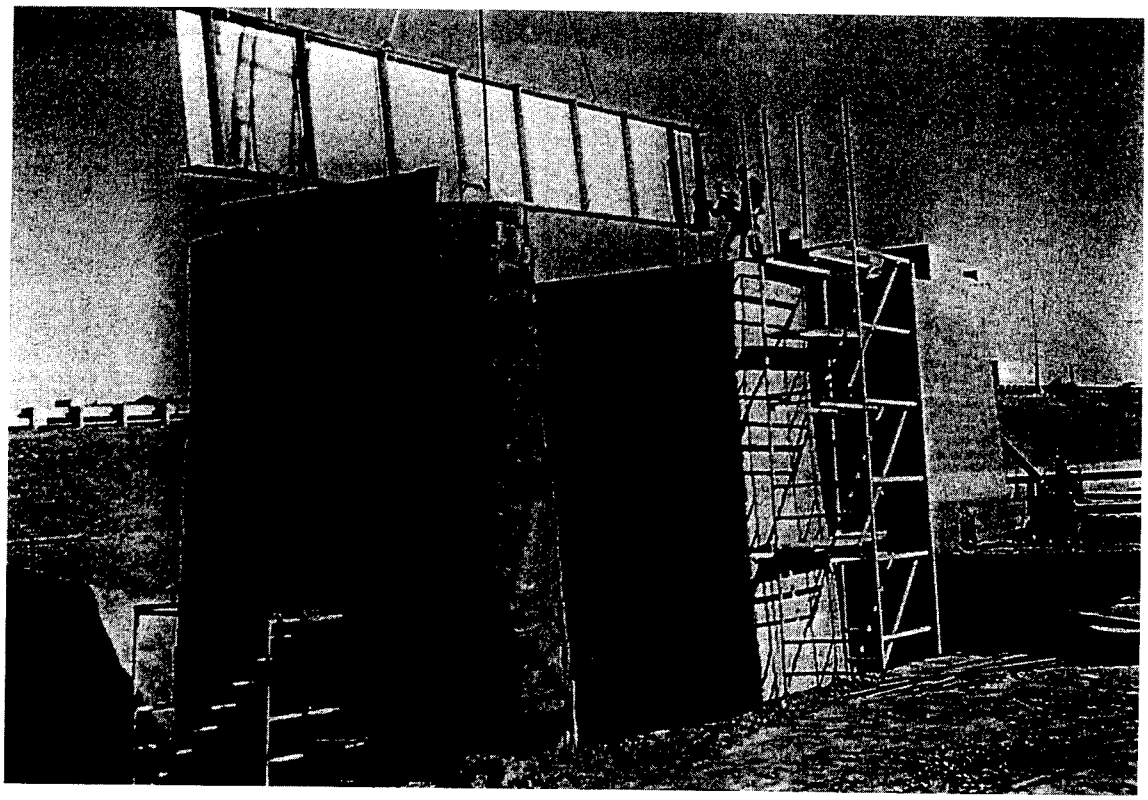

Plate 3.10 Placement of a Steel Bridge Girder

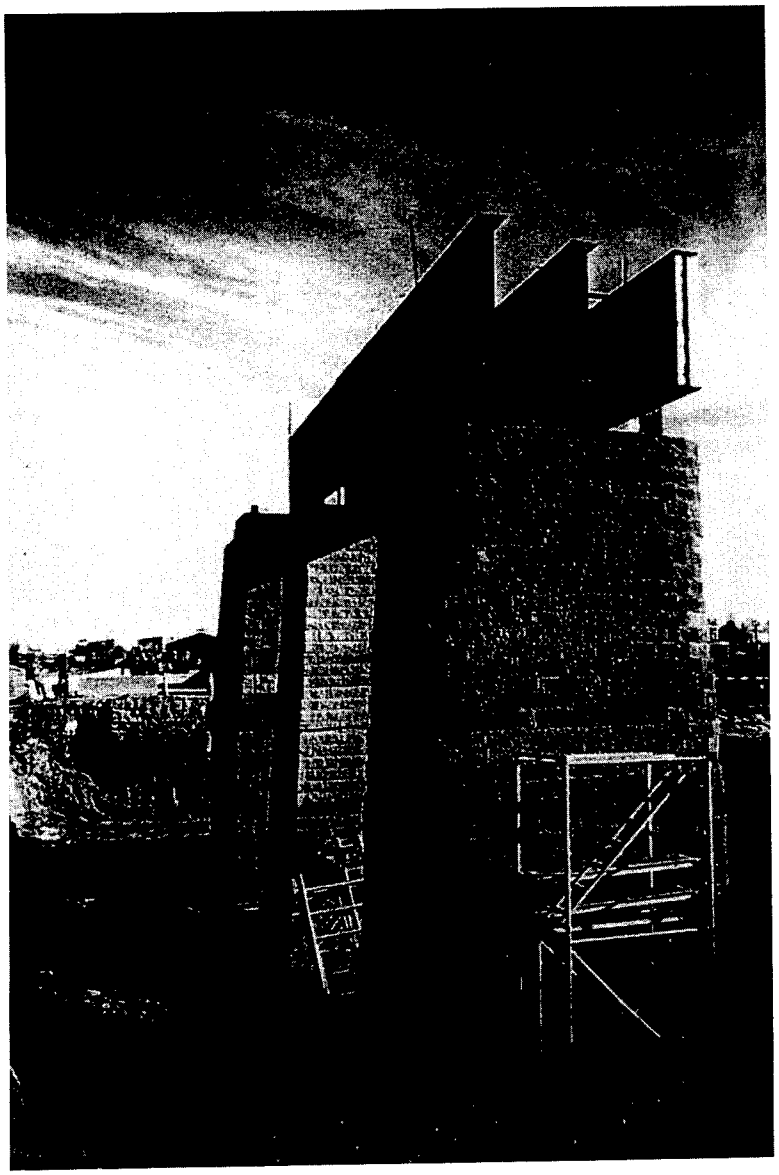

Plate 3.11 Three Steel Bridge Girders Welded Together

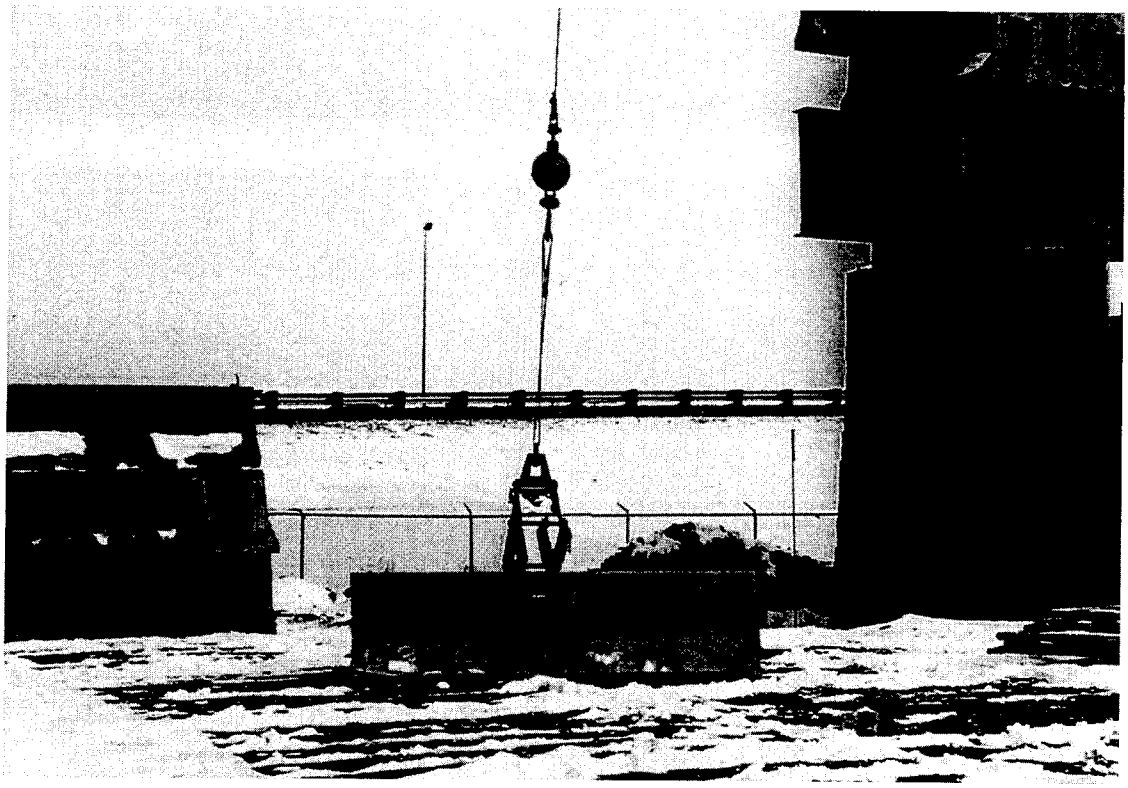

Plate 3.12 A Forklift Clamp is Used to Lift a Jersey Barrier

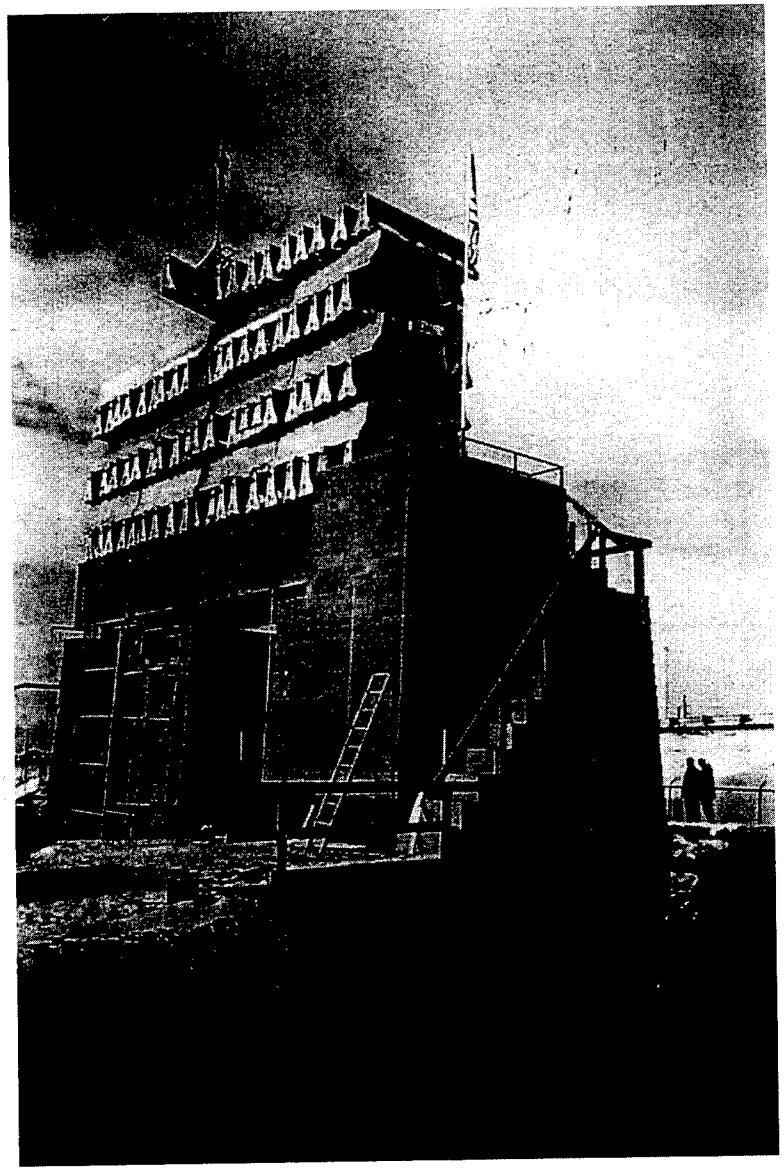

Plate 3.13 Placement of Jersey Barriers

resting on the concrete pads. The steel bearing plates were located along the center line of the top concrete pad of the outer pier, and a 0.3 m offset from the back face of the abutment facing blocks. The span of the girders was 10.4 m. A total of 124 concrete blocks ("Jersey Barriers") was placed on the girders in seven layers as shown in Figure 3.4. The total load was 2,340 kN, which corresponded to an applied pressure of 232 kPa on the outer pier. Note that such a pressure is slightly higher than the 200 kPa maximum pressure suggested in the FHWA Demo 82 (1996) for mechanically stabilized bridge abutments. Also note that the maximum applied pressure of the Turner-Fairbank pier was 900 kPa which was about four times higher than the suggested maximum pressure.

3.4.2 The Second-Stage Load Test

The second-stage load test on the center pier was abandoned.

3.5 Instrumentation

The focus of this project was on the second-stage load test on the center pier. Simple devices were used in the first-stage load test to obtain some quantitative measure of the lateral and vertical movements of the outer pier and the abutment.

3.5.1 Vertical Movement

A leveling rod was attached to a metal pipe, as shown in Figure 3.5, with one end fixed to either the top or the base concrete pads. The vertical movement of the concrete pads was measured by a precision survey transition of the leveling rod. Two fixed posts for survey transit were installed outside the test pit to the north and south of the outer pier and the abutment. The locations of the leveling rods are shown in Figure 3.6.

3.5.2 Lateral Movement

The term "lateral movement," unless otherwise specified, was referred to the total expansion along the perimeter of the structure. Elastic springs were

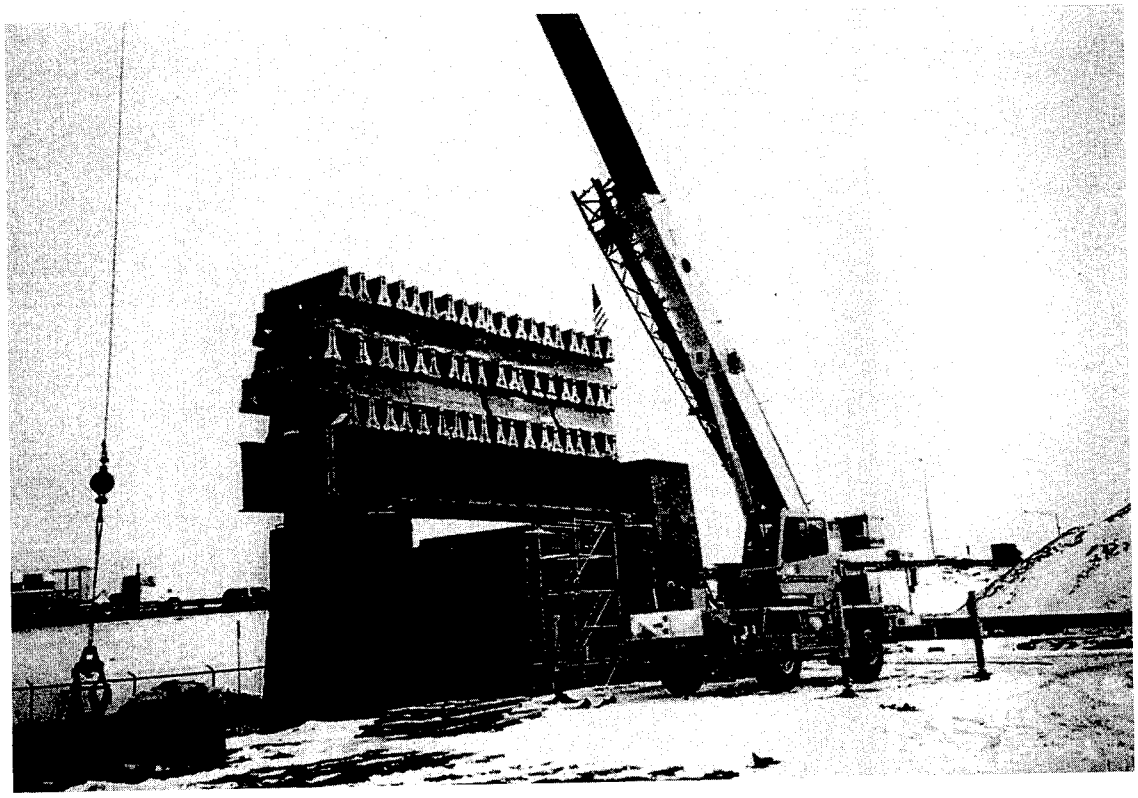

Figure 3.4 First-Stage Load Test

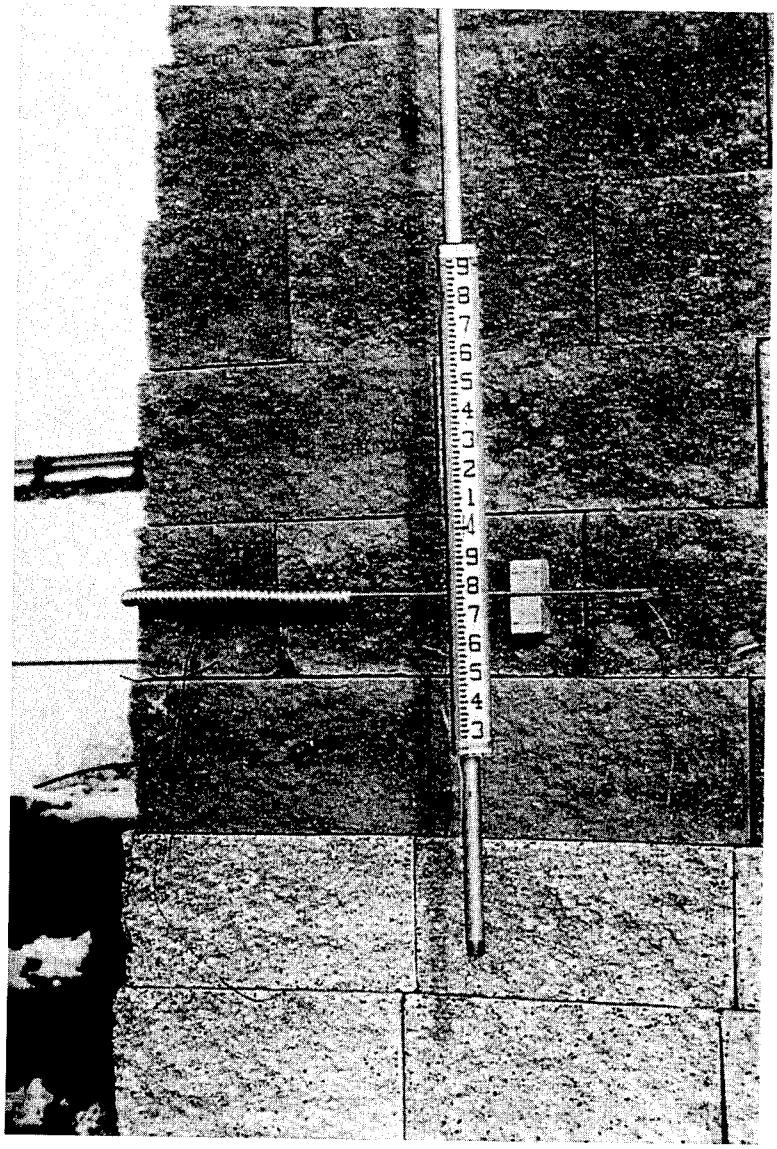

Figure 3.5 Instrumentation for Vertical and Lateral Movements

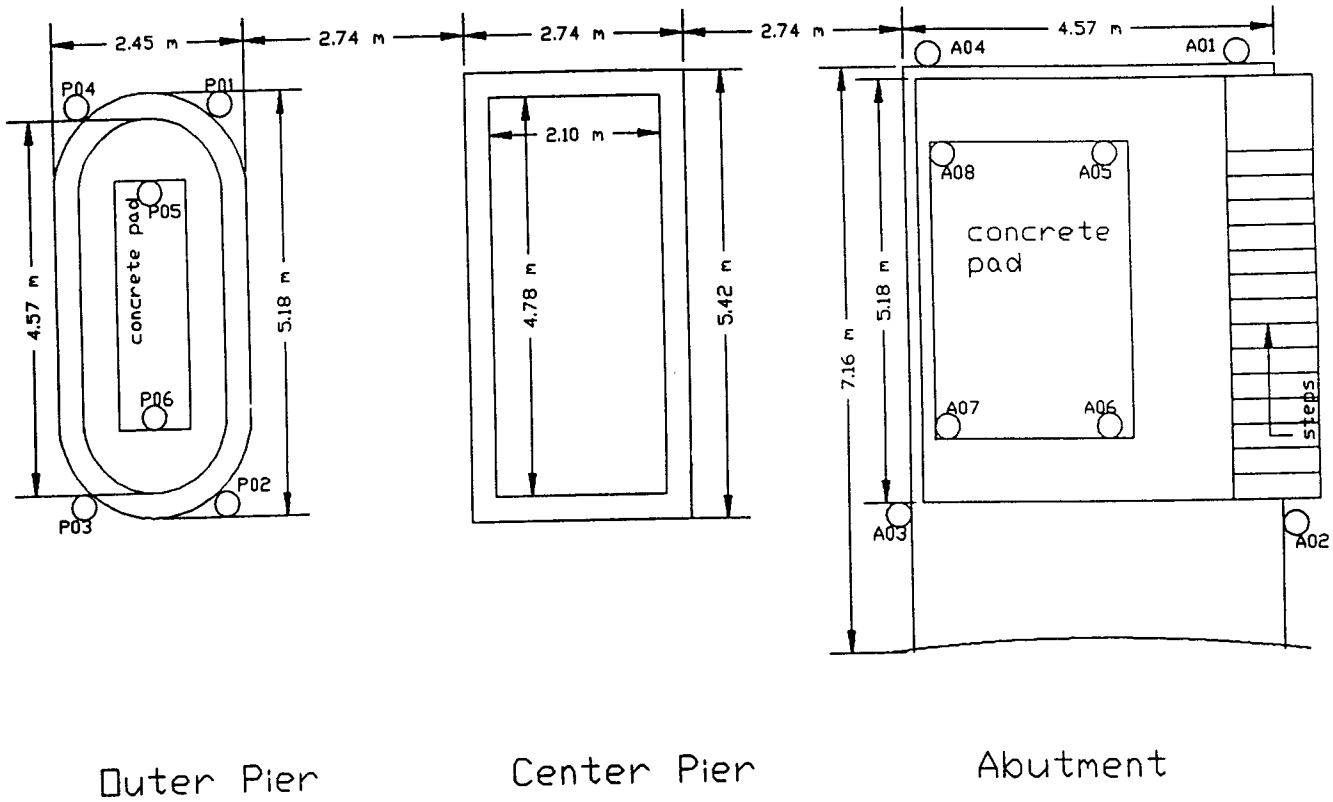

Figure 3.6 Locations of the Leveling Rods

wrapped around the circumference of the outer pier and three sides (north, west and south) of the abutment at selected heights. By measuring the elongation of the elastic spring, the lateral movement of the outer pier and the abutment was obtained. The heights at which the elastic springs were installed on the outer pier were 2.1 m, 4.6 m, and 6.6 m from the base. For the abutment, the elastic springs were located at 5.2 m, 6.0 m and 6.4 m from the base. The locations of the elastic springs (denoted as SP for the outer pier and SA for the abutment) are shown in Figure 3.7.

3.5.3 Strains in Reinforcement

High elongation strain gages, manufactured by Measurements Group, Inc. (type EP-08-250BG-120), were used to measure the strain distribution in the geotextile reinforcement. A total of six strain gages were mounted along the fill and the warp directions of each instrumented sheet of reinforcement for the outer and center piers. There were three sheets of instrumented geotextile reinforcement located at 2.0 m, 4.5 m, and 6.5 m from the base in the outer pier and 1.9 m, 4.3 m, and 6.5 m from the base in the center pier. The abutment had three sheets of instrumented geotextile reinforcement with six strain gages along the fill direction on each sheet. They were located at carrying 5.1 m, 5.9 m, and 6.5 m from the base. The locations of the reinforcement sheets with strain gages are shown in Figure 3.7.

Each strain gage was glued to the geotextile only at the two ends to avoid inconsistent local stiffening of the geotextile due to the adhesive. The strain gage attachment technique was developed at the Reinforced Soil Research Center of the University of Colorado at Denver. The gage was first mounted on a 25 mm by 76 mm patch of a lightweight nonwoven geotextile. The light-weight geotextile patch (with a strain gage and wax) was then attached to the woven geotextile reinforcement at selected locations. A microcrystalline wax material was applied over the gage to protect it from soil moisture. Figure 3.8 shows a strain gage mounted on a light-weight nonwoven geotextile patch and attached to the woven reinforcement.

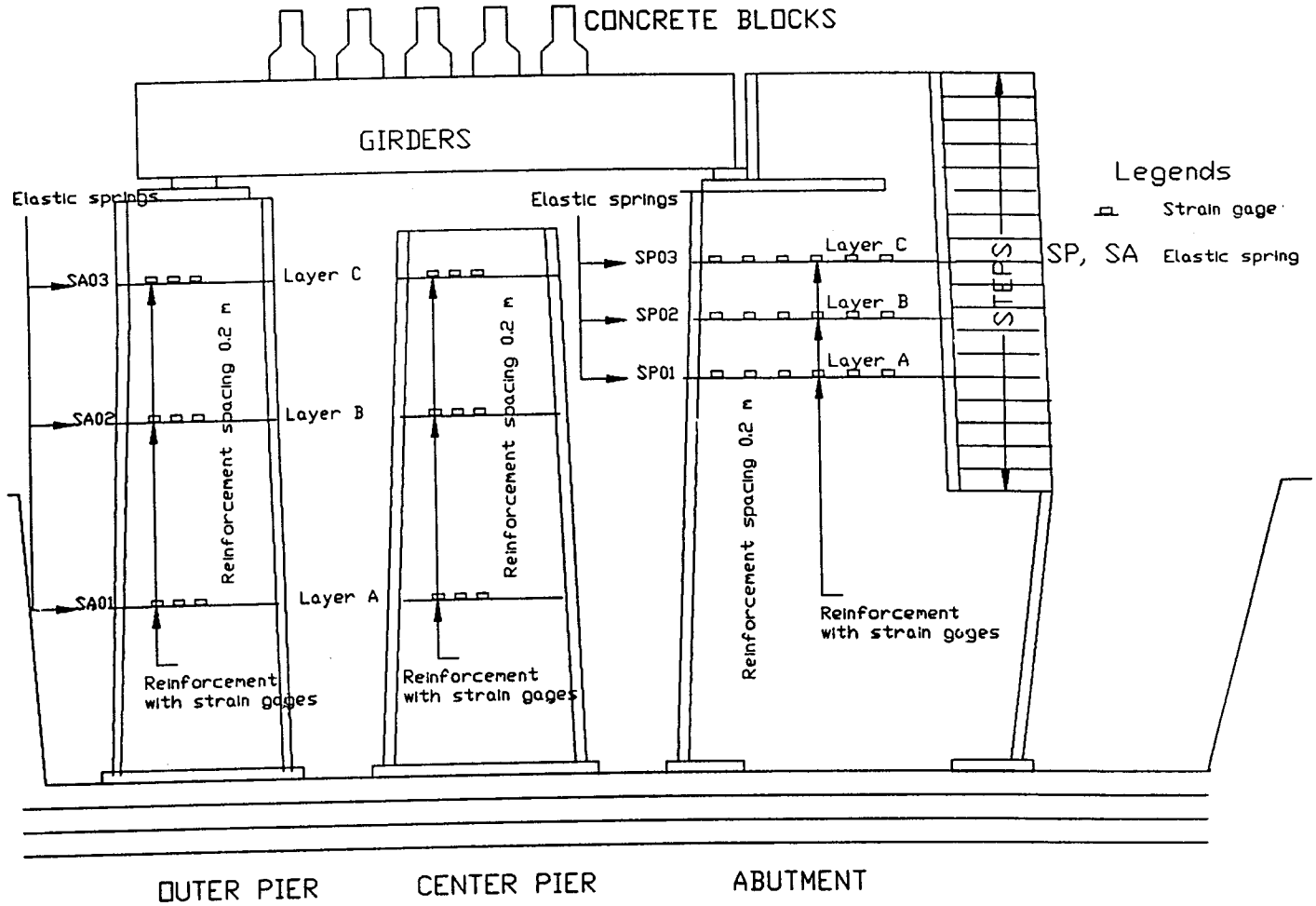

Figure 3.7 Locations of the Reinforcements with Strain Gages and the Elastic Springs

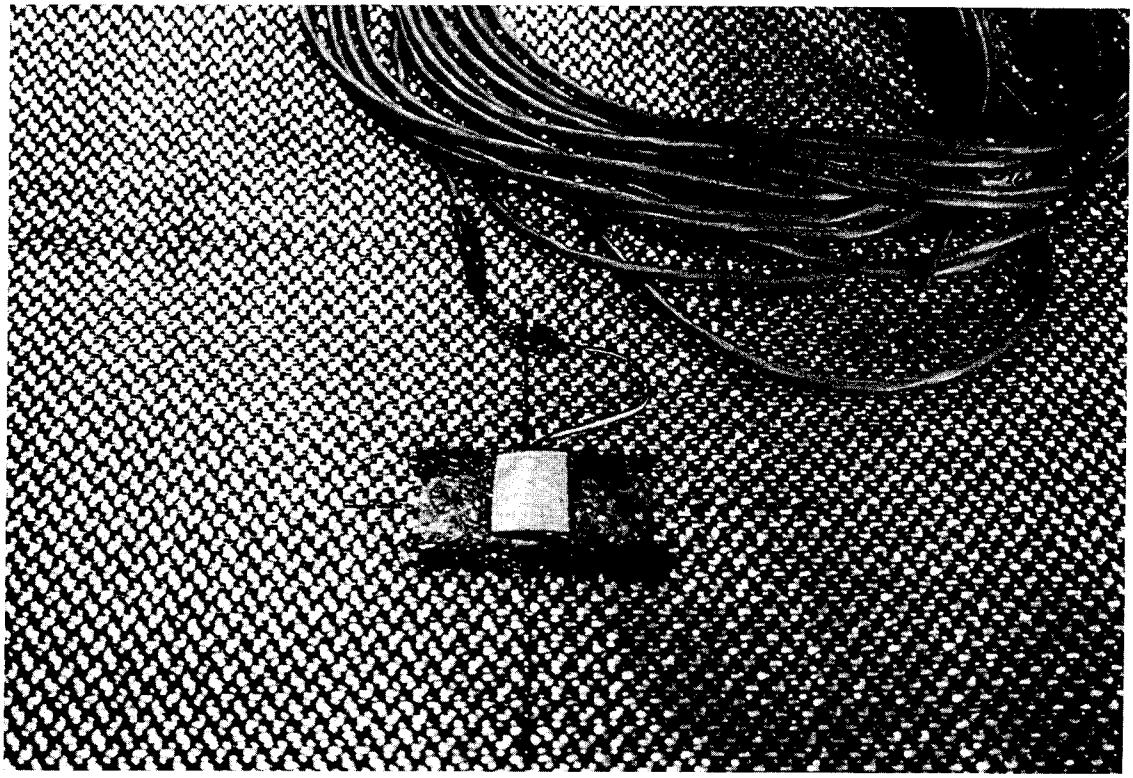

Figure 3.8 Strain Gage Attachment

Due to the presence of the light-weight geotextile patch, calibration is needed. Calibration tests were performed to relate the strain obtained from the attached strain gage to the actual strain of the reinforcement. The calibration curves along the fill and the warp directions of the woven geotextile reinforcement used in the load test are shown in Figure 3.9 and Figure 3.10, respectively.

3.6 Results and Discussion of the Results

The measured results, both short- and long-term results, and discussion of the results are presented in this section.

3.6.1 Short-Term Behavior

The measured short-term vertical and lateral displacements of the abutment and the pier, as well as the measured strains in the geotextile reinforcement soon after the load application are presented in the following sections. In addition, discussions of the measured results are presented.

3.6.1.1 Vertical and Lateral Displacements

Figure 3.11 and Figure 3.12 show the applied load versus displacement relationships of the abutment in the vertical and lateral directions, respectively. The vertical displacements were fairly uniform along the two axial directions. The maximum vertical displacements at 1,170 kN were 27.1 mm at the top and 5.2 mm at the base. The maximum lateral movement at 5.2 m from the base was 14.3 mm.

Figure 3.13 and Figure 3.14 show the applied load versus displacement relationships of the outer pier in the vertical and lateral directions, respectively. Similar to the abutment, the vertical displacements were fairly uniform along the two axial directions. The maximum vertical displacements at 1,170 kN (232 kPa pressure) were 36.6 mm at the top and 6.1 mm at the base. The maximum lateral movement at 4.6 m from the base was 12.7 mm.

Figure 3.15 shows the vertical and lateral movements of the outer pier and

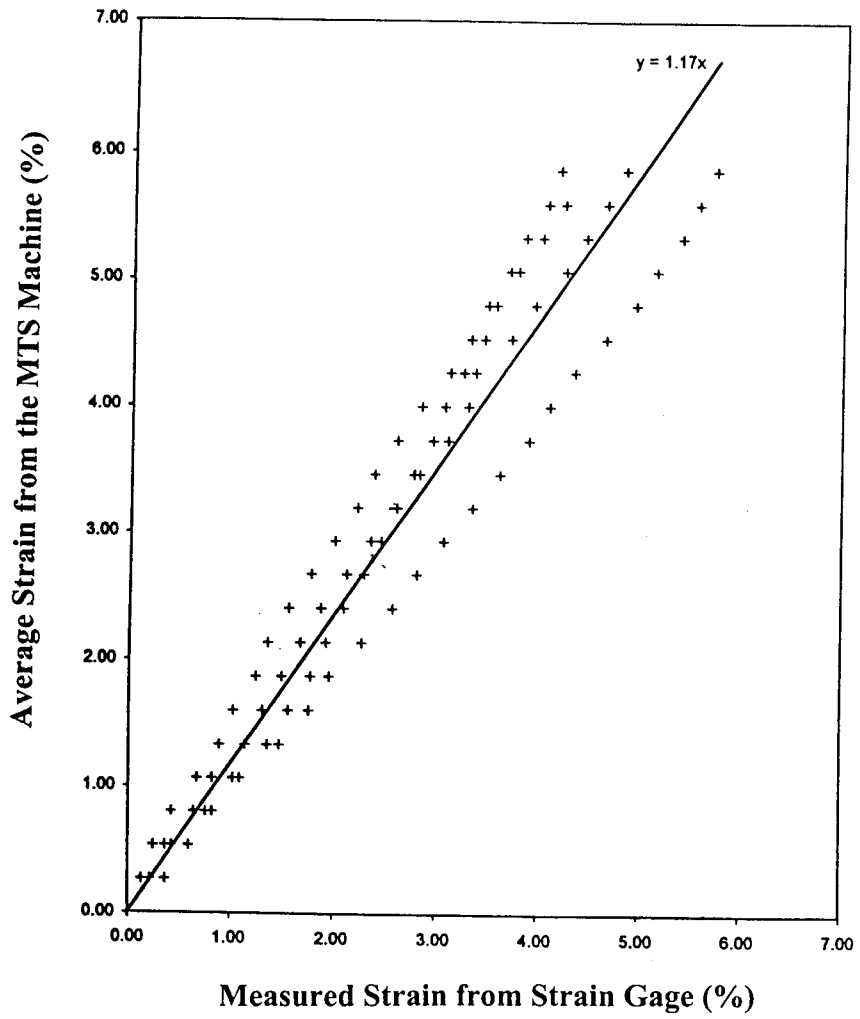

Figure 3.9 Strain Gage Calibration in the Fill Direction of the Reinforcement

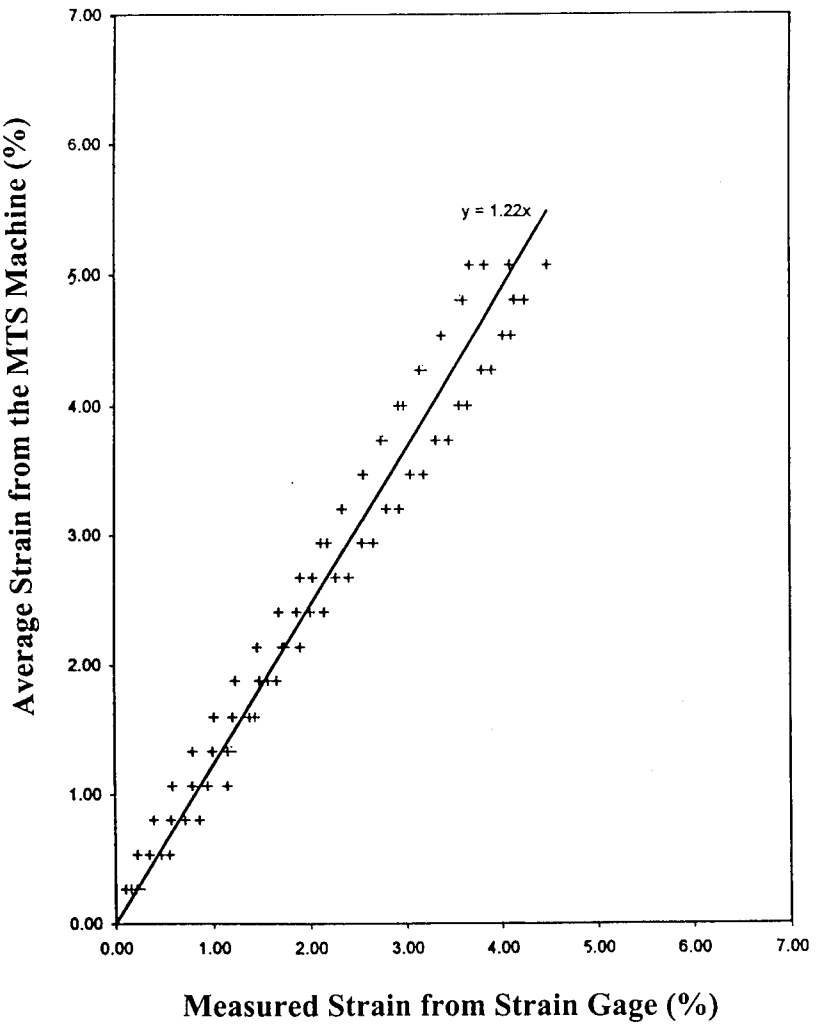

Figure 3.10 Strain Gage Calibration in the Warp Direction of the Reinforcement

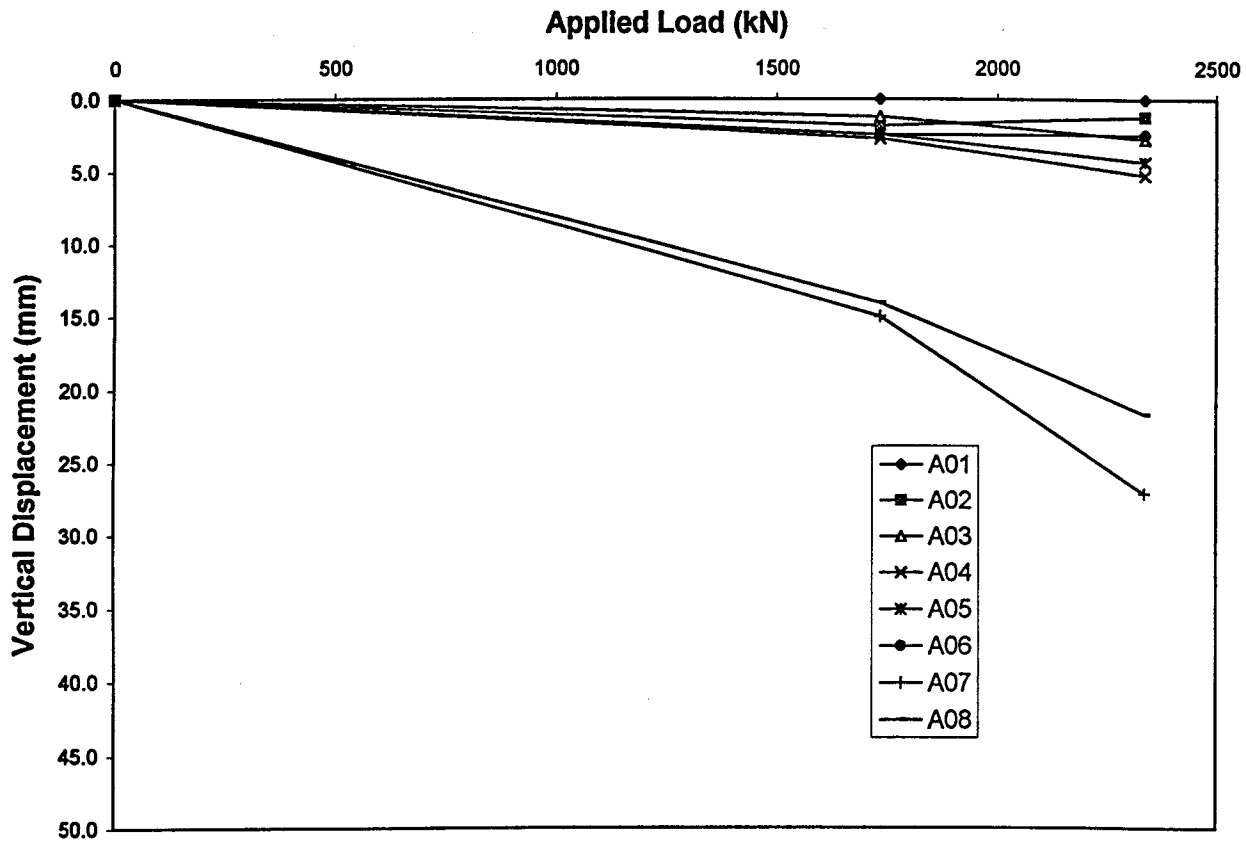

Figure 3.11 Vertical Displacement vs. Applied Load Relationships of the Abutment

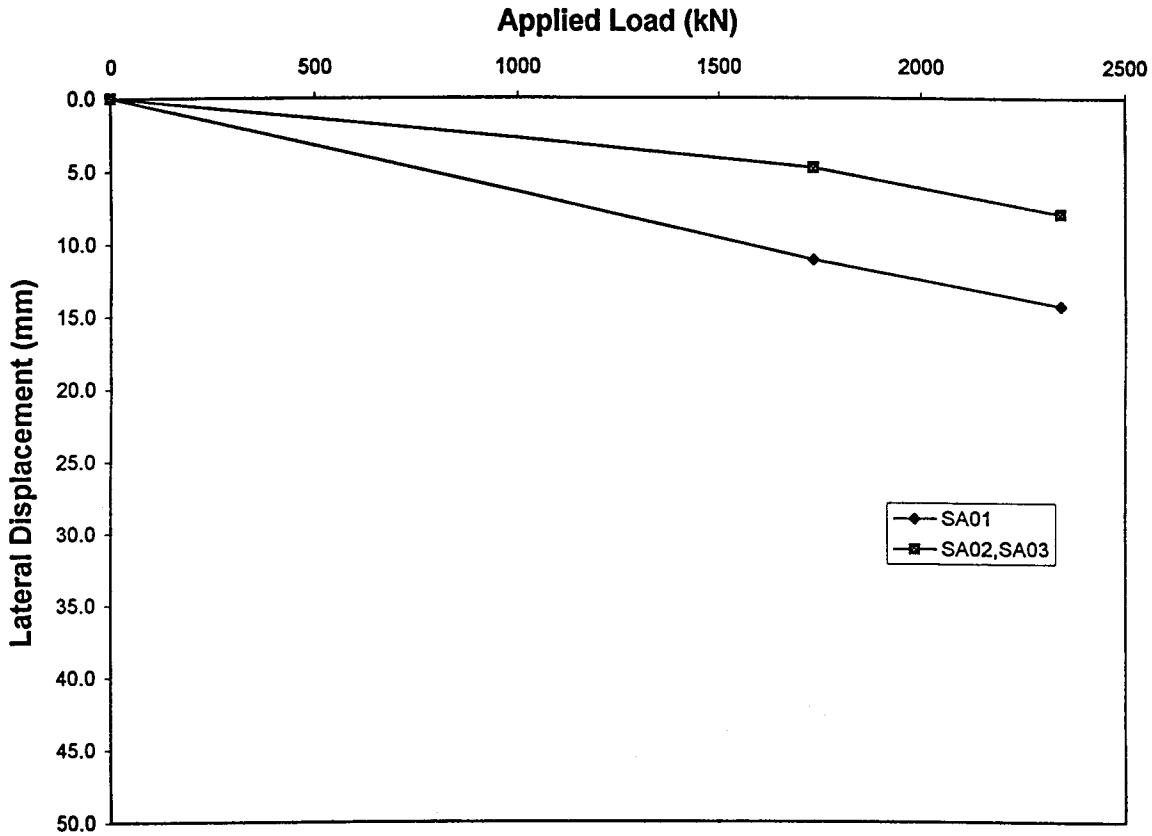

Figure 3.12 Lateral Displacement vs. Applied Load Relationships of the Abutment

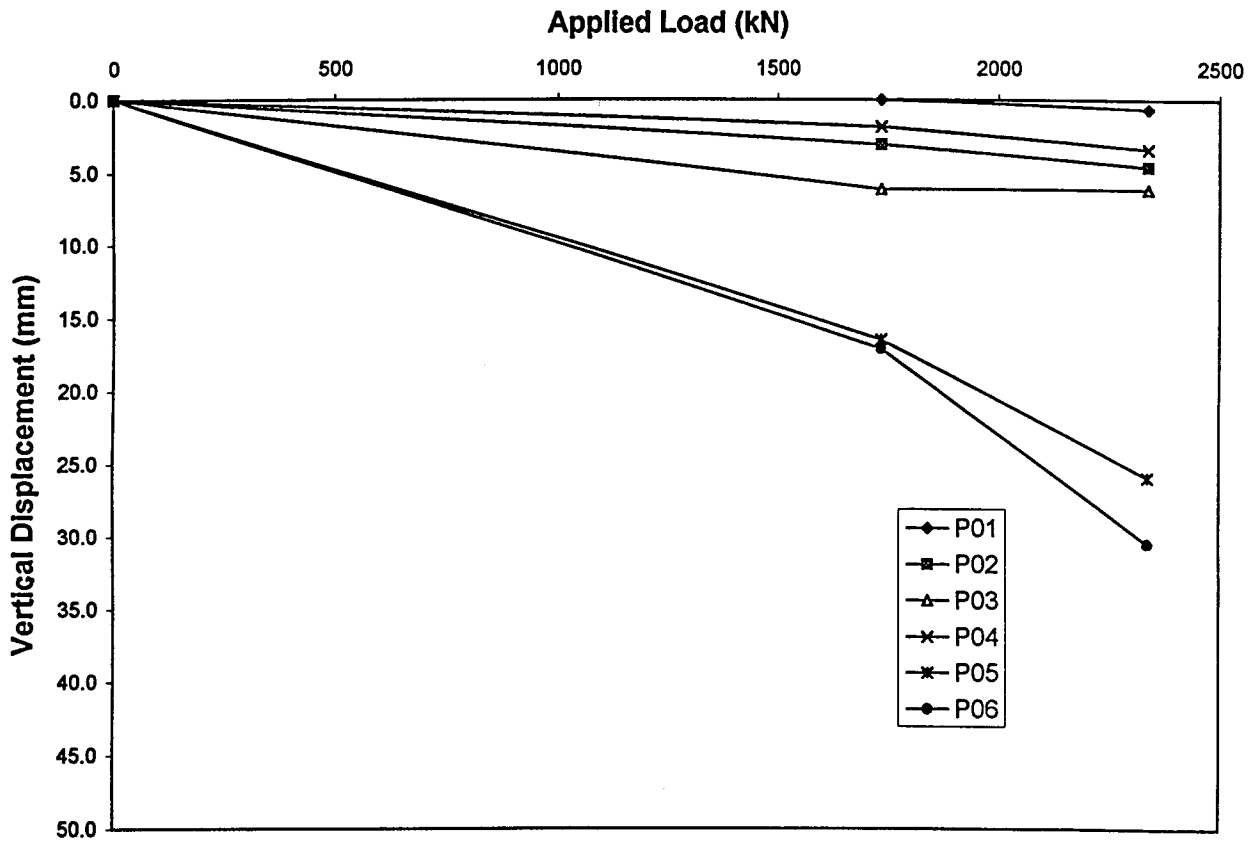

Figure 3.13 Vertical Displacement vs. Applied Load Relationships of the Outer Pier

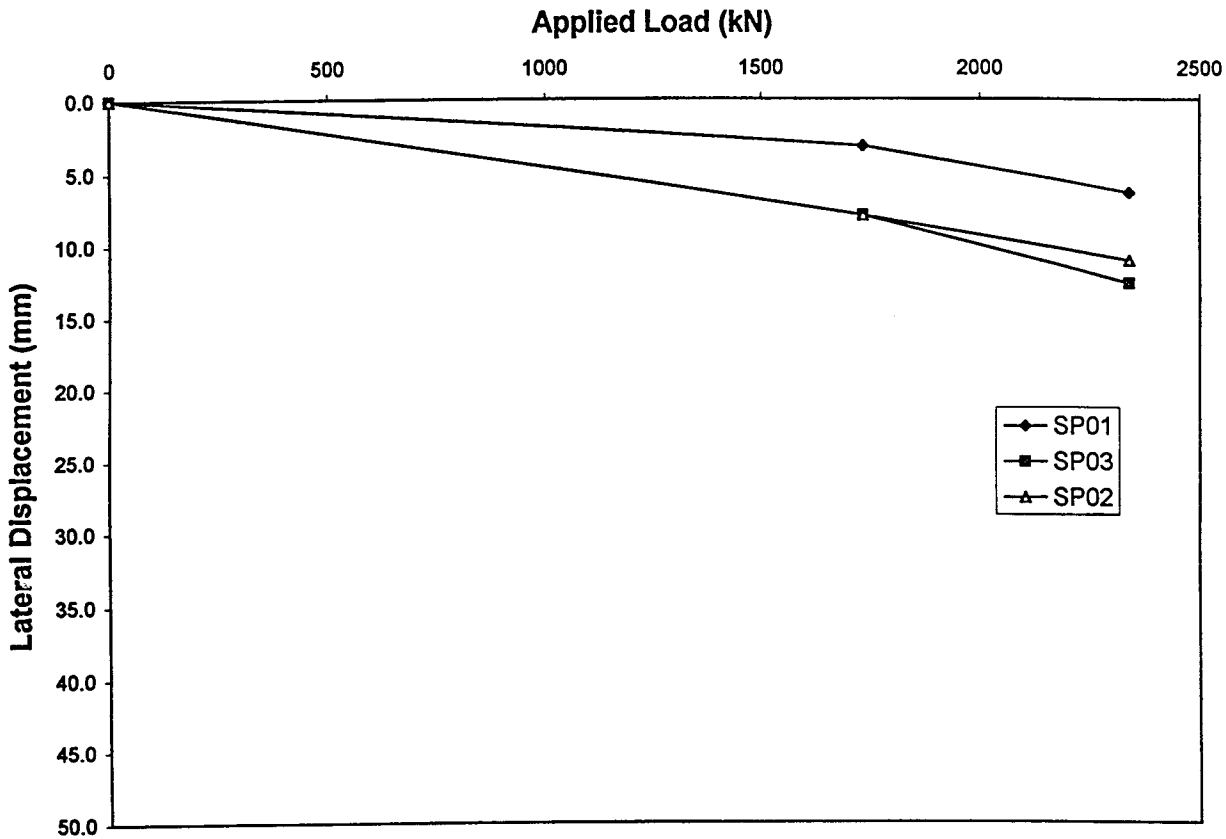

Figure 3.14 Lateral Displacement vs. Applied Load Relationships of the Outer Pier

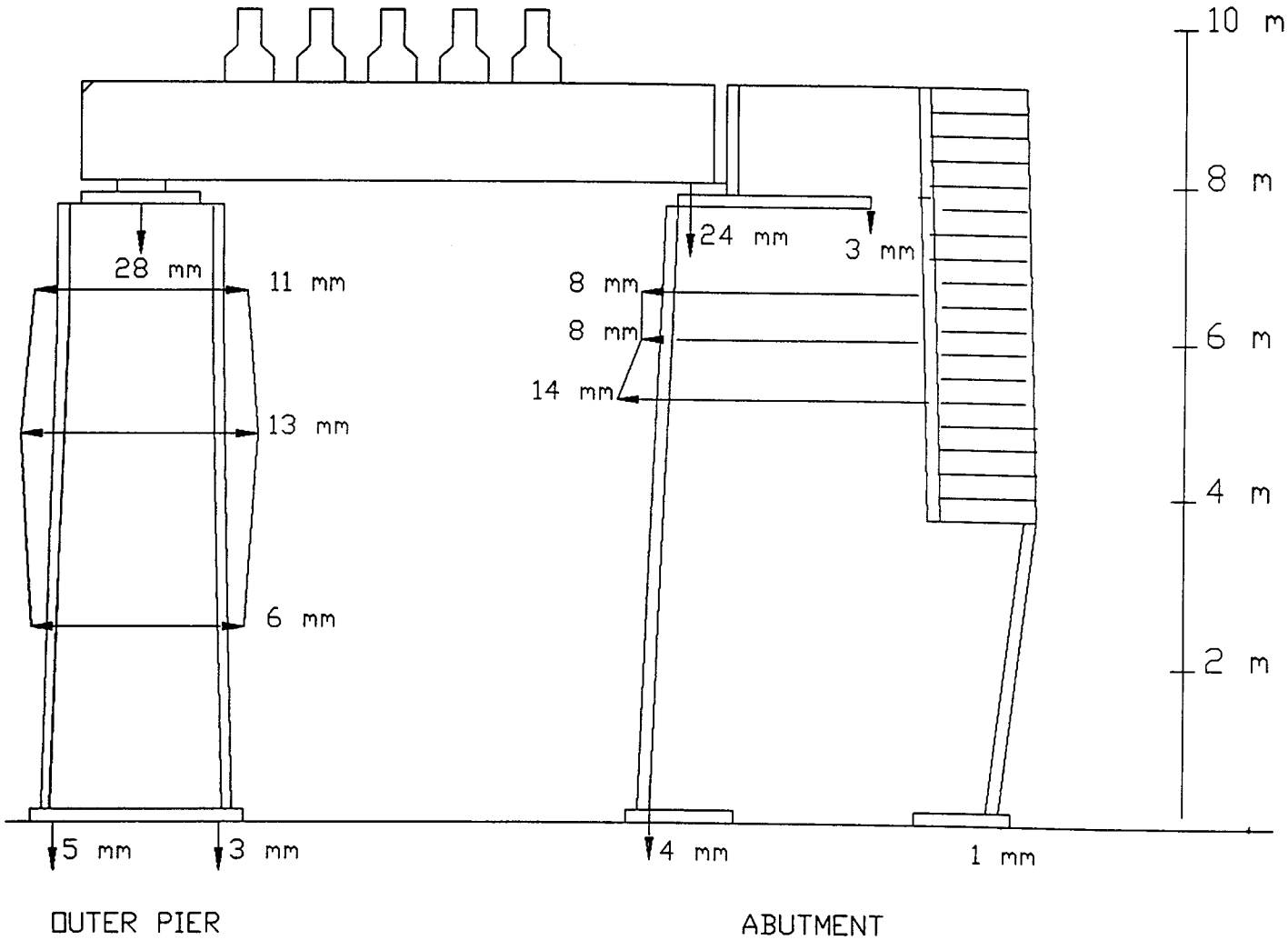

Figure 3.15 Vertical and Lateral Movements of the Outer Pier and the Abutment at 1170 kN

the abutment at the applied load of 1,170 kN. Table 3.2 summarizes the maximum vertical and lateral movements of the outer pier and the abutment. It is shown that the vertical movement of the foundations for the outer pier and the abutment was about the same (6.1 mm for the pier, 5.2 mm for the abutment). The different magnitudes of the vertical movement on top of the pier and the abutment were, therefore, a result of the different amounts of vertical compression of the structures upon loading. The maximum vertical movement of the pier was 0.48% of its height. Such a value was higher than that of the Turner-Fairbank pier which was 0.30% (without prestraining) at the same applied pressure. This may be attributed to the much lower compaction effort on the outer pier. The maximum lateral movements of the pier and the abutment were comparable (12.7 mm in the pier, 14.3 mm in the abutment).

After the load of 1,170 kN was applied, predominantly vertical hairline cracks in the facing blocks were observed along the length and the width directions of the outer pier and the face of the abutment. It was not clear when was the first crack developed. With time, however, the cracks increased both in the number and in the width.

3.6.1.2 Strains in Reinforcement

Figure 3.16 shows the strain distributions in the fill direction along the length of the three instrumented sheets of reinforcement in the abutment. The largest strains were on the order of 0.15% to 0.18% at the applied load of 1,170 kN. The largest strains occurred adjacent to the facing (the center of bearing plates was only 0.3 m from the back face of the facing blocks) and decreased toward the other end. The strains were nearly zero at 2.5 m from the facing.

The reinforcement strains in the fill direction of the outer pier were on the order of 0.2% to 0.4% at the applied load of 1,170 kN (232 kPa pressure). Note that such a magnitude of reinforcement strain was similar to that measured in the Turner-Fairbank pier at the same applied pressure. This implies that at the same applied pressure the lateral displacement of the outer pier and the Turner-Fairbank pier was comparable.

Structure	Maximum Vertical Movement (mm)			Maximum Lateral Movement (mm)
	Foundation	**Structure**	**Total**	
Outer Pier	6.1 mm	30.5 mm	36.6 mm	12.7 mm
Abutment	5.2 mm	21.9 mm	27.1 mm	14.3 mm

Table 3.2 Maximum Vertical and Lateral Movements of the Outer Pier and the Abutment at 1170 kN

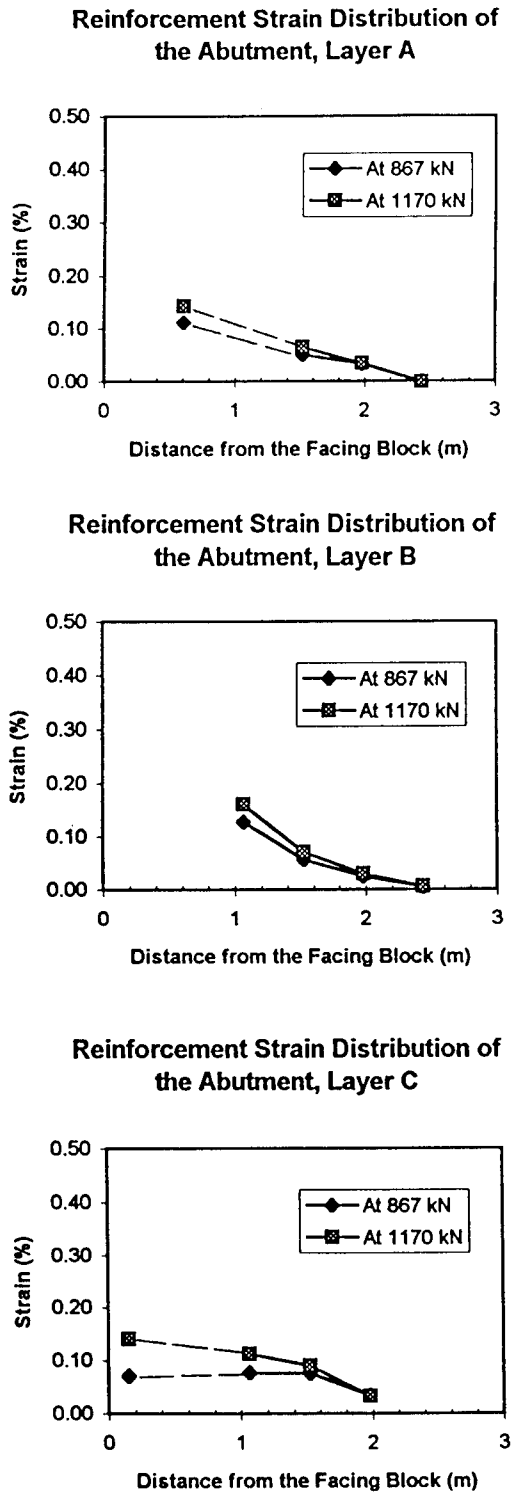

Figure 3.16 Reinforcement Strain Distributions in the Abutment

Compared the largest strains in the abutment and the outer pier (on the order of 0.2% to 0.4%) to the rupture strain (18%), the safety margin appeared to be very high against rupture failure of the reinforcement. However, the load carrying capacities of both structures may not be governed by the rupture failure of the reinforcement. Slippage between the backfill and the reinforcement or the shear failure of the backfill may occur first.

3.6.2 Long-Term Behavior under 1,170 kN Load

Time Dependent behavior of the abutment and pier -- including vertical displacements, lateral displacements, and reinforcement strains -- under a sustained load of 1,170 kN load is presented in the following sections. Discussion of the measured results is also presented.

3.6.2.1 Vertical and Lateral Creep Displacements

Figure 3.17 and Figure 3.18 show, respectively, the vertical and lateral displacements versus time relationships of the abutment under the sustained load of 1,170 kN. The maximum vertical displacements at the top and the base after 70 days were 18.3 mm and 6.7 mm, respectively. The maximum lateral displacement was 14.3 mm after 70 days. Most of the maximum vertical and lateral displacements (12 mm and 13 mm, respectively) occurred in the first 15 days.

Figure 3.19 and Figure 3.20 show, respectively, the vertical and lateral displacements versus time relationships of the outer pier under the sustained load of 1,170 kN. The maximum vertical displacements at the top and the base after 70 days were 61.6 mm and 5.2 mm, respectively. The maximum lateral displacement was 59.5 mm after 70 days. Similar to the outer pier, a large portion of the maximum vertical and lateral displacements (48 mm and 46 mm, respectively) also occurred in the first 15 days. The maximum vertical and lateral displacements of the outer pier were about four times as large as those of the abutment. This is most likely due to poor compaction by a light-weight vibrating

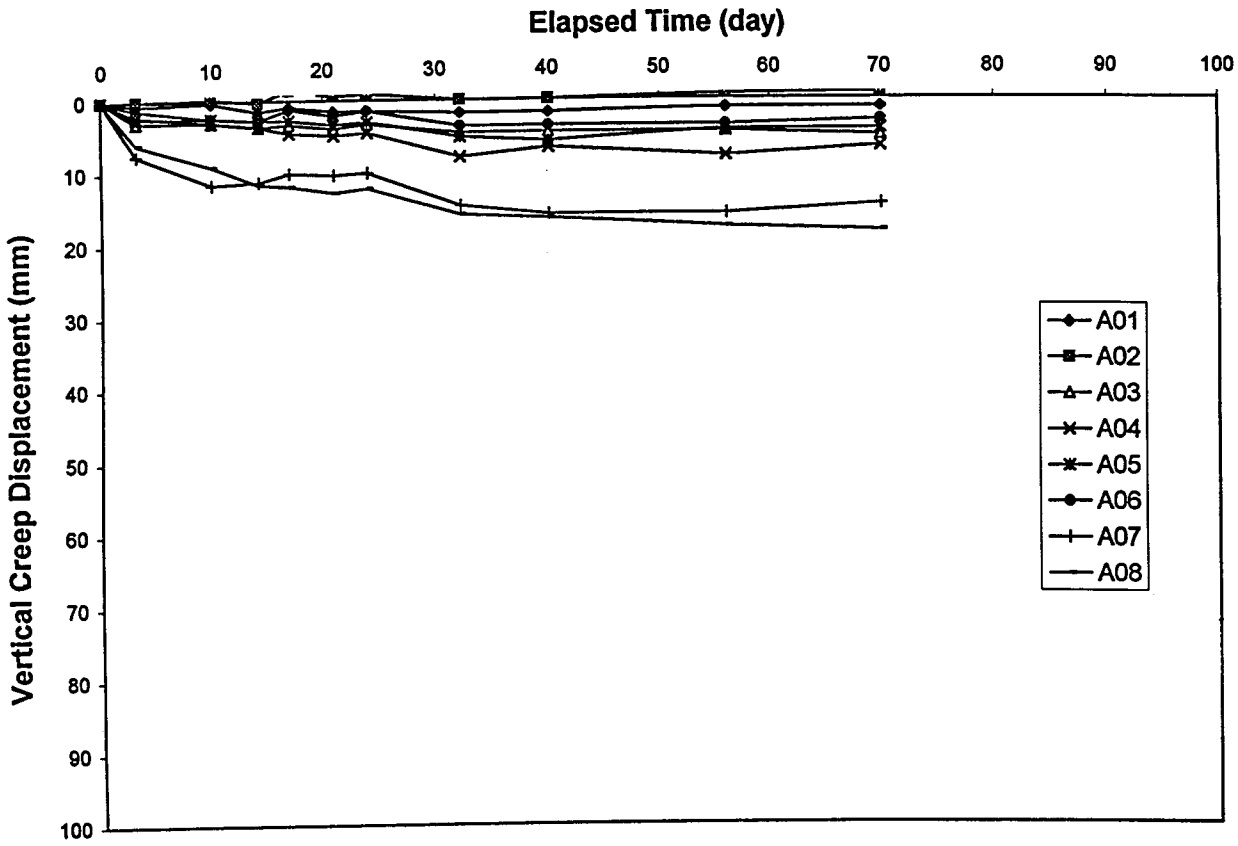

Figure 3.17 Vertical Creep Displacement vs. Time Relationships of the Abutment

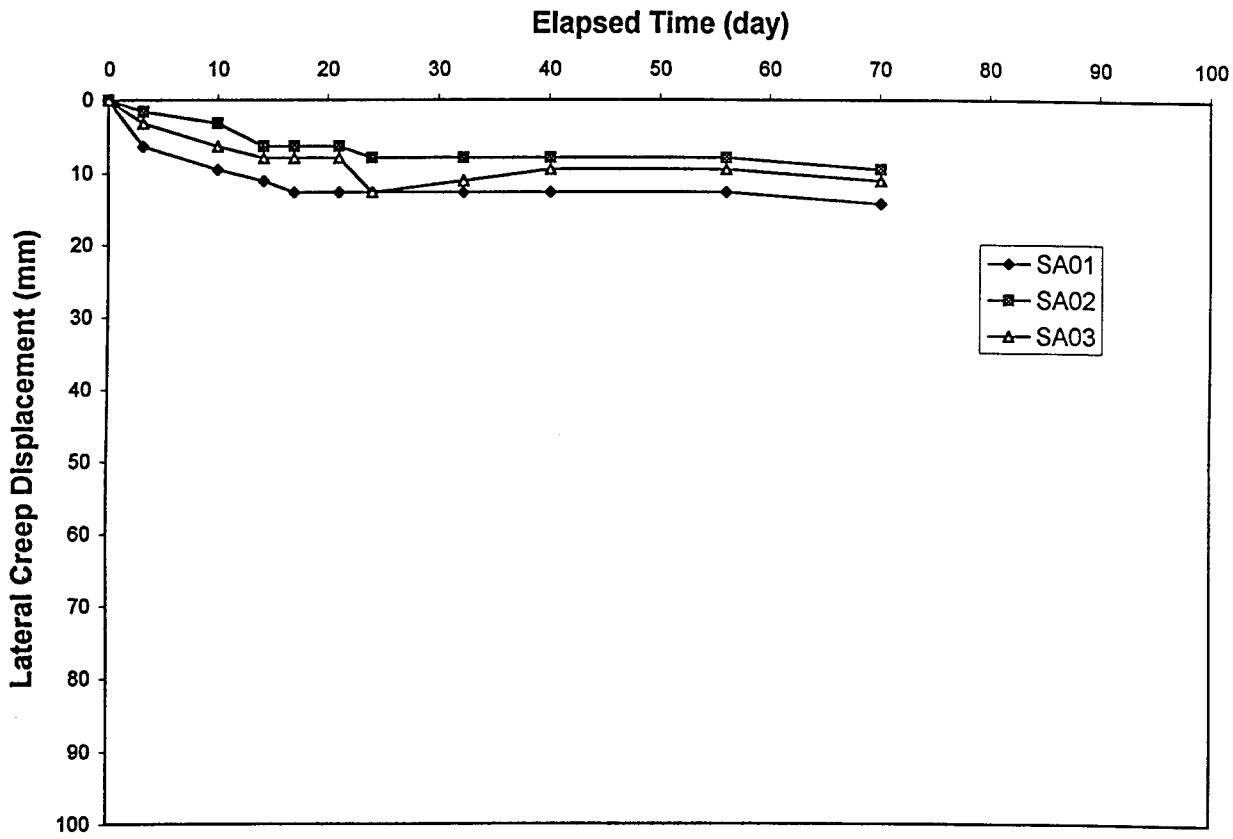

Figure 3.18 Lateral Creep Displacement vs. Time Relationships of the Abutment

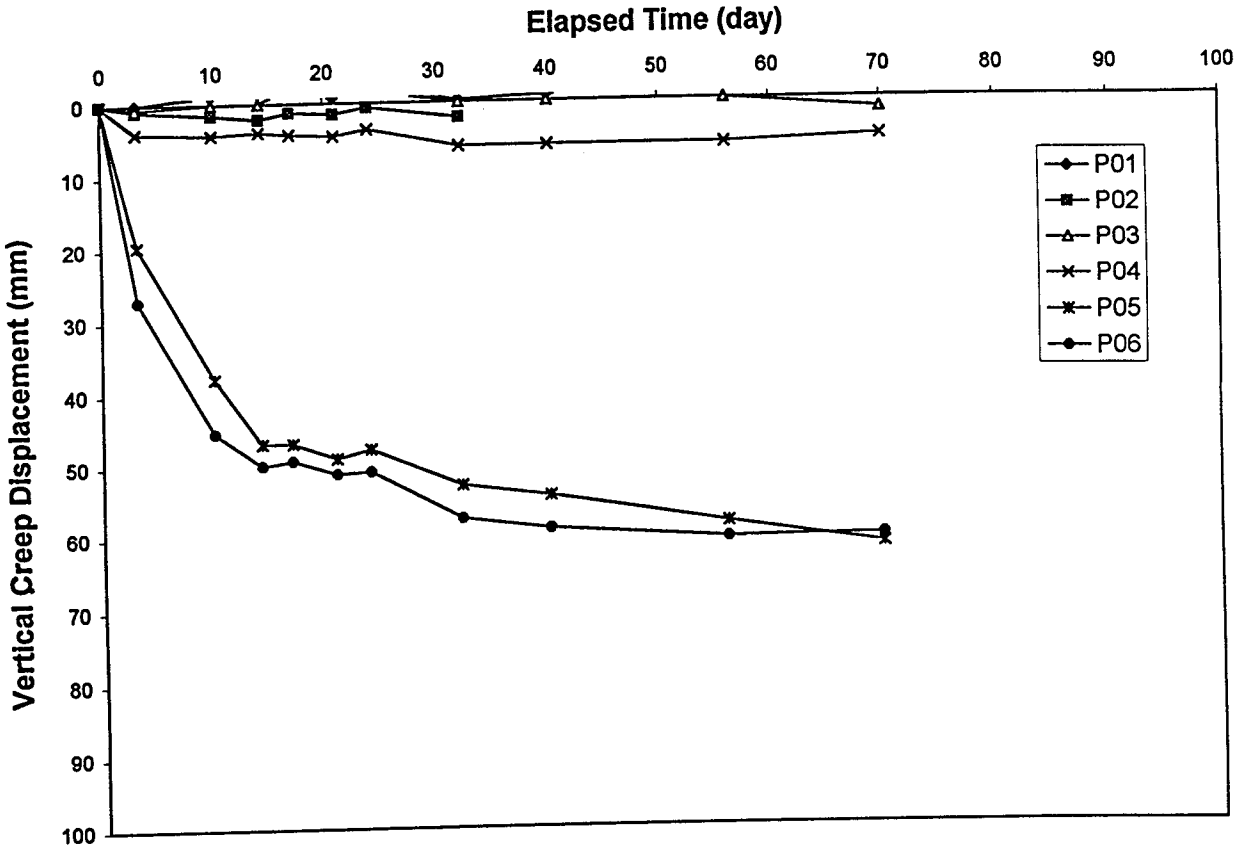

Figure 3.19 Vertical Creep Displacement vs. Time Relationships of the Outer Pier

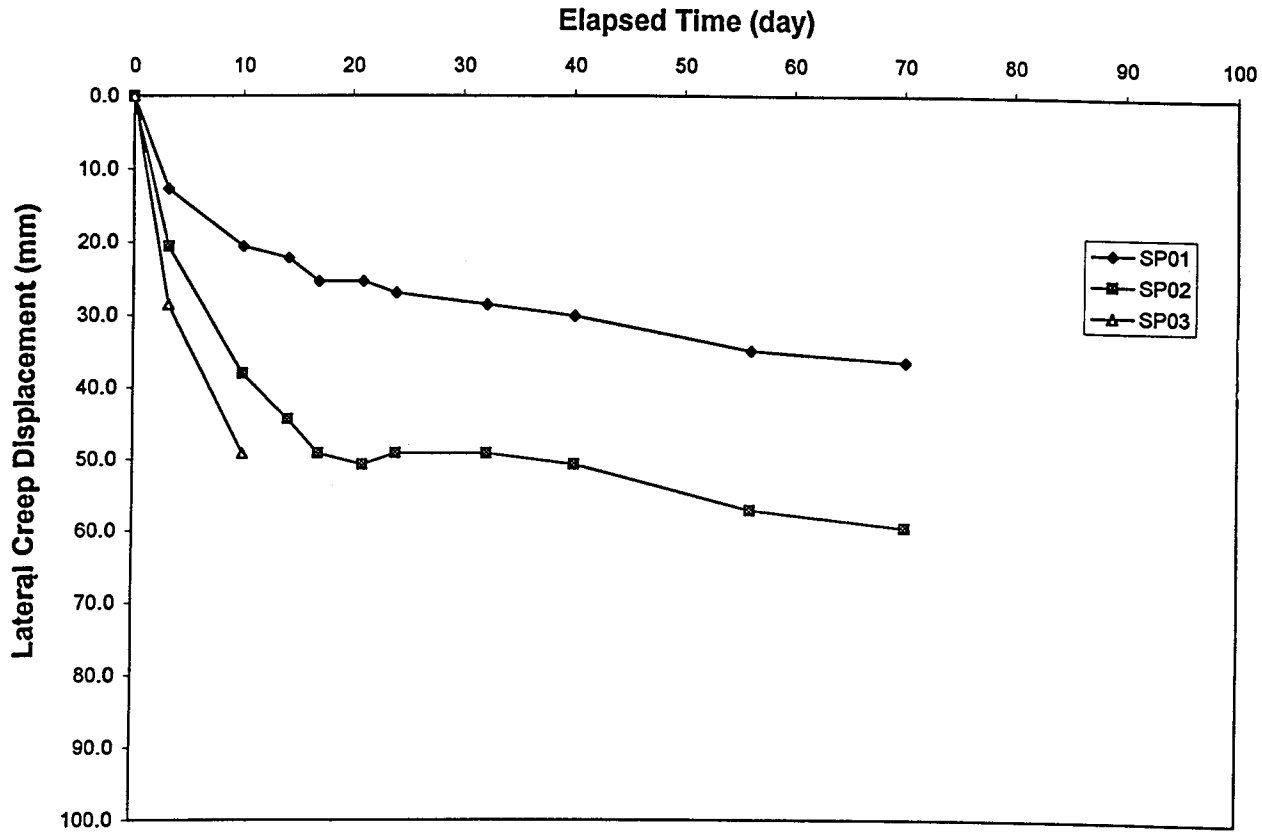

Figure 3.20 Lateral Creep Displacement vs. Time Relationships of the Outer Pier

plate used during construction.

Figure 3.21 shows the average vertical creep rate of the top-loading pad versus time relationships of the outer pier and the abutment plotted on a log-log scale. It is shown that, for the most part, the vertical creep rate of both structures reduced nearly linearly (on a log-log scale) with time. The vertical creep rates in the abutment reduced from 2.2 mm/day after 3 days to 0.03 mm/day after 70 days in the abutment. During the same period of time, the creep rate reduced from 7.5 mm/day to 0.1 mm/day in the outer pier. At around 25 days, both creep rates of the pier and the abutment significantly increased as shown in Figure 3.21. This behavior is attributed to softening of the frozen backfill due to a temperature increase following an extended period of freezing temperatures. Extrapolations of the average vertical creep rates were drawn as the shaded areas in Figure 3.21. The extrapolation may be used to obtain approximate creep rates beyond the measurement period. For instance, after a year, the vertical creep rates of the abutment and the outer pier were in the ranges of 0.003 mm/day to 0.008 mm/day and 0.012 mm/day to 0.06 mm/day, respectively.

3.6.2.2 Creep Strains in Reinforcement

Figure 3.22 shows the reinforcement creep strain distributions in layers A, B, and C (see Figure 3.7) of the abutment after 10, 25, and 70 days. The creep strain distributions were somewhat more uniform than the short-term reinforcement strain distribution. After 70 days, the maximum creep strains in layers A, B, and C were 0.30%, 0.75% (and 0.38%, respectively. Note that such maximum creep strains were also far from the rupture strain (18%) of the reinforcement.

Figure 3.23 shows the reinforcement creep strain distributions in layer A (both the warp and fill directions) and layer C (the warp direction) of the outer pier after 10, 25, and 70 days. A uniform strain distribution was assumed in the reinforcement of the outer pier. The average strain of each layer was shown in Figure 3.23. After 70 days the average creep strains of layer A were 0.20% and

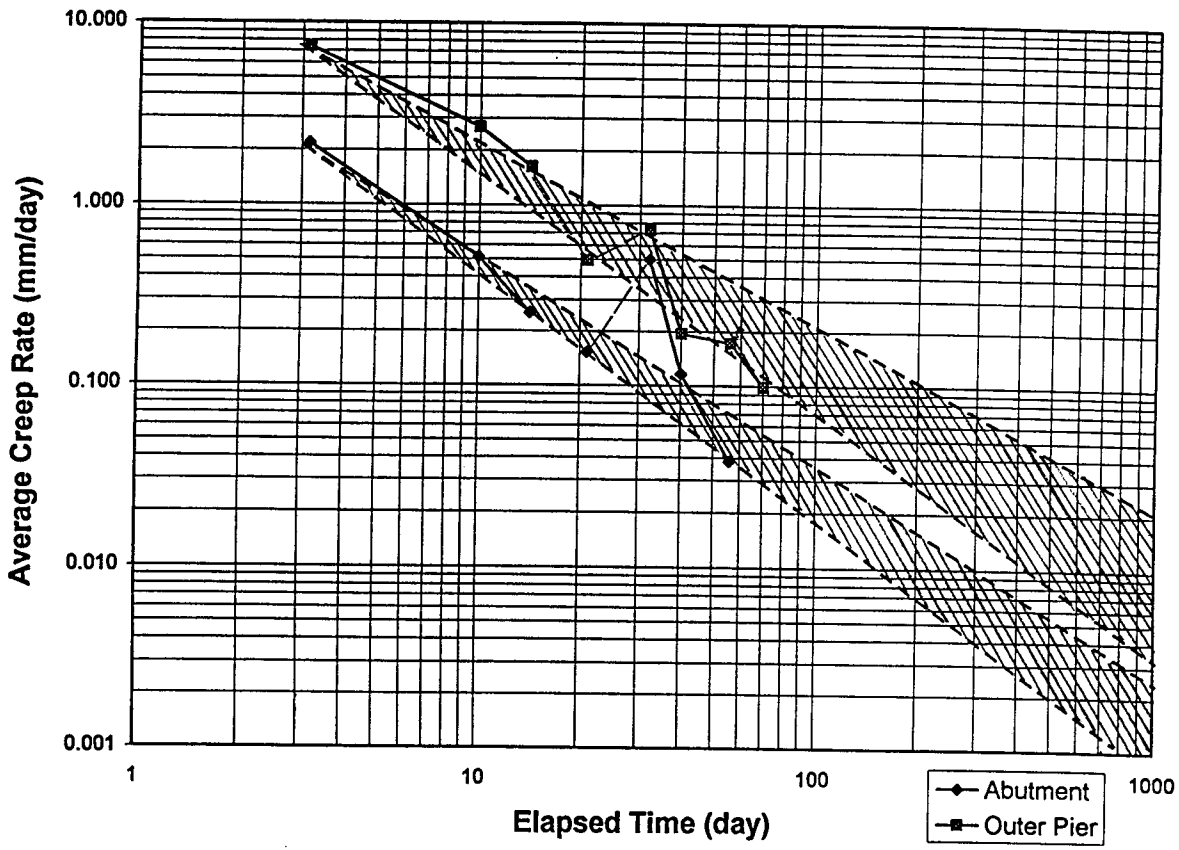

Figure 3.21 Average Lateral Creep Rate at the Top of the Outer Pier and the Abutment

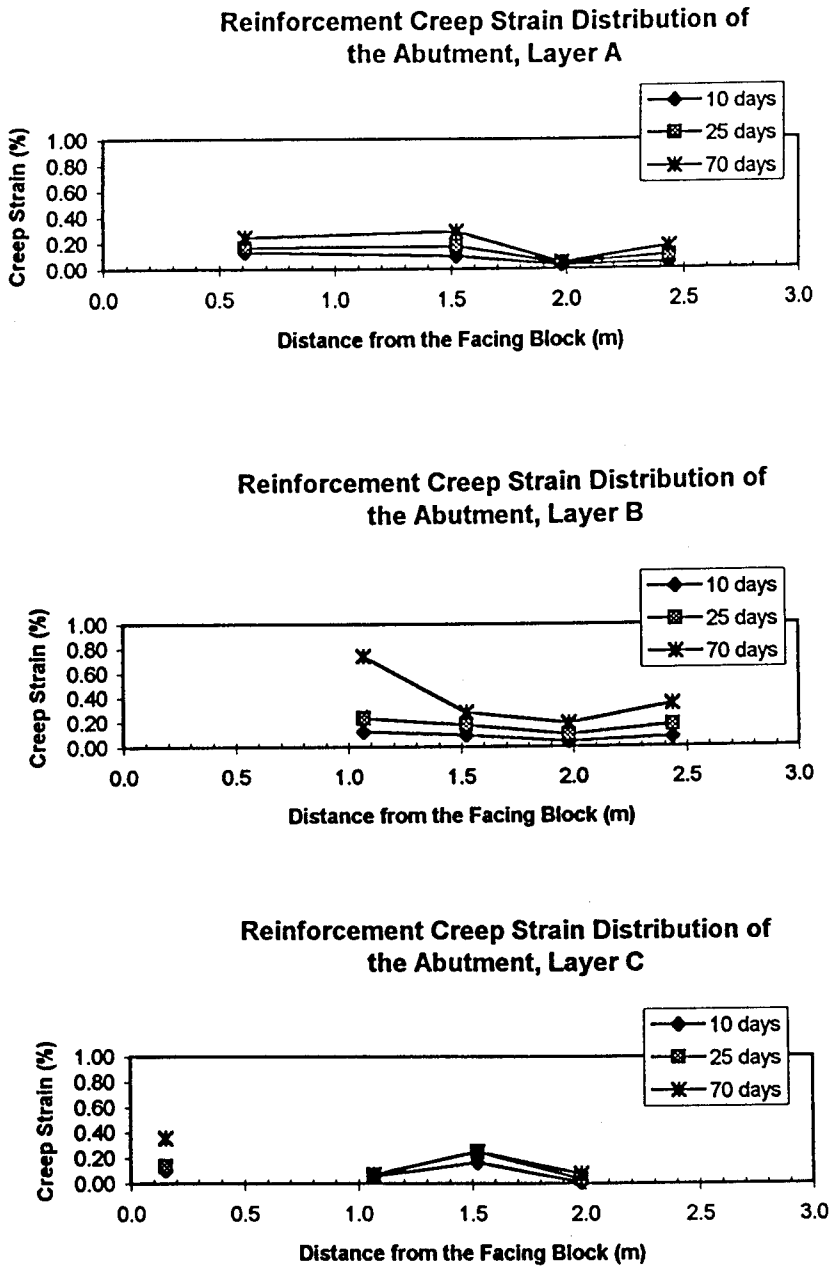

Figure 3.22 Reinforcement Creep Strain Distributions in the Abutment

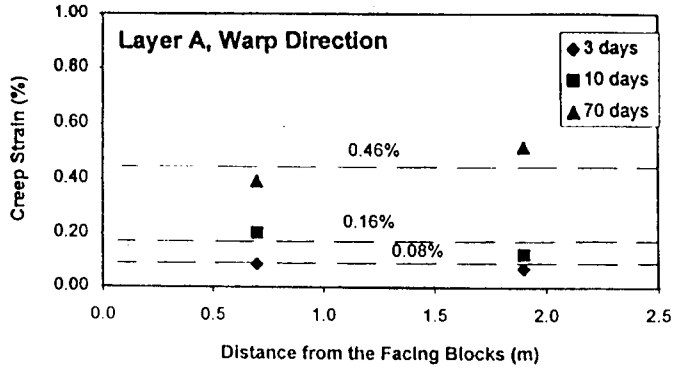

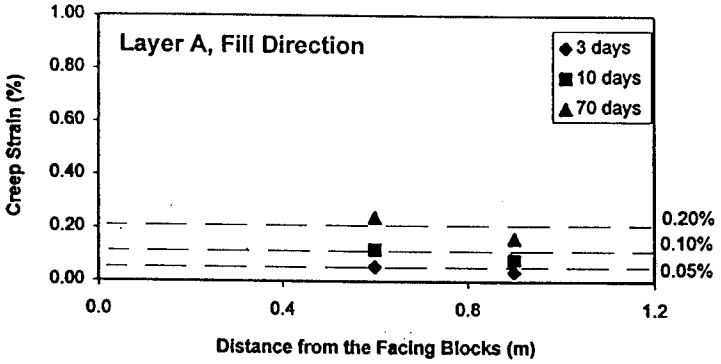

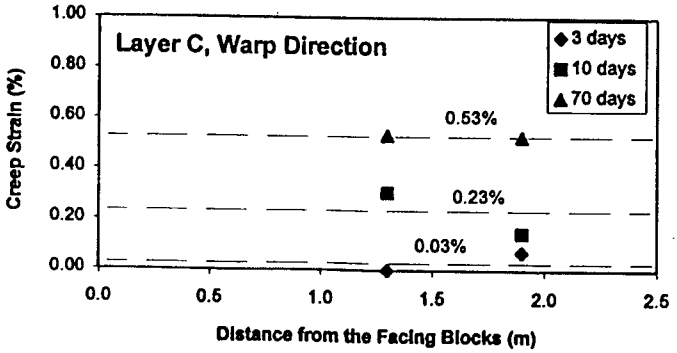

Figure 3.23 Reinforcement Creep Strain Distributions in the Outer Pier

0.46% in the fill and warp directions, respectively, and 0.53% in the warp direction of the layer C. The higher creep strains in the warp direction was mainly due to the fact that the geotextile is nearly twice as likely to creep in its warp direction (Ketchart and Wu, 1996).

From the average strains in layer A of the outer pier, the lateral creep displacements were calculated and compared to the measured lateral creep displacements. The comparison is shown in Figure 3.24. It is seen that the calculated lateral creep displacements (from the strain distributions) were in very good agreement with the measured displacements.

3.7 Summary and Conclusions

A GRS bridge abutment and two GRS bridge piers were constructed inside a 3.5-m deep pit. The structures were constructed with a "road base" backfill reinforced with layers of a woven geotextile. Hollow-cored concrete blocks were used as facing. One of the piers (i.e. the outer pier) and the abutment, both 7.6 m in height, were load tested. The load was applied using concrete barriers stacked in seven layers over three steel bridge girders. A total load of 2,340 kN, corresponding to 232 kPa pressure, was applied. The pier and the abutment were instrumented with metal pipes and elastic springs to monitor the vertical and lateral movement of the facing, and strain gages to monitor deformation of the reinforcement. The findings are summarized as follows:

- Construction of the GRS pier and abutment is indeed rapid and simple.
- Load carrying capacities of the pier and the abutment were higher than the 200 kPa maximum pressure suggested by the FHWA Demo 82 (1996).
- The displacements at 1,170 kN of the pier and the abutment were comparable. The maximum vertical displacement was slightly higher in the outer pier than in the abutment. The maximum vertical displacements were 27.1 mm in the abutment and 36.6 mm in the outer pier, corresponding, respectively, to 0.35% and 0.48% of the structure height. The maximum lateral displacement in the abutment was somewhat higher than that in the outer pier. The maximum lateral elongation of the perimeter was 4.3 mm in the abutment and 12.7 mm

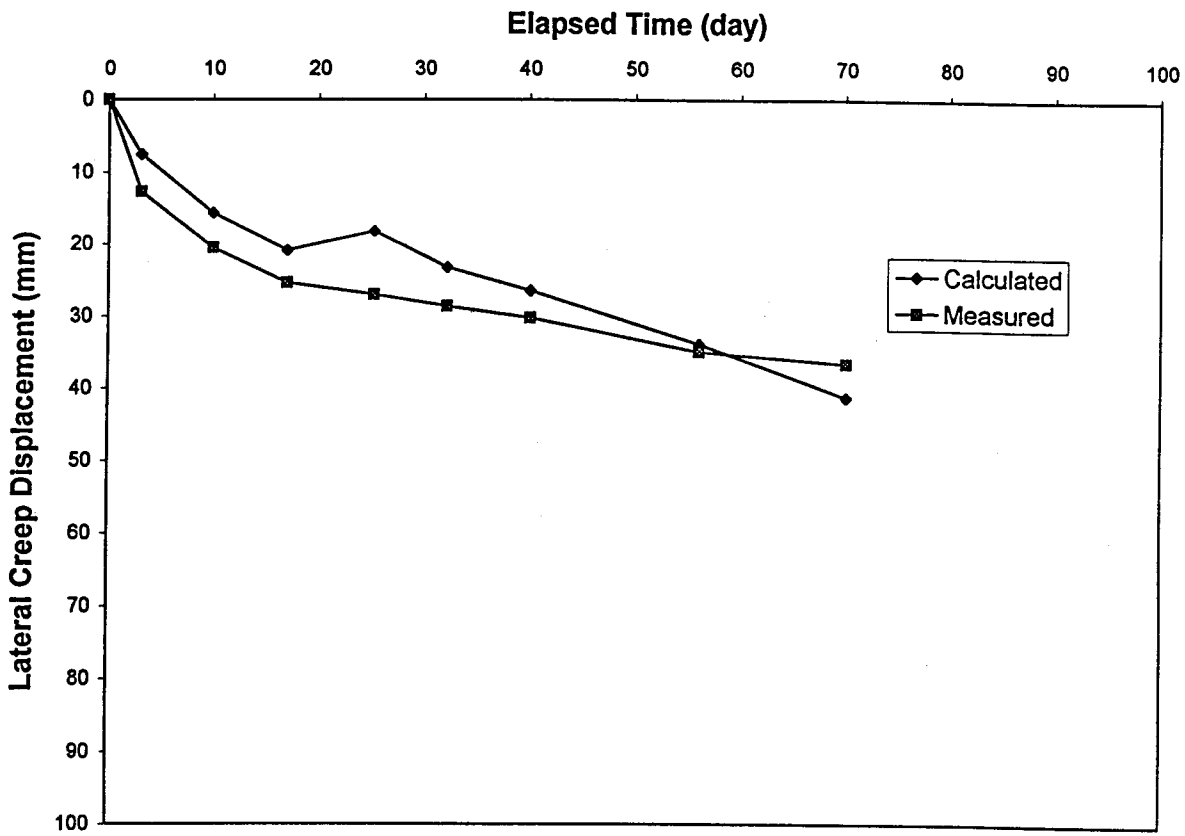

Figure 3.24 Calculated vs. Measured Lateral Creep Displacements of the Outer Pier

in the outer pier.

- The ratio of the vertical movement to the structure height at 232 kPa of the outer pier (0.48%) was higher than that of the Turner-Fairbank pier (0.30%) at the same applied pressure. This may be attributed to the much lower compaction effort on the outer pier. The reinforcement strains in the fill direction of the outer pier and the Turner-Fairbank pier, however, were on the same order of magnitude (0.2% to 0.4%). This implies that the lateral movements of both piers are comparable.
- Under a sustained load of 1,170 kN for 70 days, the creep displacements in both vertical and lateral directions of the outer pier were about four times larger than those in the abutment, due to lower compaction effort of the outer pier. The maximum vertical creep displacement was 61.6 mm in the outer pier, and 18.3 mm in the abutment. The maximum lateral creep displacement was 59.5 mm in the outer pier and 14.3 mm in the abutment.
- A significant portion of the maximum vertical and lateral creep displacements of the pier and the abutment occurred in the first 15 days. At 15 days, the maximum vertical and lateral creep displacements were about 70% to 75% of the creep displacements at 70 days in respective directions.
- Creep deformation of the structures decreased with time. The vertical creep rates reduced nearly linearly (on log-log scale) with time. The creep rate of the outer pier (7.5 mm/day after 3 days, and 0.1 mm/day after 70 days) was higher than that of the abutment (2.2 mm/day after 3 days, and 0.03 mm/day after 70 days).
- Hairline cracks of the facing blocks occurred in the outer pier and the abutment due to the lateral bulging and the down-drag force due to the friction between the backfill and the facing blocks. Installing flexible material (i.e., cushion) between vertically adjacent blocks may alleviate this problem.

- The maximum strains in the reinforcement were less than 1.0%. Compared to the rupture strain of the reinforcement of 18%, the safety margin against rupture of reinforcement appeared to be very high.
- The calculated lateral displacements from the reinforcement strain distribution were in very good agreement with the measured lateral displacements.
- With the less stringent construction condition (using a light-weight vibrating compaction plate), the outer pier showed about 1.5 times larger vertical displacement-to- height ratio than the Turner-Fairbank pier; whereas the lateral displacements were similar.

Chapter 4
THE BLACK HAWK ABUTMENT

4.1 Overview

Two GRS bridge abutments were constructed to support the Bobtail Road bridge, a 36- m span steel arched bridge, in Black Hawk, Colorado. The abutments were situated along a hill slope over a dry creek. The two abutments are on the east and west sides of the creek.

As shown in Figure 4.1, each GRS abutment comprised a two-tier rock-faced geosynthetic-reinforced soil mass, two square footings (on the lower tier), and a strip footing (on the upper tier). The square footings on the West abutment are referred to as Footing #1 and #4; whereas the square footings on the East abutment are referred to as Footing #2 and #3. The abutments were constructed with the on-site soil and reinforced with layers of a woven geotextile at a vertical spacing of 0.3 m. The front edge of each reinforcement sheet was placed between vertically aligned rocks at the wall face to form a frictional connection between the reinforcement layers and the facing rocks.

The GRS bridge abutments were constructed on a stiff soil. The base of the reinforced soil mass was located at different depths of the excavated stiff soil as shown in Figures 4.2. The thickness of the lower tier reinforced soil mass under Footing #1 and #4 were, respectively, 4.5 m and 1.5 m, and 7.5 m and 1.5 m under Footing #2 and #3, respectively (see Figure 4.2). The lower part of the GRS abutment was embedded in the ground, and the upper part was above ground. Only the portion above ground was constructed with rock facing. The above-ground portion of the abutment had different heights, varying from 1.0 m to 2.7 m for the West abutment; and from 1.0 m to 5.4 m for the East abutment (see Figure 4.3). The thickness of the upper tier reinforced soil mass was 1.8 m for both abutments. The upper tier reinforced soil mass was built to support the strip footing and the approaching ramp.

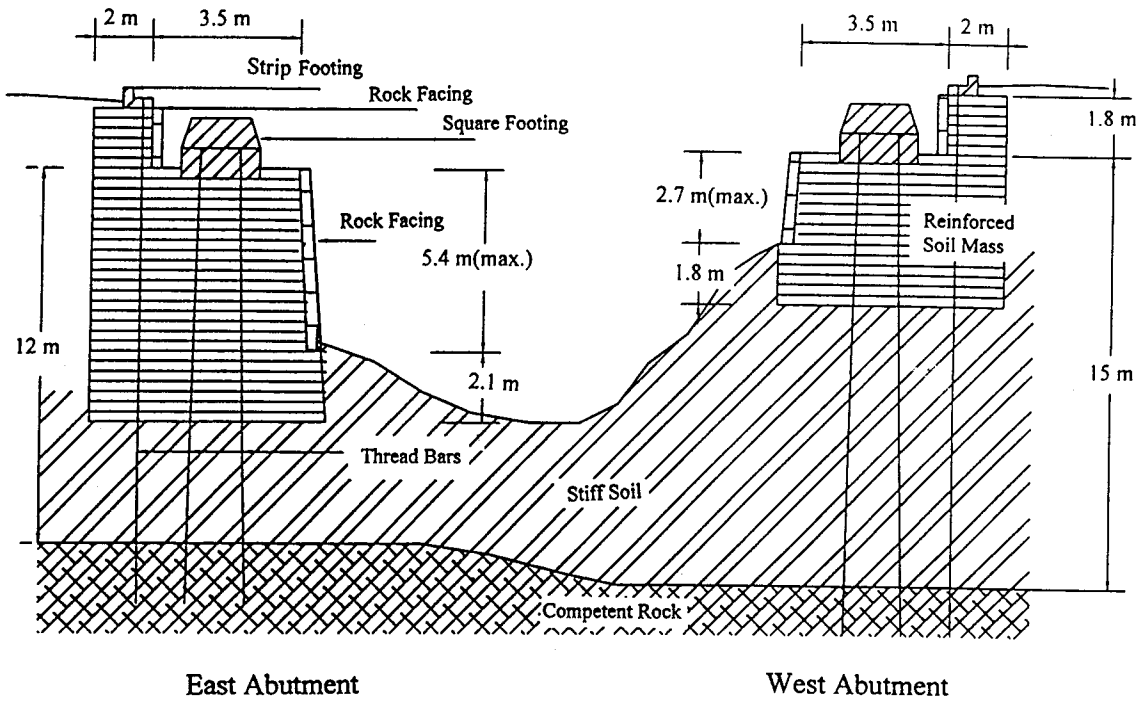

Figure 4.1 Configuration of the Black Hawk Abutment

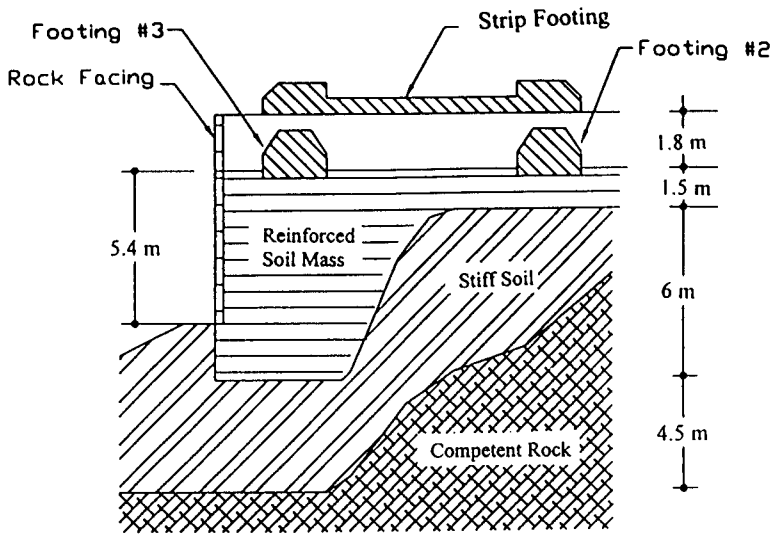

(a) East Abutment (due East)

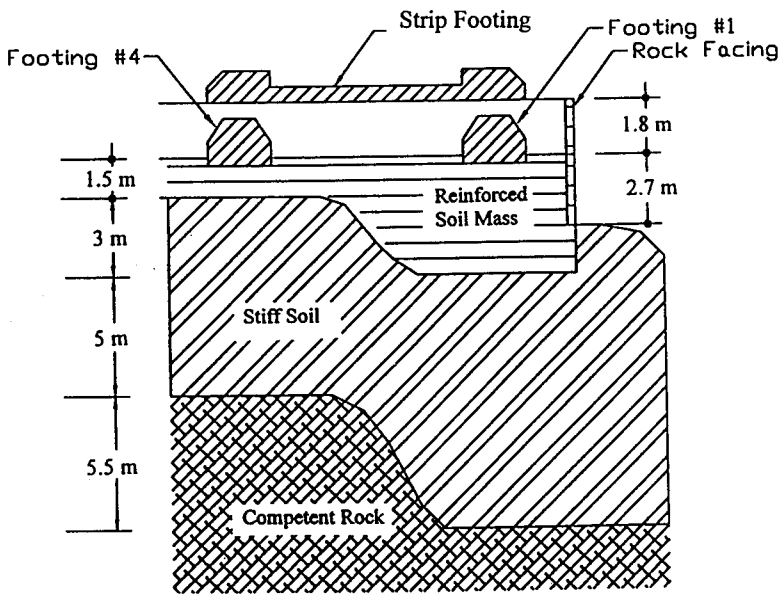

(b) West Abutment (due West)

Figure 4.2 Cross Sections of (a) East Abutment and (b) West Abutment

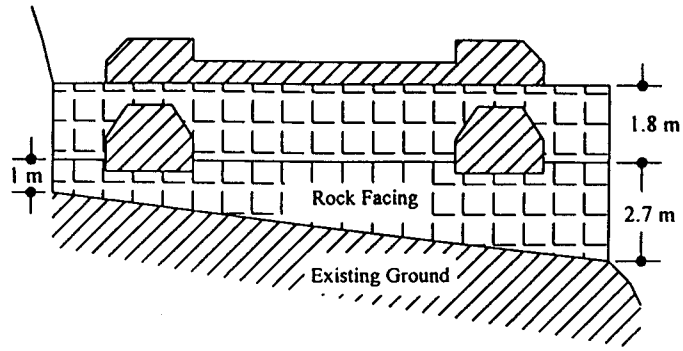

(a) West Abutment (due West)

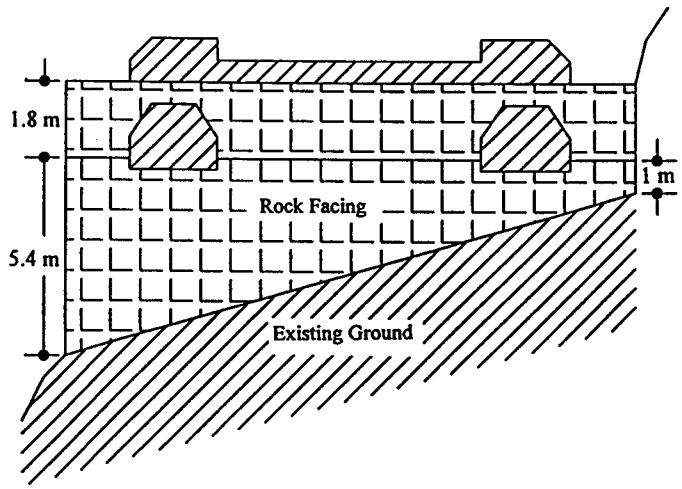

(b) East Abutment (due East)

Figure 4.3 Thickness of the GRS Abutments : (a) West Abutment and (b) East Abutment

The square footing was 2.4 m by 2.4 m with thickness of 1.65 m. The center to center distance between the square footings was 9.6 m, as shown in Figure 4.4. The front edge of square footings was 1.5 m behind the rock-faced wall. The square footings were constructed in two stages. The bottom part (0.6-m thick) of the footing was first constructed to serve as a reaction pad for pre-loading. The top part (1.05-m thick) was poured and leveled after pre-loading was completed. The strip footing was 12.0 m by 0.9 m with thickness of 0.45 m. The design loads of the square and the strip footings were 890 kN and 445 kN, respectively.

In October 1997, the GRS bridge abutments were pre-loaded. The main purpose of the preloading was to limit the post-construction settlement of the GRS abutments under service conditions.

4.2 Construction Materials

4.2.1 Backfill

The backfill was classified as SM-SC per ASTM D2487. It has 12% of fine particles (passing sieve #200). The gradation curve is shown in Figure 4.5. The plasticity index and the liquid limit were 6 and 27, respectively. The maximum dry density was 19.5 kN/m^3 with the optimum water content being 14.2% per ASTM D698. Three consolidated-drained triaxial compression tests were conducted with specimen dimensions of 152 mm in diameter and 305 mm in height. The specimen was prepared at a dry density of 15.8 kN/m^3 (91% relative compaction) with a water content of 12.2%, which were considered representative of the field condition. The results of the triaxial compression tests are shown in Figure 4.6. The internal friction angle (ϕ) was 31.3° and the cohesion was 34.3 kPa.

4.2.2 Geotextile Reinforcement

The reinforcement was a prolyproplylene woven geotextile, Amoco 2044. The wide width tensile strengths in both fill and warp directions are 70 kN/m. Some index properties of the geotextile reinforcement as provided by the

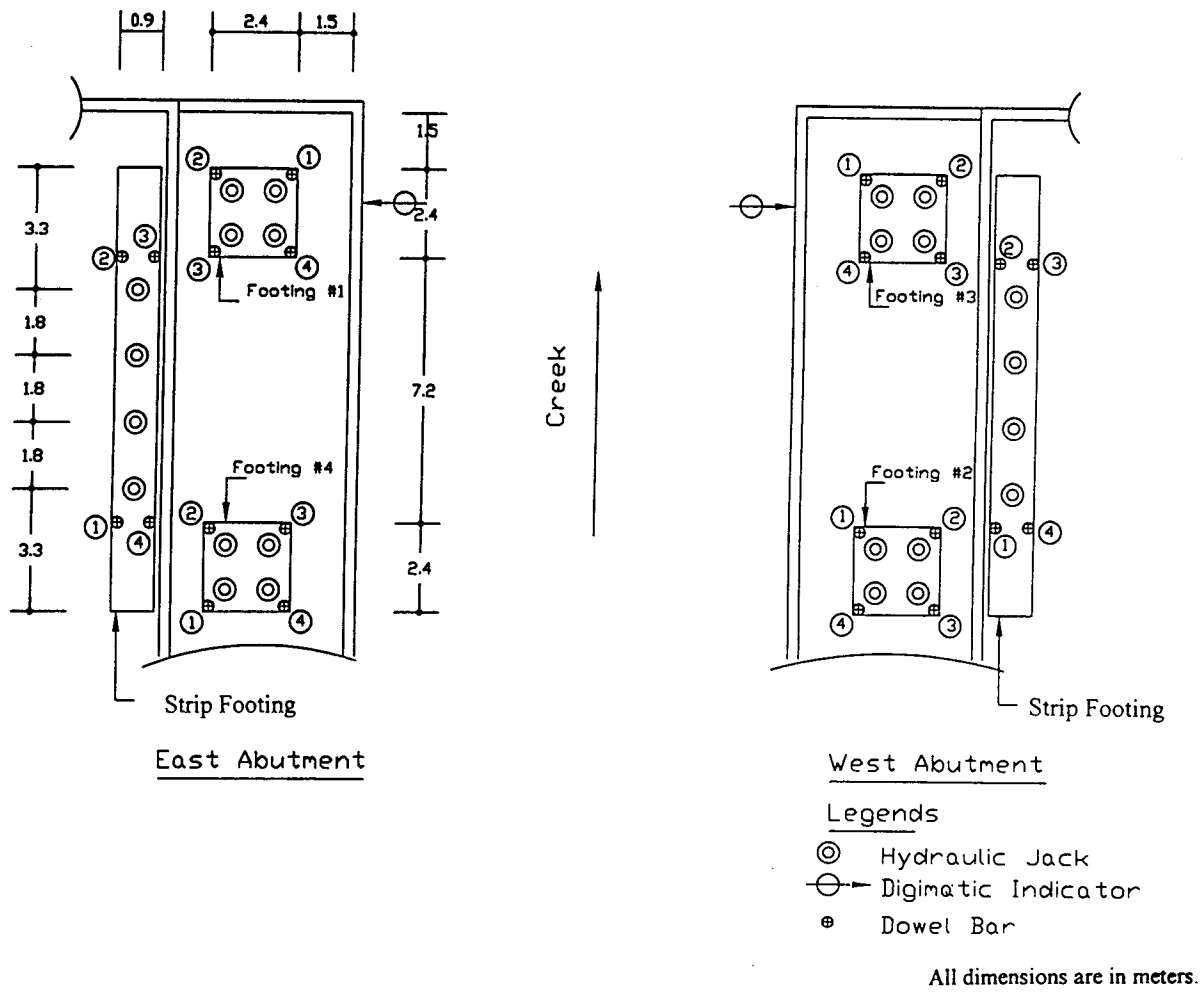

Figure 4.4 Plan View of the Footings and Preloading Arrangement

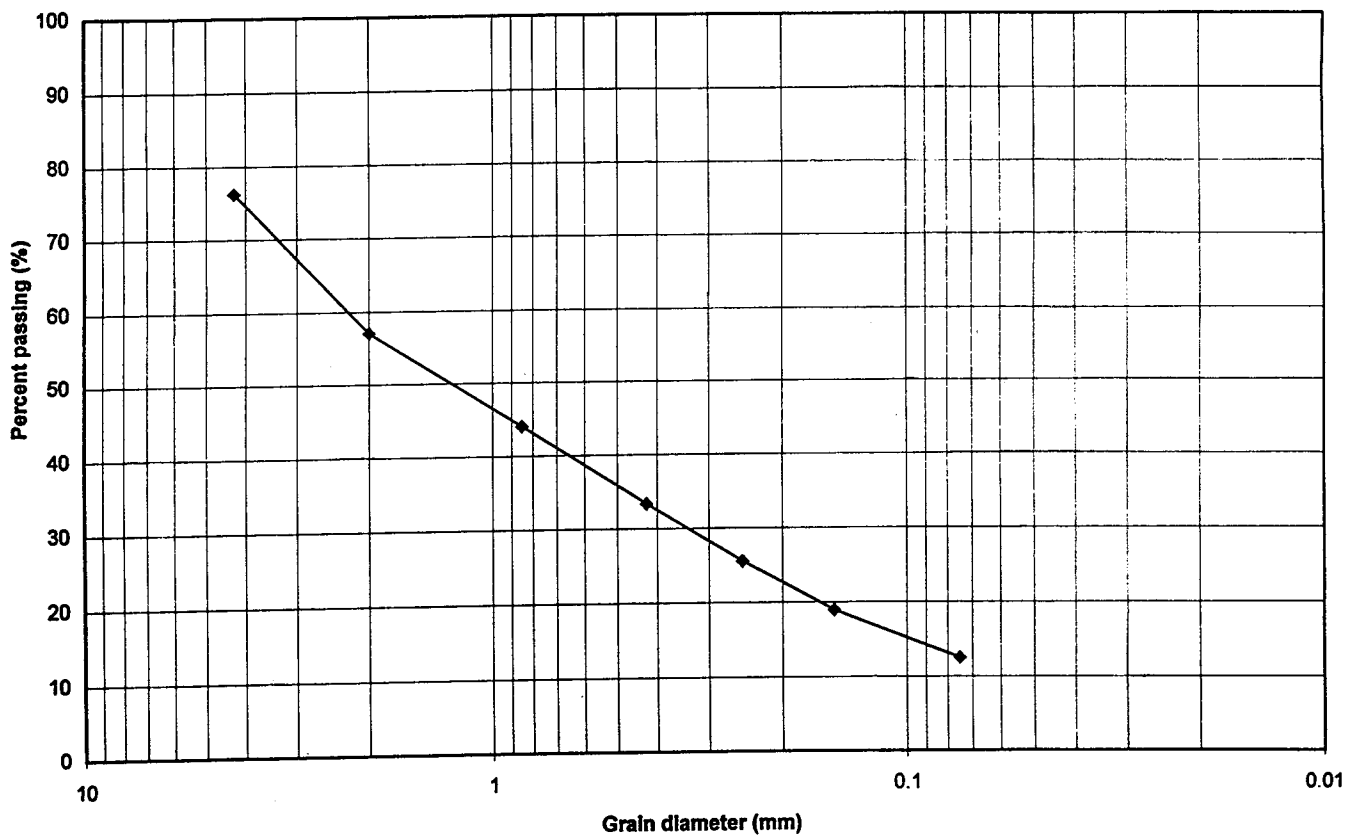

Figure 4.5 Gradation of Backfill

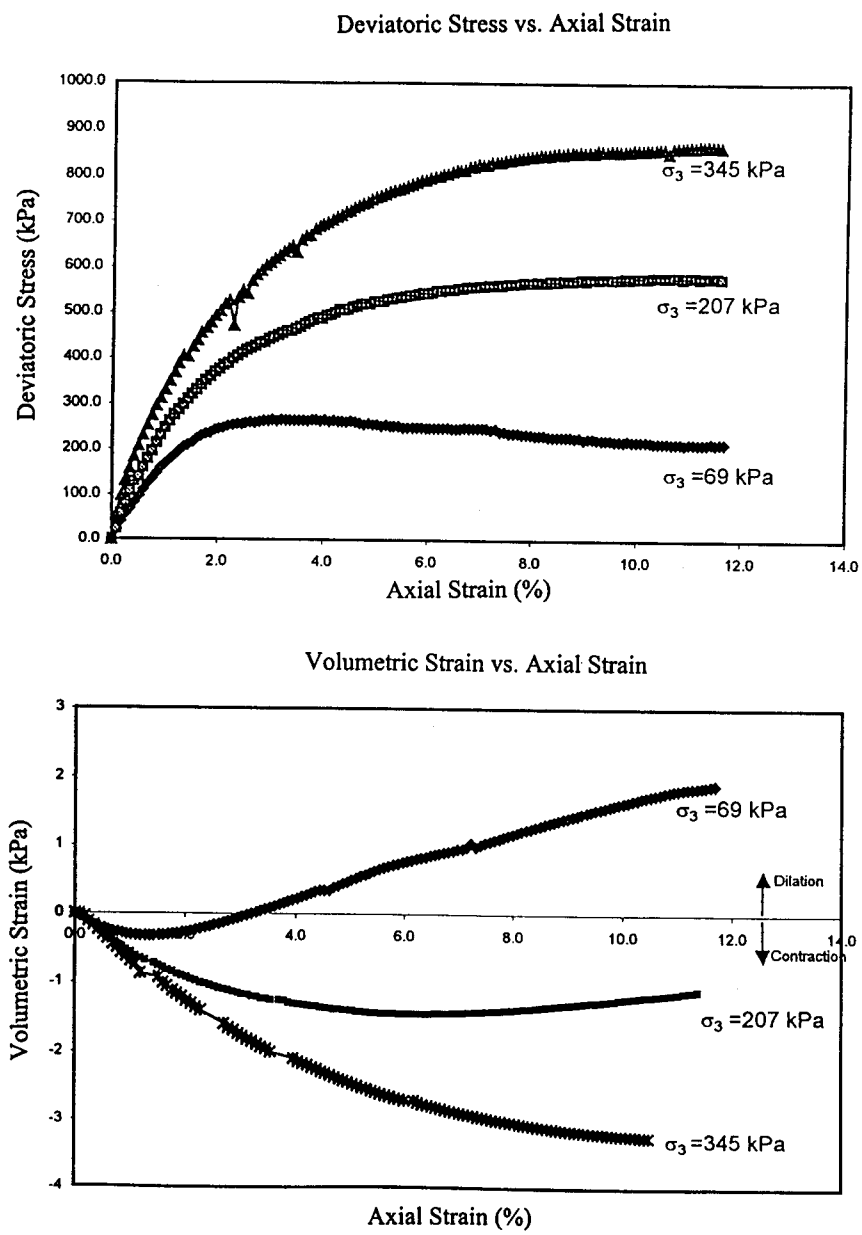

Figure 4.6 (a) Deviatoric Stress vs. Axial Strain Relationships and
(b) Volumetric Strain vs. Axial Strain Relastionships

manufacturer are shown in Table 3.1.

4.3 Instrumentation

A number of instruments were employed to monitor vertical settlements of the footings, lateral movement of the rock facing, and strains in the geotextile reinforcement during the preloading tests. The layout of the instrumentation is shown in Figure 4.7. The vertical settlement was monitored by using a precision survey transition to measure settlement of scaled dowel bars installed at four corners of each footing (see Figure 4.4). The lateral movement of the rock-faced wall was measured with digimatic indicators. The digimatic indicators were installed along the height of a fixed post in front of the wall face, as depicted in Figure 4.7. The digimatic indicators were installed at 0.6 m, 1.5 m, and 2.4 m from the base of the 2.7-m high wall on the West abutment and at 1.2 m, 2.1 m, and 3.3 m from the base of the 5.4-m high wall on the East abutment.

High elongation strain gages (WK-13-250BG-350 gage type) were used to measure the strains in the geotextile reinforcement. Four strain gages were mounted along the fill direction of each instrumented sheet of reinforcement for the 1.8-m tall GRS wall on the west abutment. There were three sheets of instrumented geotextile reinforcement, located at 0.3 m, 0.6 m, and 1.2 m from the base of the wall.

Each strain gage was glued to the geotextile only at the two ends to avoid inconsistent local stiffening of the geotextile due to the adhesive. The gage was first mounted on a 25 mm by 76 mm patch of a lightweight nonwoven geotextile. The lightweight geotextile patch, with a strain gage and covered with wax, was then attached to the geotextile reinforcement at selected locations. A microcrystalline wax was applied over the gage to protect it from percolation of moisture.

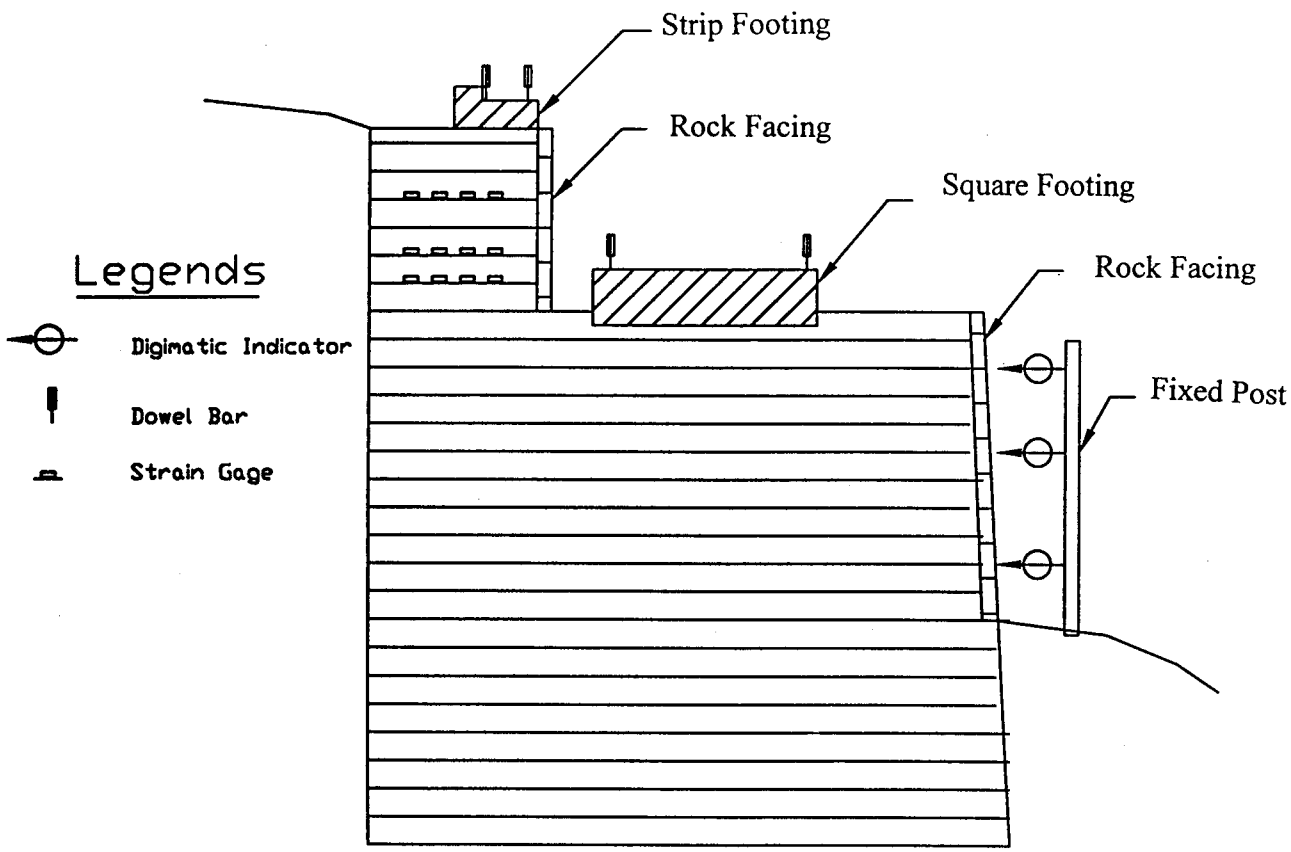

Figure 4.7 Layout of Instrumentation

4.4 Preloading Configuration and Loading Sequence

The test setup for preloading a footing, consisted of four high-strength thread bars, four steel reaction plates, and four hydraulic jacks, is shown in Figure 4.8. After construction of the GRS abutments, the thread bars were penetrated through the footing and the reinforced soil mass and anchored 3 m into a competent bedrock below the stiff soil layer. The reinforced mass was, thus, sandwiched between the footing and the competent rock layer. Upon applying pressure to the hydraulic jacks, the reinforced soil mass was "squeezed" between the footing and the bedrock.

Figure 4.9(a)-(d) shows the loading sequences of Footings #1, #2, #3, and #4, respectively. Typically, a vertical load was incrementally applied on top of each square footing by the hydraulic jacks. A vertical pressure was of 245 kPa (1.6 times of the design load of 150 kPa) was applied and sustained for 100 minutes then unloaded to zero. This first loading cycle is referred to as the "preloading cycle." Three loading-unloading cycles, referred to as "the reloading cycles" typically followed the preloading cycle. In the reloading cycles, the typical applied pressure was the design load (150 kPa).

Figure 4.9(e) shows the loading sequence of the strip footing. A vertical load was increased incrementally to 80 kPa (2 times the design load of 40 kPa), sustained for 120 minutes, then unloaded to zero. The vertical load applied in the reloading cycle was 40 kPa (the design load). The load was maintained for 120 minutes before unloading.

4.5 Test Results and Discussions

The results of loading tests on the square footings and the strip footings as well as the discussions of the test results are presented in this section.

4.5.1 Loading Tests on the Square Footings

Figure 4.10 shows the settlement at four corners of Footings #1, #2, #3, and #4 versus applied pressure relationships. At 245 kPa, the maximum settlements of Footings #1, #2, #3, and #4 were, respectively, 39 mm, 20 mm, 87

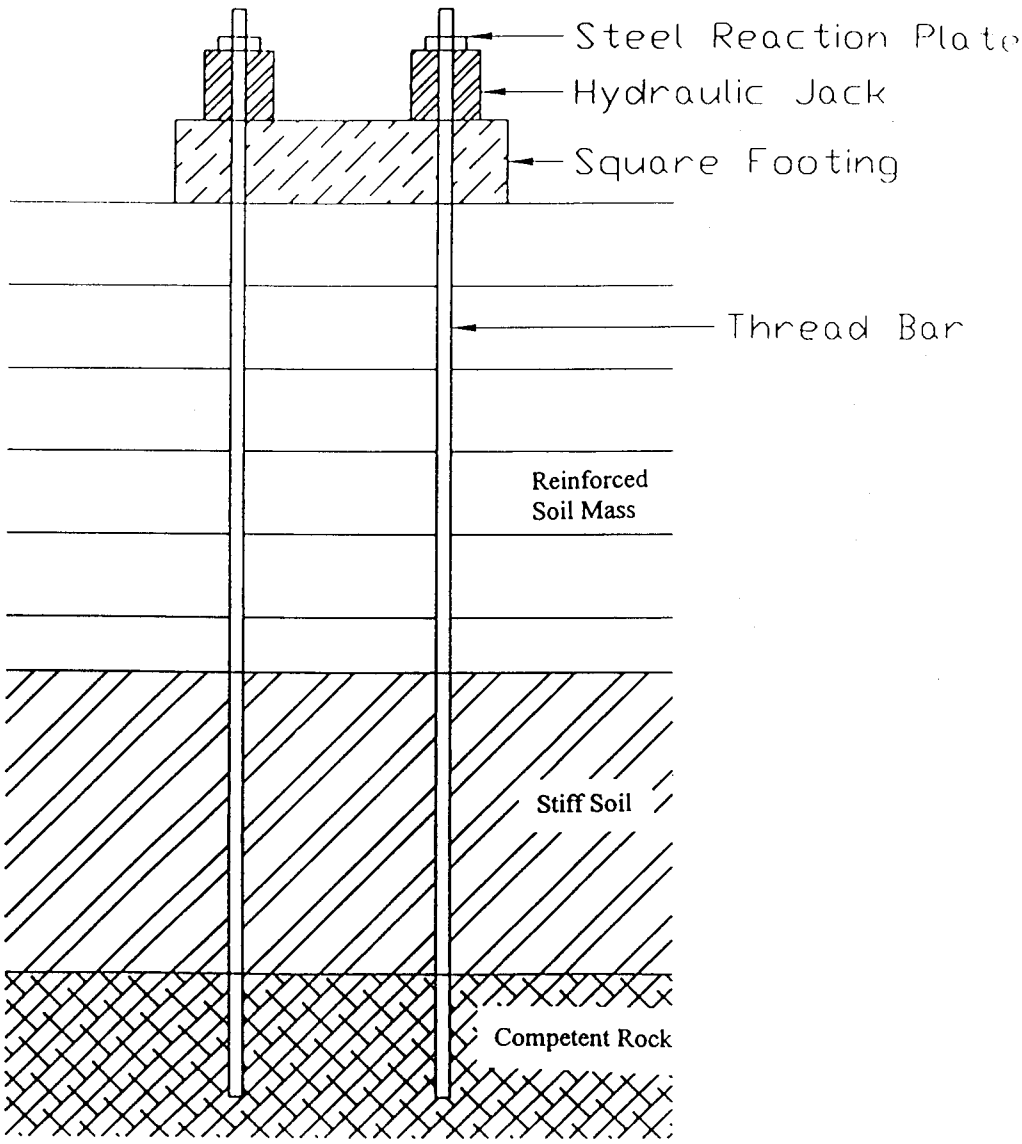

Figure 4.8 Setup for Preloading

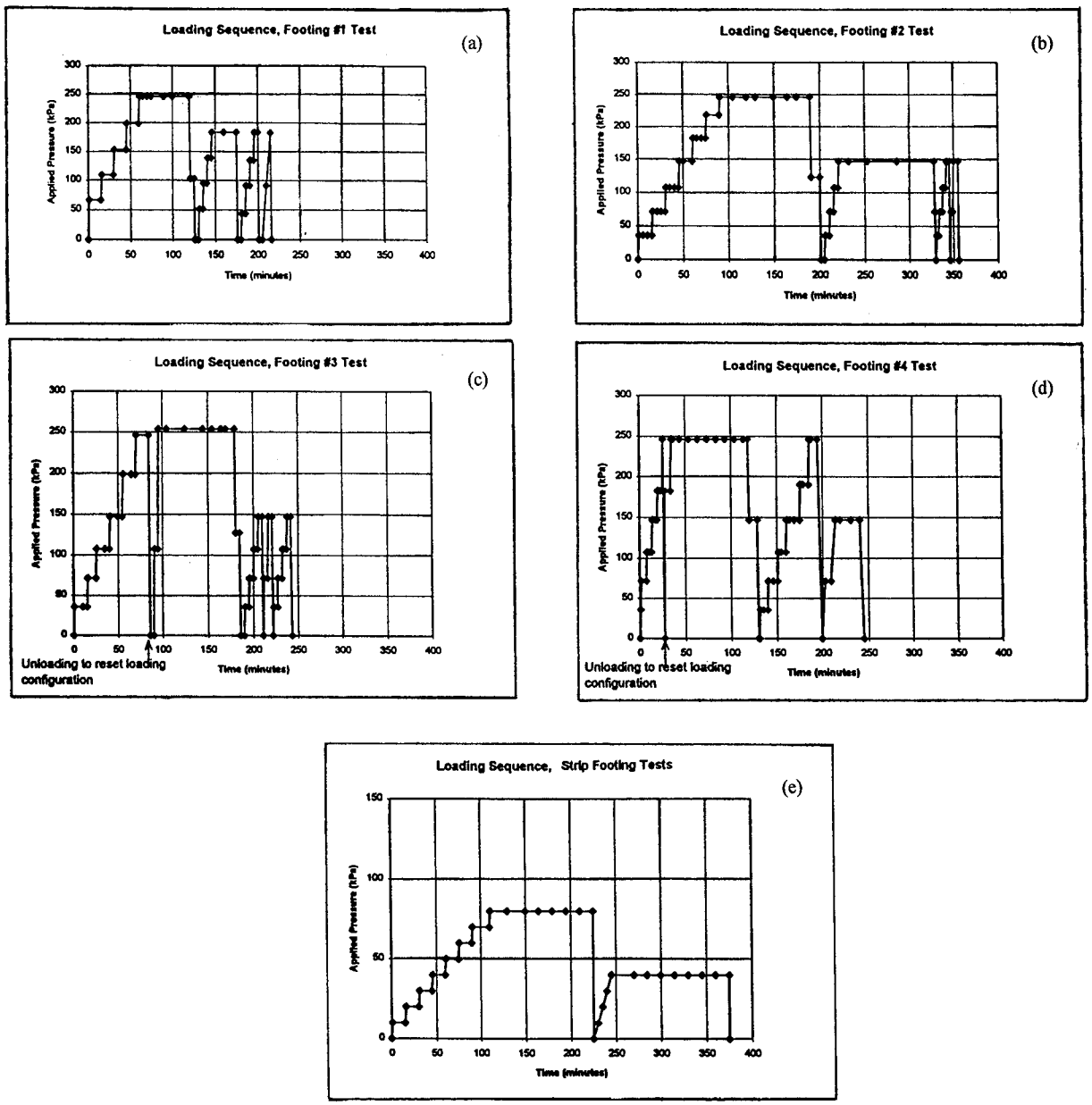

Figure 4.9 Loading Sequence Used for Each Footing

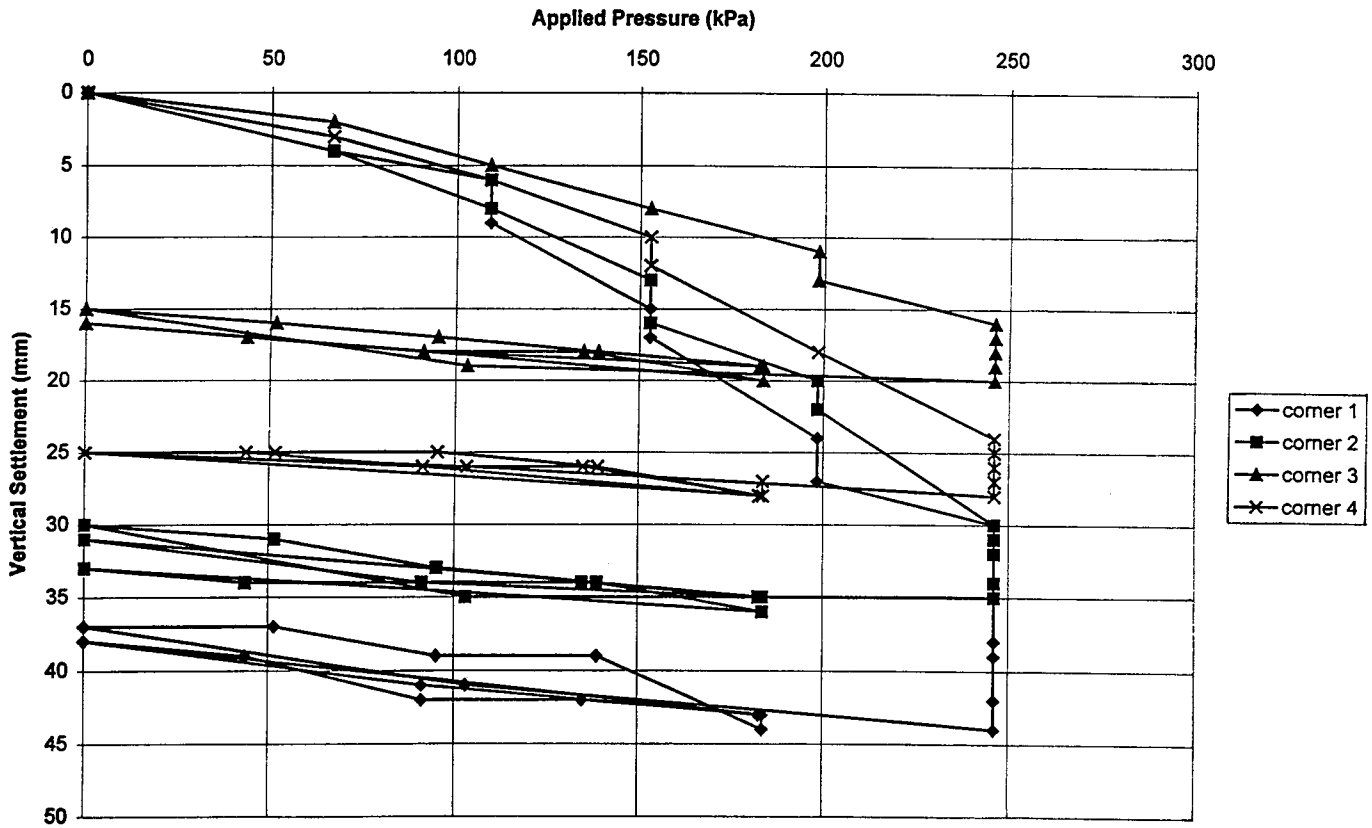

Figure 4.10(a) Relationships Between Settlement at Four Corners of Footing 1 and Applied Pressure

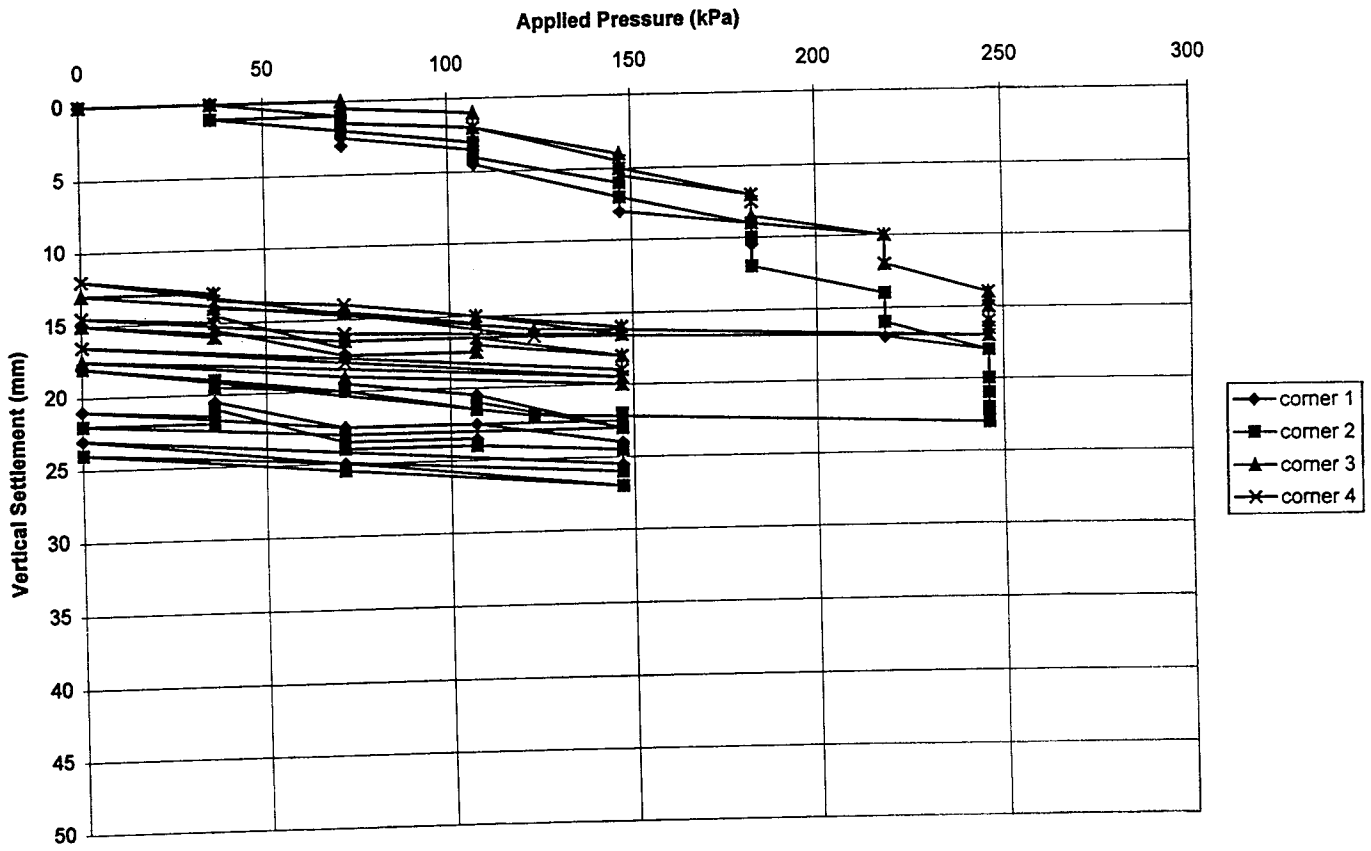

Figure 4.10(b) Relationships Between Settlement at Four Corners of Footing 2 and Applied Pressure

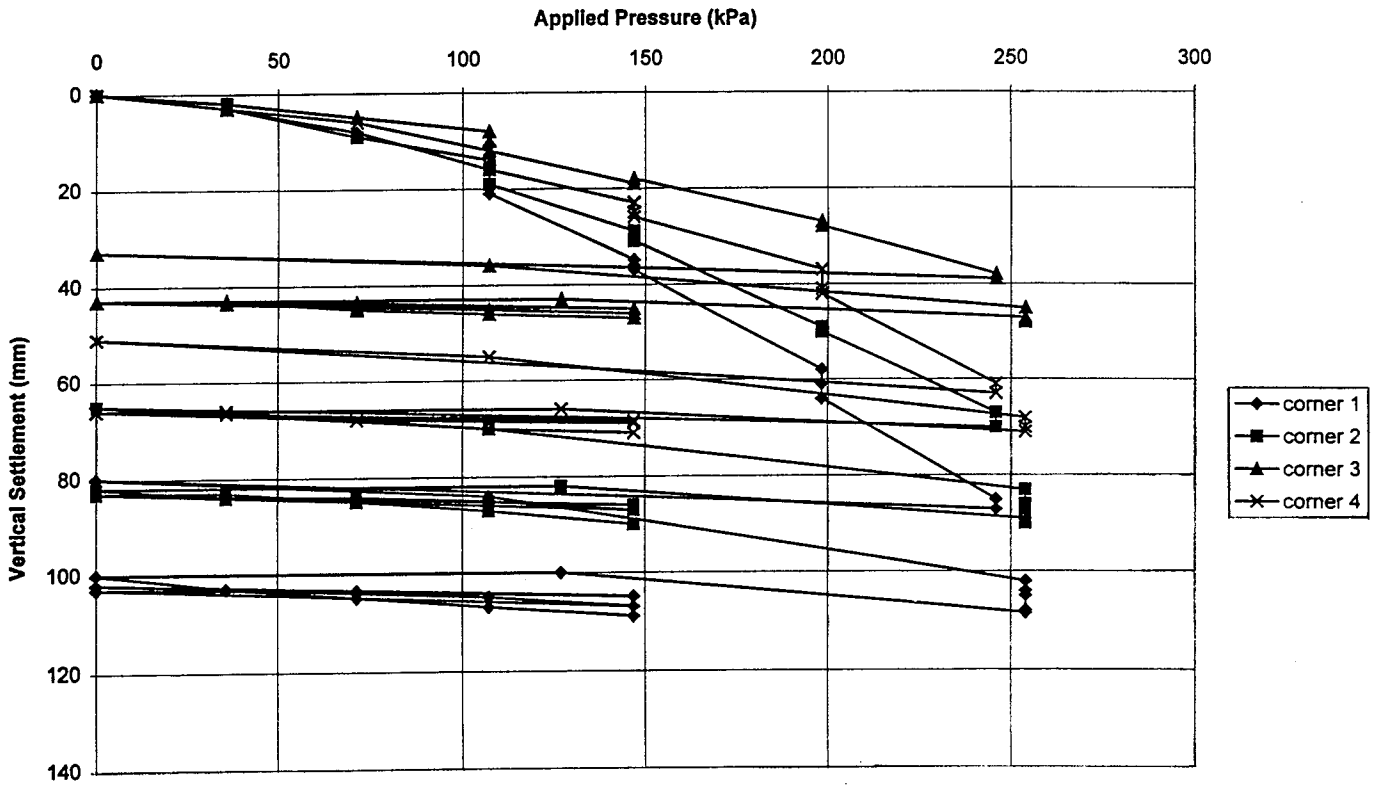

Figure 4.10(c) Relationships Between Settlement at Four Corners of Footing 3 and Applied Pressure

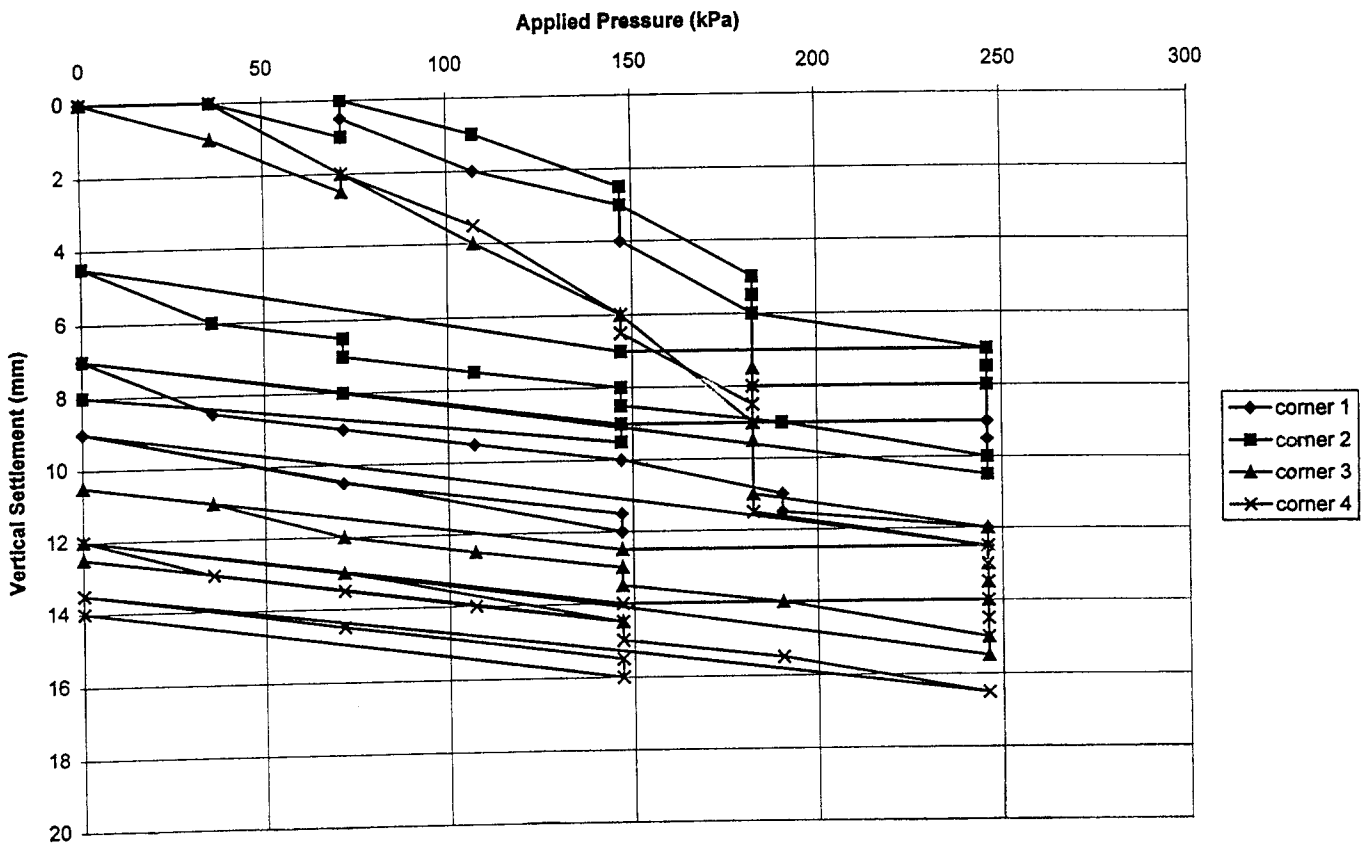

Figure 4.10(d) Relationships Between Settlement at Four Corners of Footing 4 and Applied Pressure

mm, and 13.5 mm. These maximum settlements occurred at the corner #1 (see Figure 4.4) of Footings #1, #2, and #3 and at the corner #3 (see Figure 4.4) of Footing #4. This is because these corners were adjacent to the least lateral constraint boundary of the GRS abutments.

At 150 kPa of the preloading cycle, the maximum differential settlements within Footings #1, #2, #3, and #4 were, respectively, 9 mm, 2.5 mm, 19.0 mm, and 3.5 mm. At 150 kPa of the reloading cycle, the maximum differential settlements were reduced to 3.0 mm, 1.0 mm, 4.0 mm, and 3.3 mm for Footings #1, #2, #3, and #4. The reduction in the differential settlements indicates that the preloading alleviated tilting of the footings which may be a result of an eccentrically applied load and/or non-uniformity of the soil foundation.

Figure 4.11 shows the relationship between the average settlement of each square footing and the applied pressure. The settlements increased with increasing applied pressure. At 150 kPa (the design load) of the preloading cycle, the average settlements were 13.3 mm and 4.9 mm in Footings #1 and #4 (West abutment) and 6.4 mm and 28 mm in Footings #2 and #3 (East abutment). At 245 kPa of the preloading cycle, the average settlements were 29.5 mm and 10.9 mm in Footings #1 and #4, and 17.1 mm and 64.8 mm in Footings #2 and #3. At 150 kPa of the first reloading cycle, the average settlements were 2.5 mm and 3.3 mm in Footings #1 and #4 and 3.8 mm and 4.5 mm in Footings #2 and #3. These results revealed that, by preloading the reinforced soil mass to 1.6 times the design load, the settlements of the square footings at the design load was reduced by factors of 1.5 in Footings #2 and #4, and 4 to 6 in Footings #1 and #3. The reduction in the settlement was minute in the subsequent reloading cycles.

The differential settlements between the two footings were 8.4 mm on the West abutment and 21.6 mm on the East abutment. Such differential settlements were primarily due to the different thickness of the reinforced soil mass (4.5 m and 1.5 m in the West abutment and 7.5 m and 1.5 m in the East abutment). The differential settlement between the footings at the design load was reduced to less tan 1 mm in both the East and West abutments.

Figure 4.12 shows the lateral displacement profiles at different applied

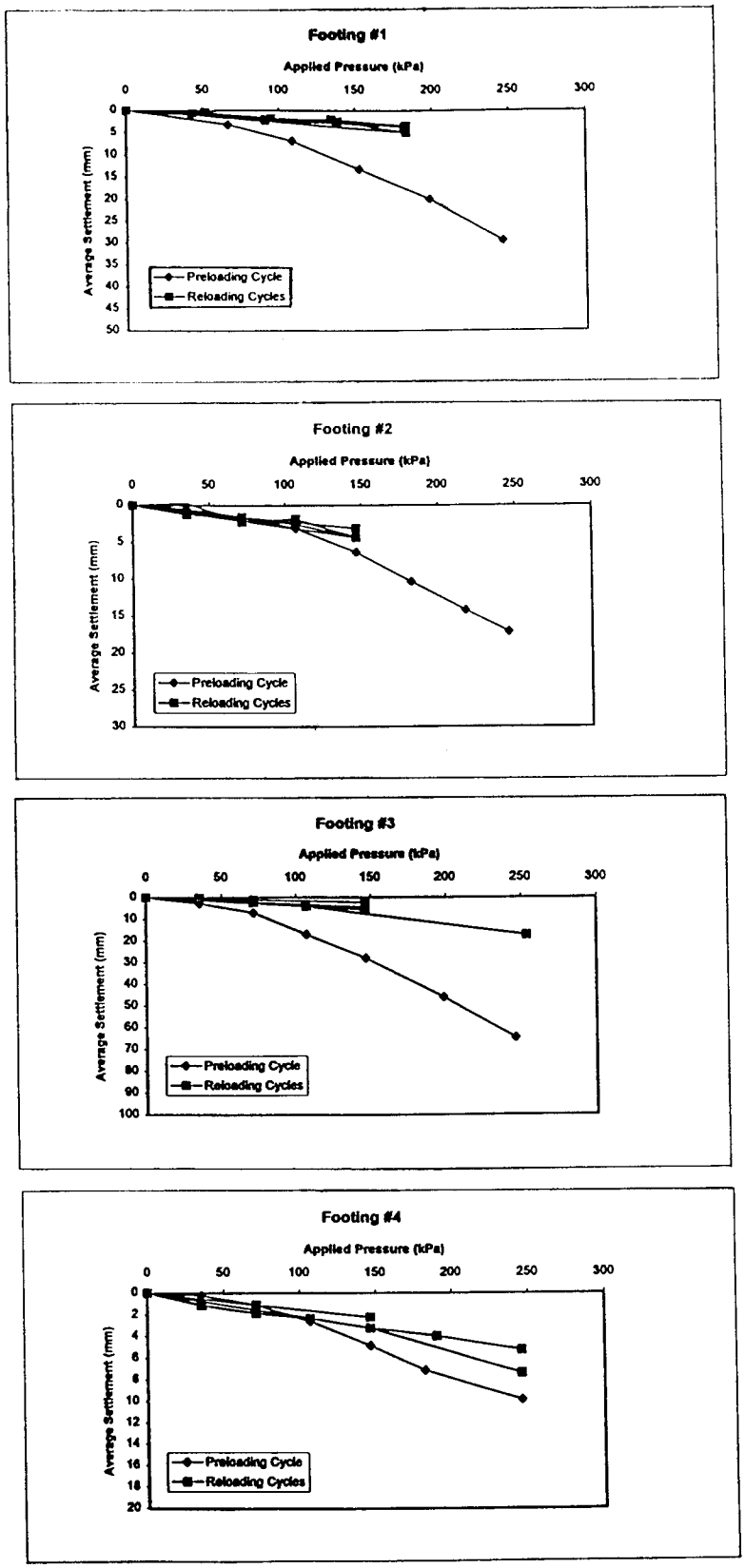

Figure 4.11 Relationships Between Average Settlement and Applied Pressure

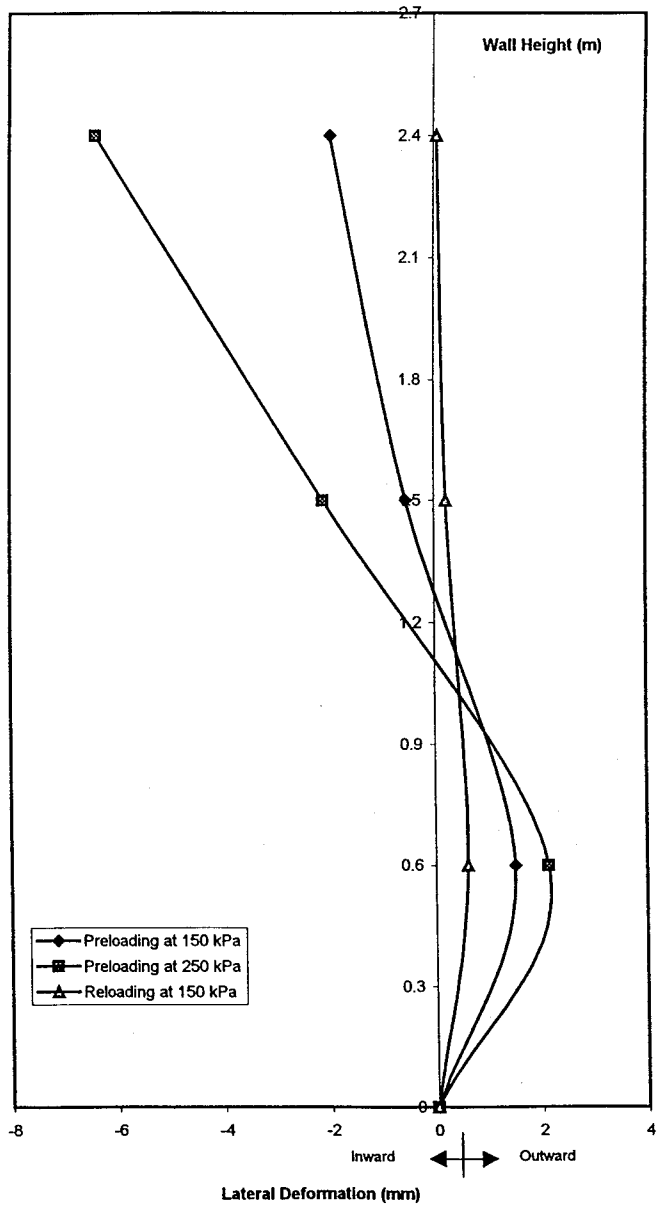

Figure 4.12(a) Lateral Deformation Profiles of the Wall Under Footing 1

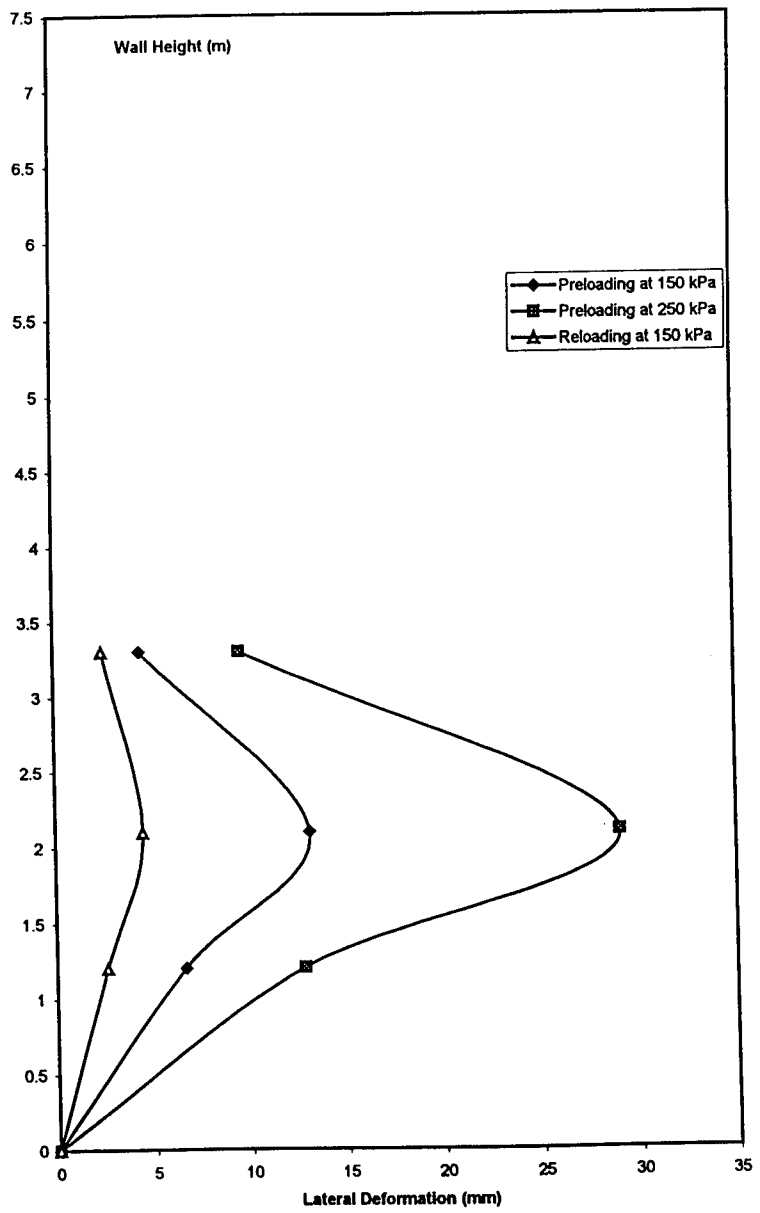

Figure 4.12(b) Lateral Deformation Profiles of the Wall Under Footing 3

loads. The deformed shapes for Footing #1 and #3 were similar in the preloading cycle. The bottom part of the wall moved outward, while the top part moved inward (toward the backfill). This may be related to the deformed shape of the reinforcement sheets in the top portion of the wall. As the vertical load was applied to the footing, the top layers of the reinforcement deformed in a "bowl" shape with a maximum vertical displacement occurred beneath the footing. The top reinforcement layers which were attached to the facing, thus, pulled the rock-face inward.

The largest outward movement (positive sign) occurred at 0.6 m (0.2H, H = wall height) from the wall base for Footing #1 and 2.1 m (0.37H) from the wall base for Footing #3. The largest inward displacement (negative sign) for Footing #1 was at 2.4 m from the wall base. The maximum outward displacements for Footing #1 and #3 were, respectively, +1.5 mm and +13.2 mm, at 150 kPa of the preloading cycle, and +2.1 mm and +29 mm at 245 kPa of the preloading cycle, and +0.6 mm and +4.5 mm at 150 kPa of the reloading cycle. The maximuminward movements for Footings #1 were -2.5 mm at 150 kPa and -6.4 mm at 245 kPa. Neither walls showed any inward movement in the reloading cycles.

Preloading reduced the maximum lateral movement at 150 kPa by a factor of 2.5 to 3 (from 1.5 mm to 0.6 mm in Footing #1 and from 13.2 mm to 4.5 mm in Footing #3). This is not the case with the Turner-Fairbank pier of which preloading did not produce any reduction in the lateral movement. This may be due to the difference in the soil placement density and in the lateral restrain offered by the facing. The backfill in the Black Hawk abutments was of much lower density than in the Turner-Fairbank pier. The looser backfill became stiffer in the lateral direction due to the preloading, thus experienced less lateral movement when reloaded. The lateral restrain of the Black Hawk abutment was greater than that in the Turner-Fairbank pier due to the difference in weight (rocks vs. cinder blocks). The greater restrain induced larger "lock-in" lateral stress after removal of the load, and resulted in smaller lateral movement upon subsequent loading.

Figure 4.13 shows the average vertical creep displacement versus time relationship of the square footings. In the preloading cycle, under a load of 245 kPa sustained for 60 minutes, the vertical creep displacements of Footings #1, #2, #3, and #4 were, respectively, 6.7 mm, 4.0 mm, 7.2 mm, and 2.1 mm. In the reloading cycle, under the sustained load of 150 kPa, the vertical creep deformation was insignificant. The maximum vertical creep displacement was 0.5 mm in 30 minutes.

Figure 4.14 shows the maximum lateral creep displacement versus time relationship. The maximum lateral creep displacements at the sustained load of 245 kPa of the preloading cycle for Footing #1 and #3 were, respectively, 0.7 mm and 2.0 mm in 60 minutes. The lateral creep displacement at the sustained load of 150 kPa of the reloading cycle, similar to the vertical creep, was insignificant. The maximum lateral creep displacement was 0.02 mm in 30 minutes.

4.5.2 Loading Tests on the Strip Footings

Figure 4.15 shows the average settlement of the West abutment strip footing versus applied pressure relationship. The settlements at 40 kPa (the design load) and 80 kPa in the preloading cycle were 10.7 mm and 11.1 mm, respectively. The applied pressure of 80 kPa was sustained for 120 minutes. During the 120-minute period, the footing moved upward and downward over a range of 1.5 mm. In the reloading cycle, the fill continued to moved upward under the applied pressure of 40 kPa. The footing rebounded for a total of 5 mm during the reloading cycle.

Figure 4.16 shows the strain distribution in the reinforcement of the West abutment. The maximum strains at 80 kPa of the preloading cycle in layer A (1.2 m from base), layer B (0.6 m from base), and layer C (0.3 m from base) were 0.18%, 0.04%, and 0.06%, respectively. At 40 kPa of both preloading and reloading cycles, the maximum strains in layers A, B, and C were on the order of 0.005% to 0.05%.

Figure 4.17 shows the creep strains in the reinforcement layers at 0.75 m from the facing. The creep strains of layers A, B, and C were 0.032%, 0.009%,

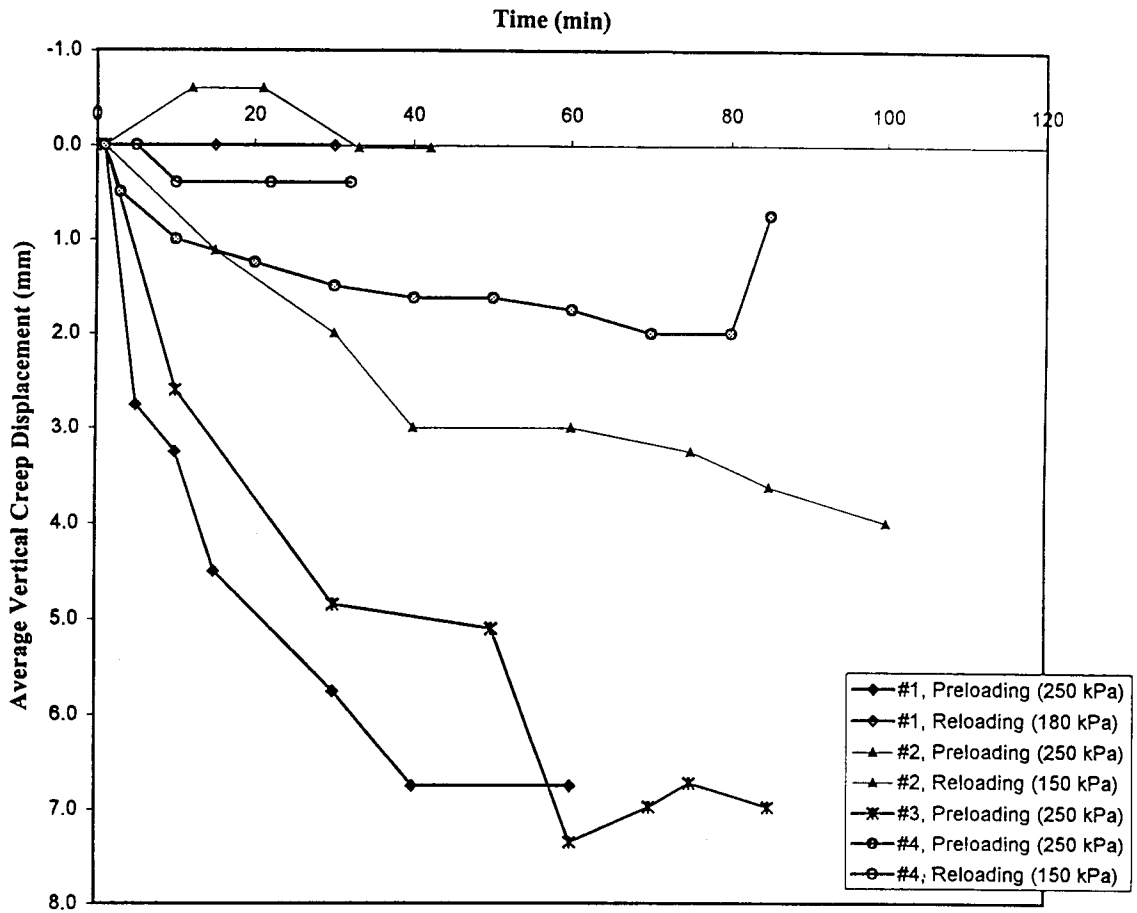

Figure 4.13 Average Vertical Creep Displacements of the Square Footings

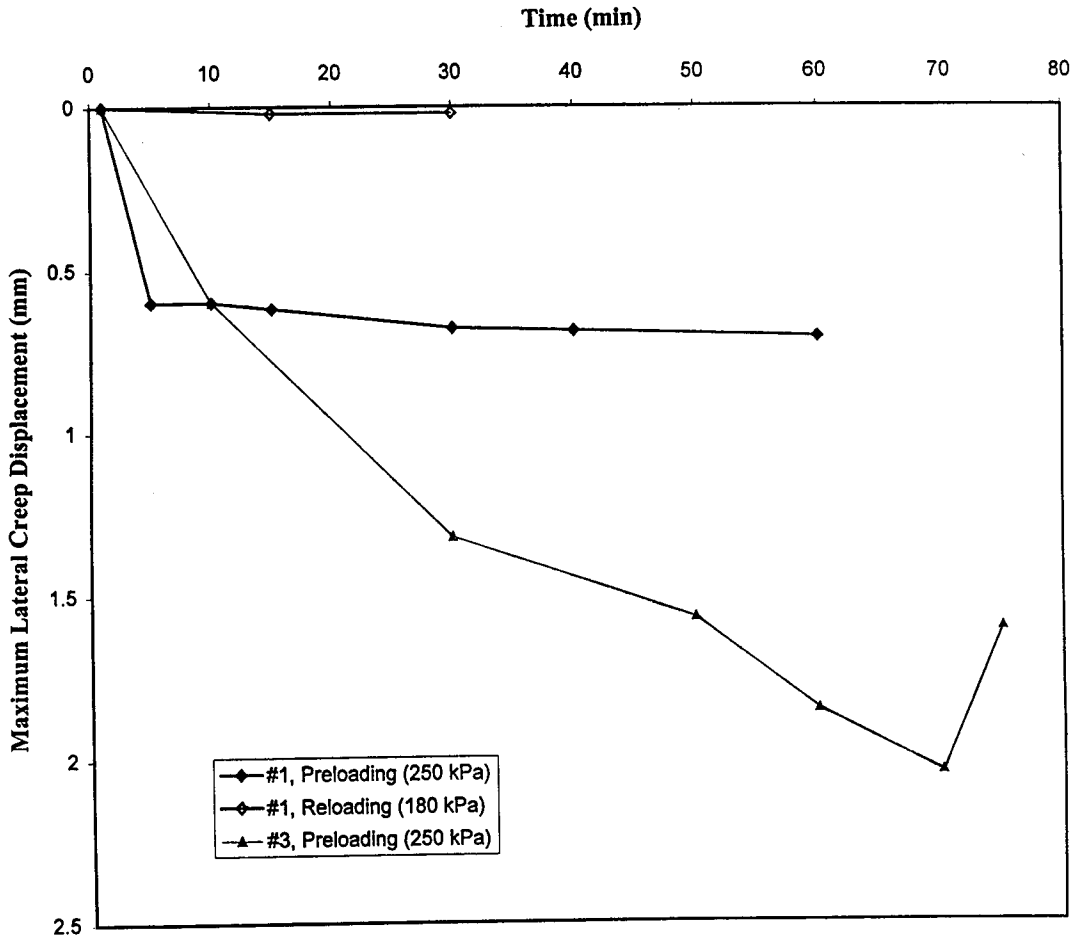

Figure 4.14 Maximum Lateral Creep Displacements of Footings 1 and 3

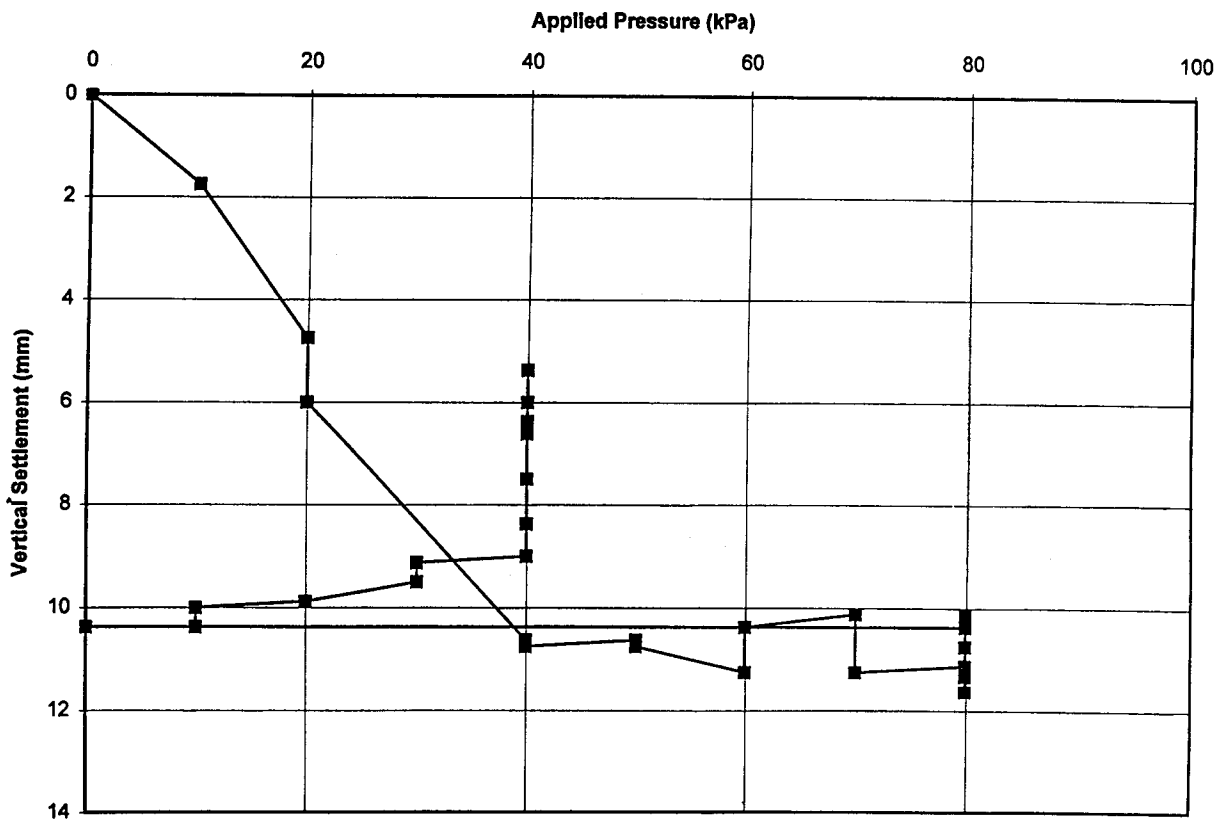

Figure 4.15 Average Vertical Sattlement vs. Applied Pressure Relationships of West

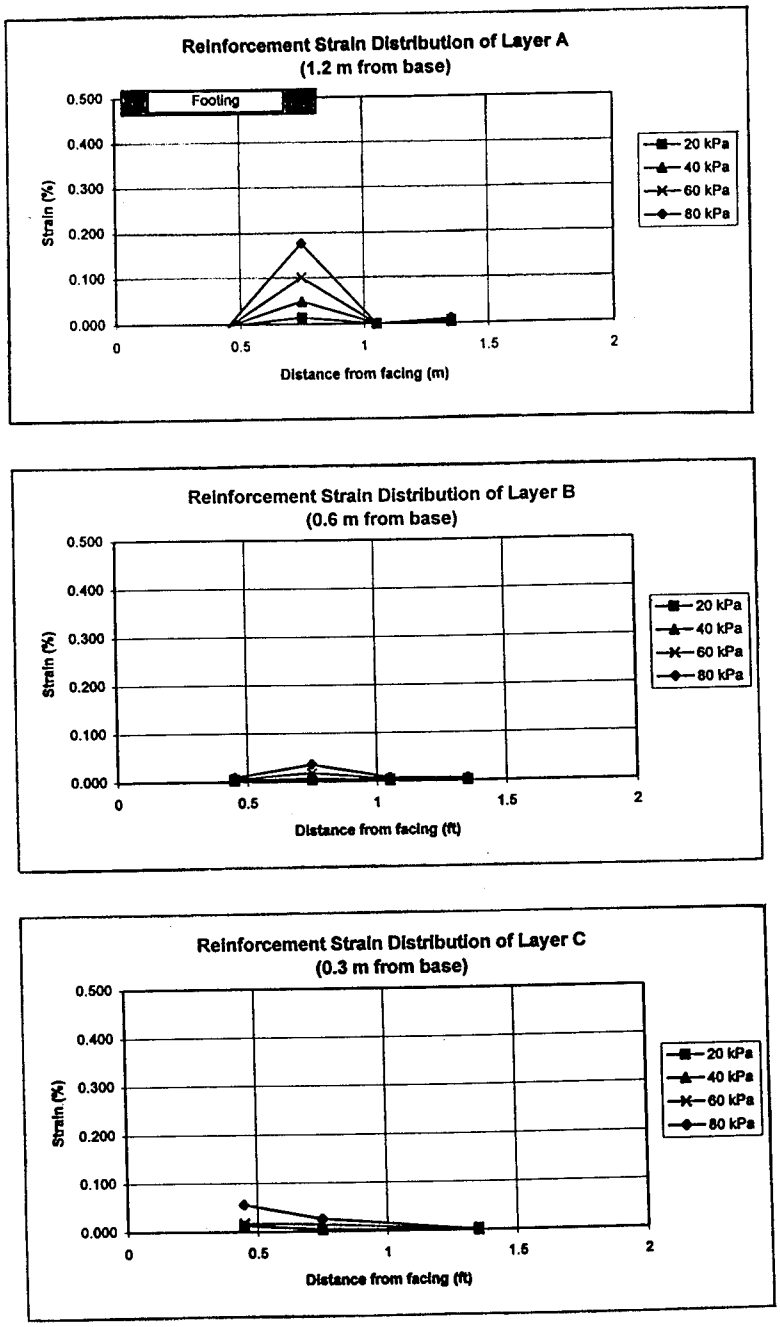

Figure 4.16 Strains in Geosynthetic Reinforcement Beneath the West Strip Footing

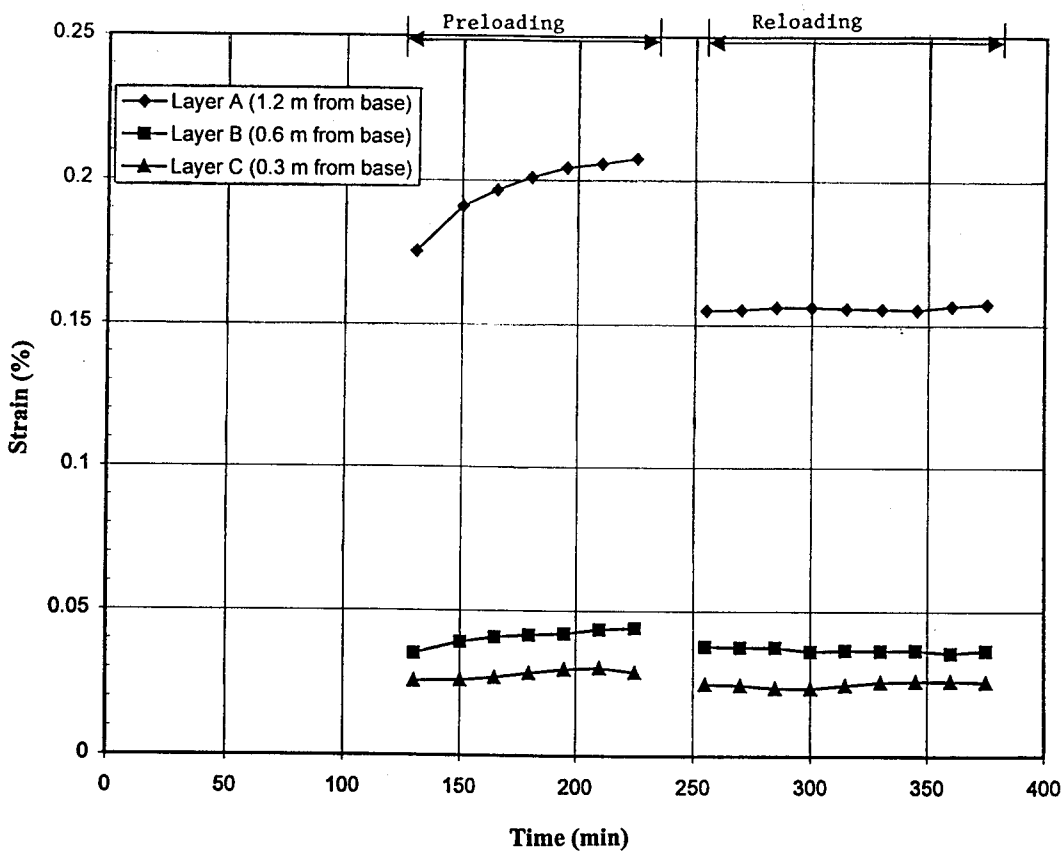

Figure 4.17 Creep Strains Under Sustained Pressures of 80 kPa in the Preloading and 40 kPa in the Reloading

and 0.003%, respectively, at the sustained load of 80 kPa of the preloading cycle. The creep strains became insignificant (on the order of $\pm$0.002%) at the sustained load of 40 kPa of the preloading cycle. It shows that the preloading reduces creep strains in the geotextile reinforcement. This agrees with the finding of the Turner-Fairbank pier presented in Chapter 2.

4.6 Summary and Conclusions

Two GRS bridge abutments were built in Black Hawk, Colorado to support a 36-m span steel arch bridge. The GRS abutments were constructed in two tiers with on-site backfill and reinforced with layers of a woven geotextile. Dry-stacked rocks were used as facing. The GRS abutments were situated over a stiff soil layer overlaying a competent rock. Each abutment has two square footings on the lower tier and a strip footing on the upper tier. The reinforced soil mass under Footing #2 and #3 was 1.5-m and 7.5-m thick, respectively on the East abutment; and was 4.5-m and 1.5-m thick under Footings #1 and #4, respectively, on the West abutment. The design loads for the square footings was 890 kN, and 445 kN for the strip footing. To reduce post-construction settlement, especially the differential settlement between footings, the GRS abutments were preloaded. The preloading was conducted by using anchored thread bars and hydraulic jacks. The abutment was preloaded up to 245 kPa (1.6 times the design load of 150 kPa) for the square footing and to 80 kPa (2 times the deign load of 40 kPa) for the rectangular footing. The abutments were instrumented to monitor the settlements of the footings, the lateral deformation of the rock-faced wall, and the strains in the geotextile reinforcement.

The finding and conclusions of the preloading tests are summarized as follows:

- By preloading the reinforced soil mass to 245 kPa, the settlement at the design load of 150 kPa was reduced by a factor of 1.5 to 6 for the four square footings. The settlements of the two square footings at 150 kPa of the preloading cycle were 13.3 mm and 4.9 mm in the West abutment, and 28 mm and 6.4 mm on the East abutment. After preloading, the

settlements at 150 kPa of the reloading cycle were reduced to 3.3 mm and 2.5 mm on the two footings of the West abutment, and 4.5 mm and 3.8 mm on the footings of the East abutment.

- Due primarily to the large difference in the thickness of reinforced soil mass, significant differential settlements between footings occurred in the preloading cycle. Preloading substantially reduced the differential settlement. The differential settlements at 150 kPa of the preloading cycle in the West and the East abutments were 8.4 mm and 21.6 mm, respectively. At 150 kPa of the reloading cycle, the differential settlement of both abutments was less than 1 mm.
- Preloading also reduced the lateral movement of the GRS abutments. The maximum lateral displacements in the West abutment (2.7 m in height) and the East abutment (5.4 m in height) were 1.5 mm and 13.2 mm, respectively, at 150 kPa of the preloading cycle. They were reduced to 0.6 mm and 4.5 mm, respectively, at 150 kPa of the reloading cycle. This was not the case with the Turner-Fairbank pier of which preloading did not produce any reduction in the lateral movement. The difference is believed to be due to differences in soil placement density and in facing rigidity.
- After the first reloading cycles, there was no significant reduction in the magnitude of the lateral and vertical deformation of the GRS abutments in the subsequent reloading cycles.
- The vertical creep displacements at a sustained load of 245 kPa of the preloading cycle were 6.7 mm and 1.5 mm in the West abutment and 3.0 mm and 4.7 mm in the East abutment. In the reloading cycles at a load of 150 kPa (sustained for 30 minutes), the creep settlement was insignificant. The maximum lateral creep displacements of the West and East abutments at the sustained load of 245 kPa were less than 1 mm in 100 minutes.
- The settlements of the strip footings in the West abutment at 40 kPa (the design load) and at 80 kPa of the preloading cycle were 10.7 mm and 11.1 mm, respectively. After unloading, the footing rebounded back and

continued to move upward even under a reloading pressure of 40 kPa. The footing moved upward a total of 5 mm in 30 minutes.

- Preloading reduced creep strains in the geotextile reinforcement. The reinforcement strains were on the order of 0.01% to 0.05% at 40 kPa and 0.05% to 0.2% at 80 kPa. The creep strain at a sustained load of 80 kPa of the preloading cycle were in a range of 0.003% to 0.032% in 100 minutes. The creep strains at the sustained load of 40 kPa of the reloading cycle were insignificant (on the order of $\pm$0.002%).

Chapter 5
CONCLUDING REMARKS

This report describes three studies on geosynthetic-reinforced soil (GRS) bridge supporting structures: load test of the Turner-Fairbank pier, load test of the Havana Yard piers and abutment, and pre-loading of the Black Hawk abutment. Findings and conclusions of each of the projects are presented at the end of Chapters 2, 3, and 4.

The following are some concluding remarks regarding GRS bridge supporting structures:

1. The three projects have clearly demonstrated that construction of GRS bridge piers and abutments is indeed rapid and simple. The use of lightweight concrete (cinder) blocks as facing (without mechanical connections between blocks) results in satisfactory performance of the structures under service loads.
2. It is believed that the small vertical reinforcement spacing (0.2m to 0.3m) contributes significantly to the satisfactory performance of the GRS bridge supporting structures.
3. With good compaction, the Turner-Fairbank pier has a load carrying capacity over 900kPa; whereas, with poor compaction, the Havana Yard pier and abutment had a load carrying capacity higher than 200kPa. Good compaction is essential to satisfactory performance of GRS structures.
4. Under an average surcharge of 230kPa, the settlements at the top of the Turner-Fairbank pier and the Havana Yard pier were 0.30% and 0.48% of the respective pier height. This is due to the difference in the compaction effort of the two piers.
5. With granular backfill and good compaction, as in the case of the Turner-Fairbank pier, long-term creep deformation under service load was negligible. On the other hand, with poor compaction, as in the case of the

Havana Yard outer pier, creep deformation can be quite significant. The creep deformation does decrease rapidly with time.

6. The reinforcement strains in both test piers were on the order of 0.2% to 0.4% under a surcharge pressure of 230kPa. The maximum strain was 0.5% at 400kPa and 2.3% at 900kPa in the Turner-Fairbank pier. Compared with the rupture strain of 18% for this geosynthetic reinforcement, the safety margin against rupture of reinforcement was very high.
7. Pre-loading (pre-straining) of the Turner-Fairbank pier was very effective in reducing vertical settlement. Upon reloading to 415kPa (following loading to 900kPa and unloaded to zero), the vertical settlement was about 50% of that occurred during the initial loading.
8. Pre-loading (pre-straining) did not reduce the lateral movement, except near the top of the pier (the Turner-Fairbank pier) where the blocks were bonded together with glue. This is not unexpected with lightweight block face as they provide little restrain to lateral movement during pre-loading.
9. Pre-loading in the Black Hawk abutment was critical to the satisfactory performance of the abutment. By pre-loading the footings to 1.6 Times the design load, the vertical settlements at the design load were reduced by a factor of 1.5 to 6.0. More importantly, the maximum differential settlement at the design load was reduced from 23mm to 2mm. The large differential settlement before pre-loading was due primarily to the large difference in the thickness of the reinforced soil mass.
10. GRS pier and abutment are clearly viable alternatives to conventional bridge pier and abutment and metallic reinforced pier and abutment.

REFERENCES

Adams, M. (1997), "Performance of a Prestrained Geosynthetic-Reinforced Soil Bridge Pier," Keynote Lecture, *Mechanically Stabilized Backfill*, A. A. Balkema Publisher, Netherlands, p. 35-53.

FHWA Demonstration Project 82 (1996), "Mechanically Stabilized Earth Walls and Reinforced Soil Slopes Design and Construction Guideline," Pub. No. FHWA-SA-96-071, Federal Highway Administration, US Department of Transportation.

Ketchart, K. and Wu, J.T.H. (1996), "Long-Term Performance Tests of Soil-Geosynthetic Composites," Report No. CDOT-CTI-96-1, Colorado Department of Transportation.

Recycled
Recyclable

HRDI-08/1-01(799)E